MODELLING THE SPONTANEOUS COMBUSTION OF COAL BEDS

Steven Martin Bradshaw

A thesis submitted to the Faculty of Engineering, University of the Witwatersrand, Johannesburg, in fulfilment of the requirements for the degree of Doctor of Philosophy.

Johannesburg, 1989.

DECLARATION

I declare that this thesis is my own unaided work, except where otherwise acknowledged in the text. It is being submitted for the degree of Doctor of Philosophy in the University of the Witwatersrand, Johannesburg. It has not been submitted before for any degree or examination in any other University.

S. M Bradshaw

26 day of June 1989

ABSTRACT

Spontaneous combustion can occur in a coal stockpile if the heat generated by oxidation cannot be dissipated at near ambient temperature. Spontaneous combustion of stockpiled coal occurs because [illegible] reaction between atmospheric gases and coal, and causes pollution, as well as the potential loss of all or part of the stockpile. Determination of conditions for which combustion occurs is of great [illegible] of coal stockpiles.

[illegible] small coal stockpiles [illegible] the finite element method. For coal [illegible] of superficial cross section, two [illegible] the case where only one flow [illegible] point is well described by [illegible] a simple one-dimensional model [illegible] pile is made flatter Benard-like [illegible] the ignition point is described [illegible] It is shown that the Benard-like [illegible] It is shown how to [illegible] what their approximate

[illegible] critical convection patterns [illegible] downwards at [illegible] table flow platform. A [illegible] criteria for the point [illegible] readily measurable parameters. This [illegible] ignition points in the interior of [illegible] the numerical work in which a [illegible] the edge of a stockpile when [illegible] It is shown that the cells which are [illegible] those found in the numerical

[illegible] approximate are derived which allow [illegible] criteria for ignition of coal beds in [illegible] properties of the coal and the size of the [illegible] pile. These criteria will allow the practitioner to [illegible] coal [illegible] and should prove very useful to the [illegible]

For my wife Zelda whose love and support made this work possible

ACKNOWLEDGEMENTS

I would like to thank my supervisors, Professor David Glasser, Dr. Kevin Brooks and Donald Williams for their advice, support and encouragement throughout the course of this study. Professor Glasser in particular provided invaluable insight, enthusiasm and guidance that were much appreciated. My former colleague Paul Anderson generously allowed me to use the early version of his finite element program which was subsequently modified and improved by the two of us to provide the powerful tool that provided the results of Chapter 2. Many enjoyable and profitable hours were spent discussing our respective projects. Dr. Henk Viljoen willingly provided much needed expert advice during the early stages of the work described in Chapter 3. Financial support for the author was provided by the Foundation for Research and Development of the Council for Scientific and Industrial Research, and latterly by the National Energy Council. Computer facilities were provided by Council for Scientific and Industrial Research. Without these facilities much of this work would not have been possible.

TABLE OF CONTENTS

LIST OF FIGURES

LIST OF TABLES

NOMENCLATURE

a	Horizontal wave number = $\sqrt{(k^2 + l^2)}$ Eq. (3.41)
a_n	Integral defined in Appendix E where n is an integer subscript
A	Matrix Eq. (3.59)
A	Geometric parameter Eq. (2.19g)
A_m	Fourier coefficient
b	Constant Eqs. (2.47) and (4.6)
$\underline{b}$	Time dependent part of unknown Eq. 2.28
B	Geometric parameter Eq. (2.19h)
Bi	Biot number Eq. (2.19d)
B_{rsg}	Fourier coefficient
c	Constant Eqs. (2.11a and 2.11b)
c	Molar concentration of oxygen in air
C_{rsg}	Fourier coefficient
c_p	Gas specific heat
D	Molecular diffusion coefficient
D_p	Particle size or area-based mean particle size used in Eq. (4.12)
D_{pc}	Particle size at "combustion"
D_{pe}	Particle size at extinction
D_{pi}	Particle size at ignition
E	Activation energy
e_{ij}	Element of Jacobian matrix Eq. (2.31)
$f_{t_i}(A,B)$	Unspecified function of geometry in ignition criteria Subscript used to differentiate between functions
$F(a,z)$	Function contained in trial functions Eq. (D.14)
$F_{t_i}(A,z)$	Function contained in trial functions Eqs. (D.17 and D.28)
$\underline{F}_e$	Element vector forcing function Eq. (2 25)
$\underline{F}$	System vector forcing function Eq. (2.26)
$\underline{f}$	Vector function Eq. (2.28)
$f_i(\underline{z},p)$	Unspecified function Eq. (2.29)
FK	Frank-Kamenetskii parameter = $\beta\ \varphi_h^2\ \gamma$ Eq. (2.36)
FK^*	Modified Frank-Kamenetskii parameter = FK $\sqrt{Ra^*}$ Eq. (2.38)
g	Acceleration due to gravity
G	Fourier coefficient
H	Height of coal bed
h	Heat transfer coefficient
J	Jacobian matrix Eq. (2.30)
k_e	Bed thermal conductivity
k_0	Pre-exponential factor in rate equation

k	x-component of the wave number
$k(T_a)$	$= \dfrac{6\, k_o \rho_a \exp\left(-\dfrac{E}{R_g T_a}\right)}{M}$
K_e	Element stiffness matrix Eq. (2.25)
K	System stiffness matrix Eq. (2.26)
l	y-component of the wave number
L	Length of one-dimensional bed or width of coal bed
$L(u)$	Differential operator
Le	Lewis number $= \epsilon D \rho_a c_p / k_e$ Eq. (2.19a)
M	Gas molecular mass
M	System mass matrix Eq. (2.27)
m_j	Mass fraction of coal with nominal particle size D_{pj}
n	Outward normal to surface of coal bed
N	Number of terms in continuation sequence Eq. (2.33)
$\underline{N}$	Vector of shape functions
p	Bifurcation parameter Eq. (2.29)
P	Pressure
P^*	Pressure in bed - ambient pressure P_a
r	Dimensionless horizontal coordinate Eq. (2.6d)
r^*	Horizontal coordinate
r_A	Reaction rate expression Eq. (1.4)
R_1	Upper flat surface of bed
$R(x)$	Residual Eq. (2.23)
R_g	Universal gas constant
R	Base radius of frustum or base length of edge
R_o	Radius of chimney in simplified three-dimensional model
R_{top}	Top radius or length of trapezoid
Ra	Rayleigh number $= \dfrac{\rho_a^2 g c_p H D_p^2 \epsilon^3 \eta T_a}{150 \mu k_e (1-\epsilon)^2}$ Eq. (2.19e)
Ra^*	Modified Rayleigh number $= Ra/\gamma$ Eq. (3.17)
Ra_L	$= Ra/(\eta T_a)$
S	Surface area per unit volume
T	Bed temperature
t	Time
t_o	Time to reach chimney Eq. (1.10)
t_c	Time for convection Eq. (2.20b)
t_d	Time for diffusion of species Eq. (2.20e)
t_g	Time for generation Eq. (2.20c)
t_r	Time for reaction Eq. (2.20d)
t_λ	Time for conduction Eq. (2.20a)

$\underline{U}$ Velocity vector

$\underline{u}$ Normalized velocity vector = $\underline{U}/(\alpha/H)$ Eq. (2.6c and d)

u_o Velocity in one-dimensional bed Eq. (1.1)

$u(x)$ Unspecified function Eq. (2.22)

$u^*(x)$ Approximation to unspecified function

w Dimensionless temperature function Eq. (3.11)

x' Horizontal co-ordinate

x Normalized horizontal co-ordinate = x'/H

$\underline{x}$ Vector of unkowns Eq. (2.29)

Y Normalized oxygen mole fraction Small stockpile model $= \dfrac{C\ M}{\rho_a\ Y_a'}$ Eq. (2.6g)

Y' Oxygen mole fraction

y Normalized horizontal co-ordinate = y'/H

y' Horizontal co-ordinate

Z Vertical co-ordinate

z Normalized vertical co-ordinate = Z/H

Greek symbols

α Thermal diffusivity = $k_e/(\rho c_p)_g$

β Dimensionless enthalpy of reaction = $-\Delta H\ y_a/(M\ c_p\ T_a)$ Eq. (2.19c)

γ Dimensionless activation energy = $E/(R\ T_a)$ Eq. (2.19b)

λ Perturbation parameter Eqs. (3.27)-(3.28)

$\underset{\sim}{\Delta}$ Vector operator Eq. (3.5)

Δ Parameter not dependent on D_p = $Ra^{1/2}\ \varphi_h^2$

ΔH Enthalpy of reaction

ϵ Voidage

ϵ_{pert} Perturbation coefficient Eq. (3.52)

η Coefficient of expansion

θ Dimensionless temperature = $(T-T_a)/T_a$ Eq. (2.6e)

κ Permeability

λ Eq. (3.36)

Λ Integer truncation number Eq. (3.40)

μ Gas viscosity

ν Equation (3.39)

Π Dimensionless pressure = $(P+\rho_a gZ)/(\alpha\mu/\kappa)$ Eq. (2.6f)

ρ_a Density of ambient air

ρ Density

σ eigenvalue

τ Dimensionless time = $t\alpha/H^2$

T Normalized oxygen mole fraction = $\dfrac{\left(C M / \rho_a - Y_a' \right)}{Y_a'}$
Interior model

ϕ_h^2 Thermal Thiele modulus = $\dfrac{6 k_o \rho_a (1-\epsilon) H^2 c_p \exp(-\gamma)}{k_e D_p}$

Φ Function of unkowns Eq. (2.27)

ρ Ratio of heat capacities = $(1-\epsilon)(\rho c_p)_s/(\rho c_p)_g$

$\phi_j(x)$ Trial functions Eq. (2.22)

χ Poloidal potential Eq. (3.5) and Eq. (H.5 and H.6)

ψ Stream function Eq. (2.11a and b)

Ψ Toroidal potential Eqs. (H.5 and H.6)

ω Vorticity Eq. (H.9)

Subscripts

1,2,... Integer numerals are used to differentiate between functions

a Refers to ambient conditions

c Conduction

crit Critical value of a parameter

E Refers to chimney exit

i Ignition condition

I Refers to chimney entrance

g Refers to gas properties

max Refers to maximum value

min Refers to minimum value

n Refers to normal component

r Refers to radial or horizontal property

s Refers to solid properties

t Refers to time derivative

top Refers to upper flat surface of coal bed

z Refers to vertical component

Superscripts

' Unit vector directed upwards

· Time derivative

(o) Steady-state coefficient

B Refers to perturbation coefficient associated with energy equations

τ Dimensionless time = $t\alpha/H^2$

T Normalized oxygen mole fraction = $\dfrac{\left(C\ M\ /\ \rho_a - Y_a' \right)}{Y_a'}$
Interior model

φ_h^2 Thermal Thiele modulus = $\dfrac{6\ k_o\ \rho_a\ (1-\epsilon)\ H^2\ c_p\ \exp(-\gamma)}{k_e\ D_p}$

Φ Function of unkowns Eq. (2.27)

φ Ratio of heat capacities = $(1-\epsilon)(\rho c_p)_s/(\rho c_p)_g$

$\varphi_j(x)$ Trial functions Eq. (2.22)

χ Poloidal potential Eq. (3.5) and Eq. (H.5 and H.6)

ψ Stream function Eq. (2.11a and b)

Ψ Toroidal potential Eqs. (H.5 and H.6)

Ω Vorticity Eq. (H.9)

Subscripts

1,2... Integer numerals are used to differentiate between functions

a Refers to ambient conditions

c Conduction

crit Critical value of a parameter

E Refers to chimney exit

i Ignition condition

I Refers to chimney entrance

g Refers to gas properties

max Refers to maximum value

min Refers to minimum value

n Refers to normal component

r Refers to radial or horizontal property

s Refers to solid properties

t Refers to time derivative

top Refers to upper flat surface of coal bed

z Refers to vertical component

Superscripts

$\hat{}$ Unit vector directed upwards

$\cdot$ Time derivative

(o) Steady-state coefficient

B Refers to perturbation coefficient associated with energy equations

C Refers to perturbation coefficient associated with concentration equation

CHAPTER 1

INTRODUCTION

1.1 Background to spontaneous combustion

It is well known that self-heating occurs in large stockpiles of coal, e.g. in above-ground storage beds, storage silos, storage holds in ships and even in dumps of mine waste material which would not burn in a domestic fireplace, but which presents a serious problem when dumped in large heaps. Self-heating is an extremely undesirable phenomenon, as it leads to a degradation of the coal properties and if the heat generated within the coal bed cannot be dissipated to the surroundings at near ambient temperature spontaneous combustion can result. Spontaneous combustion causes a serious pollution problem through the emission of noxious gases and particulate matter, can be a danger to human life and in the case of coal stockpiles may lead to a loss of all or part of the coal store, with possibly disasterous economic consequences. It is also important to prevent spontaneous combustion in dumps of mine waste material because of the pollution problem and from the safety aspect, particularly as the waste material may be required to backfill open-cast mines.

Although the problem of spontaneous combustion has been known for a long time, it is only recently that scientifically-based models of the phenomenon have appeared in the literature. Many of the early investigations were concerned with laboratory measurements of the susceptibility of particular coal samples to spontaneous combustion. Although such studies provide valuable information, they are of limited use in designing stockpiling facilities and developing contingency measures in case of fires in coal beds. Many of the methods that have been used to counteract the problem of spontaneous combustion have been developed through experience on an *ad hoc* basis, and while many are undoubtedly of considerable merit, the use of *ad hoc* procedures in new situations may be potentially disasterous. In order to gain a general understanding of a phenomenon and to be able to predict behaviour in new situations a mathematical model of that phenomenon is invaluable.

More recent models of spontaneous combustion have placed the subject on a firmer scientific foundation, and have dealt with effects such as

CHAPTER 1

INTRODUCTION

1.1 Background to spontaneous combustion

It is well known that self-heating occurs in large stockpiles of coal, e.g. in above-ground storage beds, storage silos, storage holds in ships and even in dumps of mine waste material which would not burn in a domestic fireplace, but which presents a serious problem when dumped in large heaps. Self-heating is an extremely undesirable phenomenon, as it leads to a degradation of the coal properties, and if the heat generated within the coal bed cannot be dissipated to the surroundings at near ambient temperature spontaneous combustion can result. Spontaneous combustion causes a serious pollution problem through the emission of noxious gases and particulate matter, can be a danger to human life and in the case of coal stockpiles may lead to a loss of all or part of the coal store, with possibly disasterous economic consequences. It is also important to prevent spontaneous combustion in dumps of mine waste material because of the pollution problem and from the safety aspect, particularly as the waste material may be required to backfill open-cast mines.

Although the problem of spontaneous combustion has been known for a long time, it is only recently that scientifically-based models of the phenomenon have appeared in the literature. Many of the early investigations were concerned with laboratory measurements of the susceptibility of particular coal samples to spontaneous combustion. Although such studies provide valuable information, they are of limited use in designing stockpiling facilities and developing contingency measures in case of fires in coal beds. Many of the methods that have been used to counteract the problem of spontaneous combustion have been developed through experience on an *ad hoc* basis, and while many are undoubtedly of considerable merit, the use of *ad hoc* procedures in new situations may be potentially disasterous. In order to gain a general understanding of a phenomenon and to be able to predict behaviour in new situations a mathematical model of that phenomenon is invaluable.

More recent models of spontaneous combustion have placed the subject on a firmer scientific foundation, and have dealt with effects such as

the kinetics of the oxidation reactions, the adsorption and desorption of water, the ingress of reactant gases into the bed, heat transfer mechanisms in coal beds and the physical properties of the coal stockpile. Most of these studies have considered simple, idealised geometries, because of the complexity of modelling spontaneous combustion in two or three dimensions.

In the Department of Chemical Engineering at the University of the Witwatersrand a ten year program of research into spontaneous combustion has been conducted along two fronts. Modelling of the phenomenon on the coal chemistry level has yielded valuable information on e.g. heats of reaction, reaction mechanisms, reaction rate expressions and the influence of many of the intrinsic properties of the coal. The interested reader is referred to Itay,1984, Itay et al.,1989. Concurrently with this research, considerable work has been done in the area of modelling the physical processes occurring in above-ground coal stockpiles. A hierarchical approach to the modelling has been followed, beginning with a simple one-dimensional model, which provides valuable insights while still remaining sufficiently tractable to be solved on a small computer, and culminating in the three-dimensional model described in this thesis. The more complex models are regarded as research tools, to investigate in more complex and realistic geometries the results of the simpler models, and to confirm or modify where necessary the predictions of those models. The mathematical sophistication required in the multi-dimensional models is clearly beyond what can be expected of the practitioner in industry, and the computational requirements of these models are so great that only the most powerful of mainframe computers are capable of solving the equations. However, as a means of testing and validating the predictions and criteria of the simple models they are invaluable, and lend confidence and justification to the simple expressions for safe stockpiling parameters we envisage being used by the practitioner. Although the modelling effort has been aimed at above-ground stockpiles, the principles could be applied to coal storage bunkers, coal stored in the holds of ships and even to the storage of agricultural grains.

1.2 Scope and aims of the study

The main purpose of the study described in this thesis is to investigate ignition points in realistic coal stockpiles. The ignition point is defined as the point at which the steady-state condition of the coal bed experiences a rapid qualitative change from

a low temperature solution to a high temperature burning situation as some critical parameter is changed The validity of a simple relationship for the ignition particle size developed for a one-dimensional model will be investigated for small two-dimensional coal beds, and a new criterion for ignition points developed for the interiors of large coal beds. The question of which criterion should be used for a particular coal bed will also be answered. As will be shown in section 1.3, the determination of ignition points for a coal stockpile is a vital piece of information for the coal industry, as it provides an estimate of the limit of safe stockpiling conditions. When this limit is known, the practitioner can design coal stockpiles accordingly.

The thesis is divided into two main sections, the first dealing with the determination of ignition points in small coal stockpiles, or at the edges of large ones, and the second showing how ignition points may be calculated for the interiors of large stockpiles. In Chapter 2 the equations describing energy, mass and momentum transfer in a coal stockpile are derived. This set of simultaneous non-linear partial differential equations must be solved numerically, and a brief survey of some of the methods used previously for such problems is followed by a description of the finite element program that was used in this study. A continuation method which was used to calculate ignition points in the coal bed is described, and a comparison made between the results so obtained and a simple relationship for the ignition point derived from a one-dimensional model. When the natural convection flow shows formation of Benard-like cells, a different criterion is used to predict the particle size at ignition. The chapter is concluded with an investigation, using a numerical method, into the formation of Benard-like cells in coal beds. A paper based on the work of this chapter has been published (Brooks et al.,1988c, see Appendix G).

Chapter 3 is devoted to a study of a laterally-unbounded layer of coal, in which spatially-periodic solutions can be assumed. This allows the treatment of extremely large coal stockpiles which could not be analysed by the numerical techniques of Chapter 2 because of the enormous computational effort that would have been required. By assuming spatially-periodic solutions, conditions for which Benard-like cells form can be modelled, complementing the work of Chapter 2. A review of the literature on cellular natural convection and ignition in exothermically-reacting media commences the chapter. The model for the infinite layer is then developed, and the simplifications used are introduced and justified. A brief

description is given of the Galerkin method which is used to transform the governing non-linear partial differential equations into a set of algebraic equations. The thermal explosion limit in the layer for the conduction-only case is examined as a worst-case solution and as a test of the continuation method that is used to calculate ignition points. The calculation of the conditions for the onset of convection is performed and the implications that the results have with regard to the likely stable size of the Benard-like cells is discussed. By using a continuation method similar to that used in Chapter 2, ignition points are calculated for the infinite layer, and a new simple criterion for ignition in this situation is developed. The work described in this chapter formed the basis for paper to be published in a journal (see Appendix G).

The implications of this study for the modelling of spontaneous combustion are discussed in Chapter 4, and it is shown how to choose the correct criterion for the determination of ignition points in a given coal stockpile. The ignition criteria that have been developed are simple algebraic equations containing easily measurable parameters of the coal bed. The criteria are suitable for use by the practitioner in industry and should prove extremely useful in the prevention of spontaneous combustion. The thesis is concluded with Chapter 5.

There are two areas of interest that are not covered in this thesis, and these are the unsteady-state behaviour of coal beds and the modelling of beds of very fine coal particles. The unsteady-state behaviour is of interest because in some cases a coal bed will reach steady-state only after many years. It may be that beds which will combust if left for long enough can be quite safely stockpiled for short periods, which may satisfy the needs of the practitioner. It was found that numerical solution of the unsteady-state problem was very problematical, as the the system of governing equations is stiff and cannot be solved by conventional numerical methods. It was also not possible to consider beds of very fine coal particles, for which the maximum temperature rise can be acceptably low. This was because all the reaction occurs in a thin layer on the surface of the bed, and within this layer the gradients of temperature and concentration are extremely steep. To represent these steep gradients numerically proved to be very difficult.

1.3 Historical review of models of spontaneous combustion

In this review emphasis is given to the simplified models developed by Brooks and Glasser,1986 and Brooks et al.,1988a, as it is to the verification and improvement of these models that a large part of this thesis is directed. The literature of the coal-chemistry side of spontaneous combustion has been reviewed elsewhere (Itay,1984, Schmal,1987) and only the most important results are summarised here.

There has been much work concerning coal and its oxidation (e.g. Van Krevelen,1981 and Guney,1972). Schmal,1987 and Brooks,1986 provide reviews of the subject relevant to spontaneous combustion. It has been found that the predominant reaction mechanism up to temperatures of ≈80°C when coal is exposed to the atmosphere is chemisorption leading to the formation of so-called oxy-coal complexes. The heat of reaction for the chemisorption reaction has been found by many investigators to be ≈300 kJ mol^{-1} of oxygen absorbed (Brooks,1986, Schmal,1987, Sondreal and Ellman,1974). Above 80°C chemisorption merges into chemical reaction in which the oxy-coal complexes are broken down into gaseous products (Schmal,1987). This relatively high temperature behaviour is not of great interest as it is known that a coal stockpile at 80°C is on the way to combustion. It is of more concern to us to find conditions for which a coal bed will combust than to calculate the conditions at combustion.

The rate of the oxidation reaction has been found to be a function of the reaction temperature, the surface area available for reaction, the partial pressure of oxygen in the gas, the oxidation history and the coal structure. The dependence of the reaction rate on temperature has generally been found to be well-described by an Arrhenius relation, with a value of the activation energy typically ≈60 kJ mol^{-1} K^{-1}. Itay,1984 found that the reaction rate is directly proportional to oxygen partial pressure for fresh coal. For very fine coal particles Smith,1989 has found that the rate of oxidation is not dependent on particle size, while for larger particles the dependency is less certain. Schmal,1987 reports that the rate decreases proportionally with the inverse of the particle diameter. It has been found that the reactivity of coal decreases with the degree of oxidation of the coal (Van Krevelen,1981, Van Doornum,1954). The order of the oxidation reaction has been found to be between 0.5 and 1 (Itay,1984, Sondreal and Ellman,1974, Schmal,1987).

The effects of adsorption and desorption of water on the self-heating

of coal have been discussed by Brooks,1986 and Schmal,1987 amongst others. The most dangerous situation for spontaneous combustion is when dry coal adsorbs moisture from the atmosphere. This can result in a temperature increase to the point where the rate of oxidation is significant. However, the associated temperature rise is not as great as is observed in combusting coal beds and cannot alone explain spontaneous combustion. It appears that moisture adsorption plays only an initiating effect in the spontaneous combustion process. For moist coal in contact with dry air the situation is reversed and the desorption of water will result in a lowering of the temperature.

The oxidation of pyrite is unlikely to be of great significance in spontaneous combustion, as the heat of reaction for pyrite oxidation is only about one tenth that of the oxygen chemisorption reaction and the pyrite content of coal is generally very small (Schmal,1987). The effects of coal composition on spontaneous combustion have not been conclusively established, although Smith,1989 has investigated these effects.

Early studies of spontaneous combustion were concerned mainly with the measurement of intrinsic heat generation (e.g. Schmidt and Elder,1940) which can be achieved by calorimetry or differential thermal analysis. Van Doornum,1954 presented a model which attempted to predict safe storage conditions for coal. He solved the unsteady-state conduction equation with a source term that was an exponential function of temperature but not of the Arrhenius form, and derived two dimensionless numbers that characterise the safety of the coal bed. The model has severe limitations in that natural convection is neglected, as is the consumption of oxygen. Oxygen consumption is in fact significant if conduction is the only form of heat and mass transfer in the coal bed. In addition, the model contains constants that must be measured for every coal under consideration. Sondreal and Ellman,1974 fitted data for the oxidation of lignites to empirical equations which were used in the Van Doornum,1954 model, together with an oxygen balance equation. This model also neglected natural convection, and is limited to the range of lignite properties studied by the authors.

More recent studies (Nordon,1979 and Schmal et al.,1985) have considered one-dimensional models describing the heat and mass transfer processes in the coal pile but allowing only for forced convection. These models are similar to fixed-bed axial dispersion models which are known to have multiple steady-state solutions.

Nordon,1979 incorrectly concluded that natural convection could be neglected because the gas and solid phases were assumed to be in thermal equilibrium. Although his model formulation allowed for the effects of moisture, these effects were not included in the computations. The model showed two distinct steady states, a low temperature plateau of less than ~17°C and a high temperature one of greater than ~87°C. For the low temperature plateau the reaction was limited by thermal conduction of the char, while the high temperature plateau was limited by diffusion of oxygen. Nordon found that smaller beds favoured the low temperature solution and he postulated the concept of a critical bed size. Schmal et al.,1985 found that it was necessary to include the effects of moisture evaporation, condensation and transport in their model when the temperatures were greater than 50-60°C. It was found that a dry-coal model predicted higher oxygen consumption rates than were indicated by field measurements. Inclusion of moisture effects was found to have a temperature levelling effect. Brooks and Glasser,1986 and Schmal,1987 have shown that natural convection is in fact the main mode of transport in a coal stockpile, and Brooks,1986 presented a calculation showing that diffusion alone could not account for spontaneous combustion. Young et al.,1986 considered two-dimensional mass and energy transport in a porous medium in the vicinity of a hot-spot. They found that the model predictions and experimental measurements agreed well and that natural convection supplied sufficient oxygen to support the hot-spot.

Handa et al.,1983 considered a two-dimensional model of spontaneous combustion in a coal bed. They presented time-dependent oxygen concentration profiles, isotherms and stream function contours for the sloping edge of a bed. From their results it appeared that the characteristic temperature for thermal runaway was ~50-60°C, which agreed with the results of Brooks and Glasser,1986. Morita et al.,1986 used a similar model for the prediction of self-heating effects in a coal storage silo. Their numerically-calulated results showed excellent agreement with measured values. Bowes,1984 comprehensively reviewed experimental and theoretical studies of spontaneous combustion for many different materials.

Coal stockpiles in general possess little or no symmetry; this fact complicates the modelling of their behaviour considerably. However, considerable insight into the behaviour of a stockpile can be gained by studying a simpler geometry. Brooks and Glasser,1986 considered a vertically aligned, radially-insulated bed of coal, open at both ends. In this thesis we call this model the one-dimensional analogue of a

coal stockpile. It can be seen that this model bears a strong resemblance to an adiabatic fixed bed reactor; the major difference is that the flow in the coal stockpile is caused by buoyancy forces arising from the self heating. The flowrate through the bed is thus not fixed, but rather a function of the temperature profile in the bed. Since the main concern was the long term storage of strategic stockpiles, a pseudo steady-state formulation was used i.e. it was assumed that the depletion of the coal was small.

Assuming in addition:
1) Plug-flow of the gas
2) Equal gas and solid temperatures
3) Ideal gas behaviour
4) Oxygen transport by molecular diffusion may be neglected,

the equations describing the bed were (Brooks and Glasser, 1986):

Oxygen mass balance: $$\frac{u_o \rho_a}{M} \frac{dY'}{dZ} = -r_a \qquad (1.1)$$

Energy balance: $$k_e \frac{d^2T}{dZ^2} - u_o \rho_a c_p \frac{dT}{dZ} + (-\Delta H)\, r_a = 0 \qquad (1.2)$$

Momentum balance: $$\frac{dP^*}{dZ} = - u_o \frac{\mu}{\kappa} \frac{T}{T_a} - \rho_a g \left(1 - \frac{T_a}{T}\right) \qquad (1.3)$$

The permeability was calculated using the first term of the Ergun equation, since the velocities in a coal bed are very small.

The rate expression was of the simplified form:

$$r_a = \frac{6\, k_o}{D_p} (1-\epsilon) \exp(-E/R_g T) \frac{P_a Y'}{R_g T_a} \qquad (1.4)$$

i.e. the reaction rate was assumed to be linear with respect to the oxygen partial pressure and proportional to the surface area per unit volume. While this rate expression may not be entirely realistic, it does serve as a simple expression having the right characteristics.

Boundary conditions used were:

At Z=0: $k_e \frac{dT}{dZ} = (u_o \rho_a c_p + h_I)(T - T_a)$, $Y' = Y'_a$ $P^* = 0$ (1.5a)

At Z=L: $k_e \frac{dT}{dZ} = -h_E(T - T_a)$, $P^* = 0$ (1.5b)

Two boundary conditions were imposed on the momentum balance, since u_o was to be determined. The model is shown schematically in Figure 1.1.

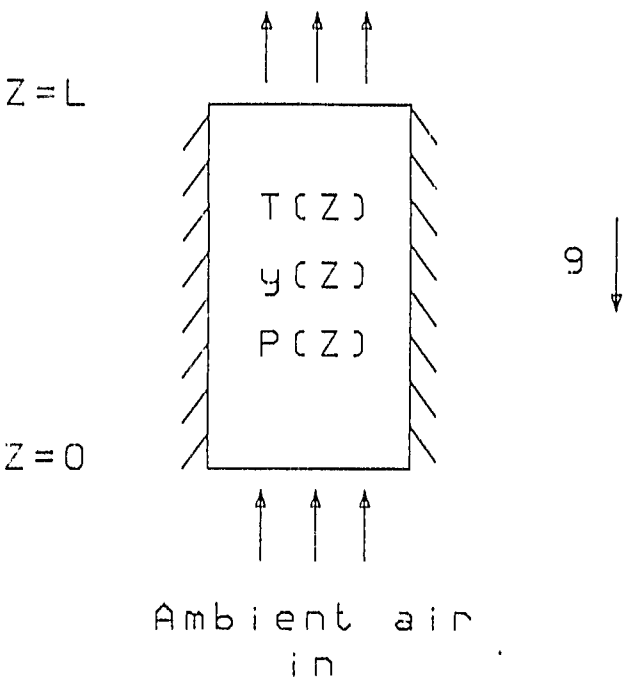

Figure 1.1 One-dimensional analogue of a coal stockpile

This set of equations has been extensively studied (Brooks and Glasser, 1986; Brooks et al., 1988a). It has been shown that the set of equations exhibits steady-state multiplicity. A schematic of a typical bifurcation diagram of average temperature versus particle size is shown in Figure 1.2. We observe an ignition point at particle size D_{pi}, and an extinction point at particle size D_{pe}. For any value of the particle size greater than D_{pe} the coal stockpile is safe and for any particle size between D_{pi} and D_{pe} the stockpile is conditionally safe. For particle sizes smaller than D_{pi} the only

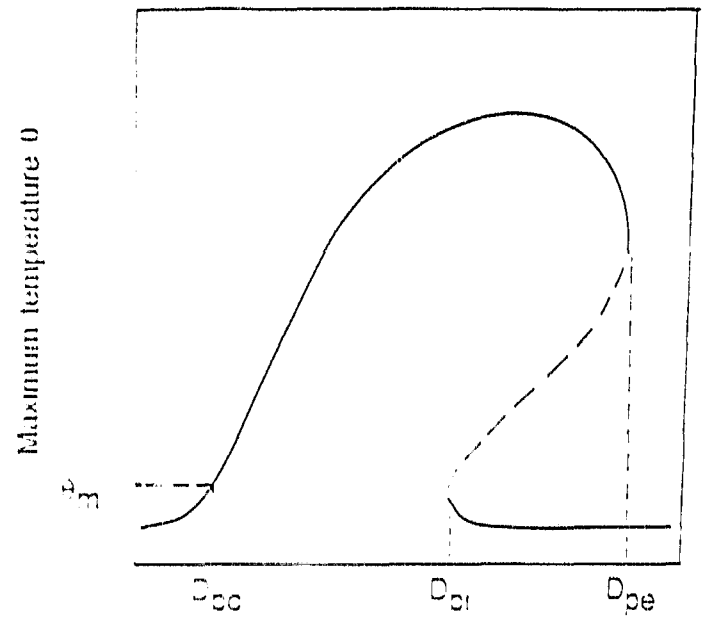

Figure 1.2 Schematic diagram of maximum temperature versus particle size for the one-dimensional coal stockpile

solution lies on what is termed the ignited branch. In practice D_{pe} is very large, and truly safe stockpiling conditions are not achieved; one has to be satisfied with conditionally safe conditions. This might not be the case if a small perturbation could move the solution from the extinguished to the ignited branch. In Figure 1.3 an example of a bifurcation diagram of particle size versus maximum temperature is shown; the calculation shown is for a pre-exponential factor of 10 m/s and a bed length of 5 m. Other model parameters are given in Appendix A. From figure 1.3 it is clear that the unstable solution, which separates the two stable solutions, rises fairly steeply from the ignition point. This implies that provided one is not too close to the ignition point, a fairly large perturbation in the temperature would be needed to ignite a conditionally safe stockpile. The ignition point is thus seen to be of crucial importance in the study of

spontaneous combustion.

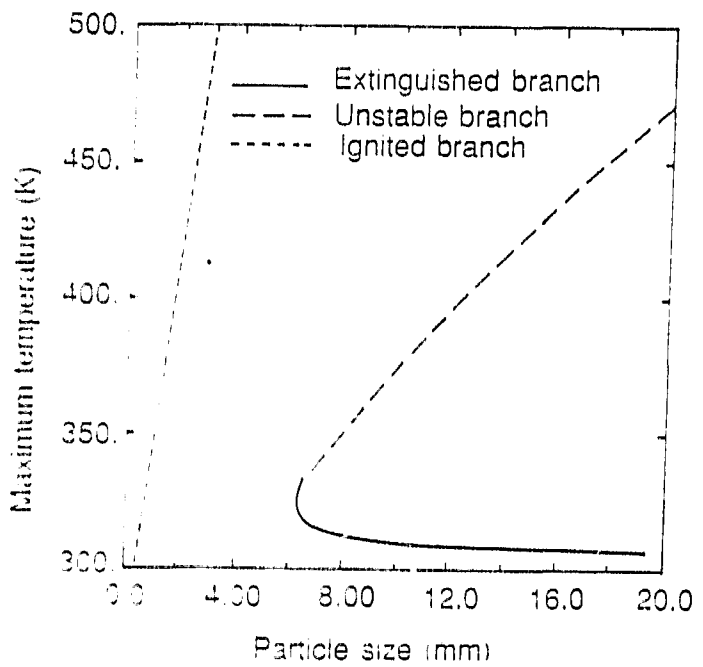

Figure 1.3 Calculated diagram of maximum temperature versus particle size showing the unstable solution for the one-dimensional coal stockpile

There exists a region of particle sizes on the ignited branch for which the temperature rise is reasonably low. This arises because in the fine coal the flowrates are very small and the coal is very reactive; thus the oxygen is scavenged close to the inlet, where the sensible heat due to reaction is easily dissipated at low temperature. Coal stockpiles in this region may be considered safe, even though they fall on what is called the ignited branch. Provided the temperature remains below for example 70°C, spontaneous combustion is not considered to have occurred; a stockpile in this situation would be considered to be acceptable to the practitioner. It can be seen that for a specified allowed maximum temperature rise (ϑ_m) a corresponding maximum allowable particle size (D_{pc}) may be

calculated. In many cases this particle size may be too small to be of practical importance. This is particularly the case with waste material of inherently low reactivity, for which the costs of crushing to this particle size would be prohibitive.

It is clear that a simple way of calculating D_{pi} would be very valuable for the practitioner. Brooks et al.,1988a showed that for values of the Rayleigh number, given by

$$Ra_L = \frac{\rho_a^2 \, g \, c_p \, L \, D_p^2 \, \epsilon^3}{150 \, \mu \, k_e \, (1-\epsilon)^2} \qquad (1.6)$$

greater than approximately 100, the value of D_{pi} could be calculated from the relationship:

$$D_{pi} = \left(\frac{1-\epsilon}{\epsilon}\right) \left[\frac{900 \, \gamma^2 \, \beta \, \mu \, k_o \, \exp(-\gamma) \, L}{g \, \rho_a} \right]^{1/3} \qquad (1.7)$$

In order to derive this relationship further assumptions were made:

a) The consumption of reactant was neglected
b) The positive exponential approximation was used (Frank-Kamenetskii,1969)
c) The temperature at the ends of the bed was assumed to be ambient, i.e. Dirichlet boundary conditions were used in place of (1.5).

These assumptions are all reasonable along the extinguished branch of solutions, up to the ignition point. This was verified by comparing the ignition point calculated from Eq.(1.7) with the ignition point calculated from the model without the above simplifying assumptions. The agreement in all cases was good.

This very powerful result allows simple calculation of the particle size at ignition, or alternatively the length required for ignition of a coal of a given particle size and reactivity. A problem that remains is the determination of L for a stockpile of more usual geometry. This is one of the main questions addressed in this thesis.

In an attempt to make the model described above more realistic, a simplified three-dimensional model has been developed (Brooks et al., 1988b). This model envisages the coal stockpile to be split into

three different regions, in each of which different effects dominate, and different assumptions are made. These regions are shown in Figure 1.4. The first of these is a central chimney in which reaction, flow and heat transfer are all considered. The second is a ball around the base of the chimney, in which only flow and heat transfer are considered. The third is physically the same as the second but only reaction is considered to occur.

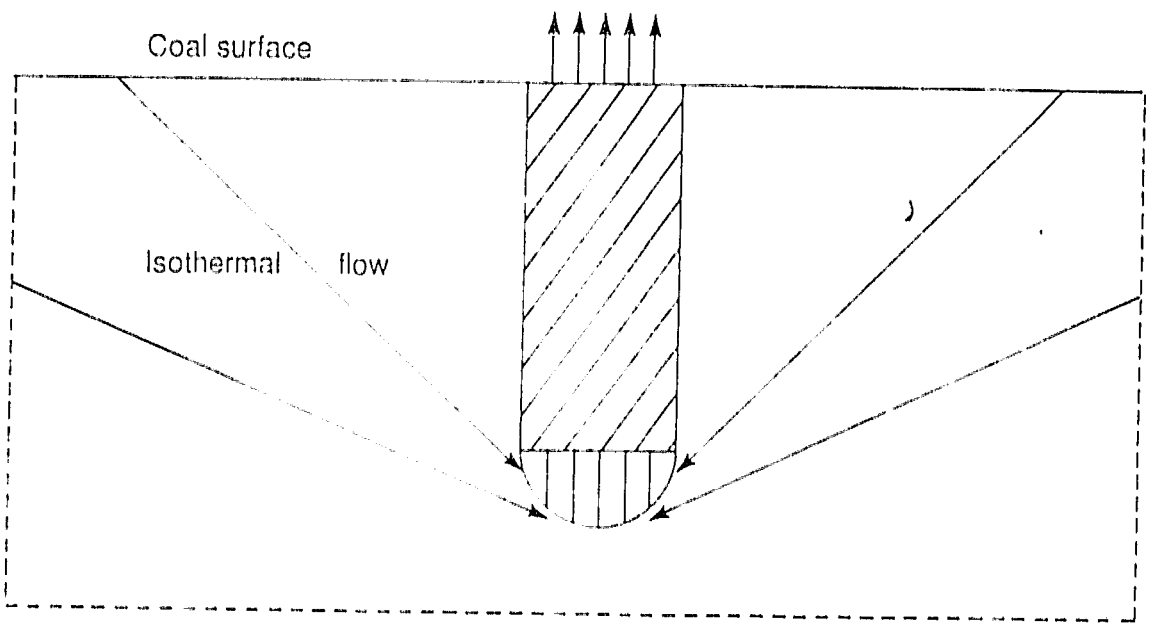

Figure 1.4 Simplified three-dimensional model

This formulation allows a more realistic boundary condition at the bottom of the bed to be derived. In addition it is possible to compute the amount of oxygen depletion occurring outside the chimney, using a residence time density function approach. This results in the expression:

$$\frac{Y'_o}{Y'_a} = \frac{(t_o)^{1/3}}{3} \int_{t_o}^{\infty} t^{-4/3} \exp(-kt)\, dt \qquad (1.8)$$

where k is the equivalent homogeneous rate constant at T_a

$$\text{i.e.} \qquad k = \frac{6\, k_o \exp(-\gamma)}{D_p} \qquad (1.9)$$

and t_o is the minimum time for oxygen to reach the chimney entrance, given by:

$$t_o = \frac{2\, \pi\, R_c}{3\, u_o} \qquad (1.10)$$

It can be seen that the amount of oxygen depletion outside the chimney will be larger for longer beds, since t_o will be larger. In the limit of an infinitely long bed, no oxygen will reach the entrance of the chimney, and thus no ignition will occur. It appeared from calculations that the bed has to be very long before this occurs.

The amount of oxygen depletion will also be larger for finer particles, since u_o will be smaller and k larger. This phenomenon may be seen in Figure 1.5; for small particle sizes the ignition points do not show the trend expected from equation (1.7). However we observe that the ignition point as calculated from equation (1.7) is a conservative bound on the particle size at ignition, i.e. it predicts that the ignition occurs for some particle size larger than that calculated from the extended model. This would be expected in view of the simplifying assumptions made in the derivation of equation (1.7).

The model exhibits somewhat different behaviour on the ignited branch, in that there exists a maximum bed temperature as a function of the depth of the chimney. This "worst-depth" comes about due to the balance between heat loss to the surface, which is large for small depths, and oxygen depletion, which is large for large depths. This worst depth is typically of the order of a few metres, which accords with the observation that the hot-spot in a stockpile is often reasonably close to the surface.

From this review it is clear that the particle size at ignition is a vital parameter and that an expression like Eq. (1.7) applicable to a more realistic geometry would be invaluable to the practitioner. The remainder of this thesis is devoted to developing such expressions.

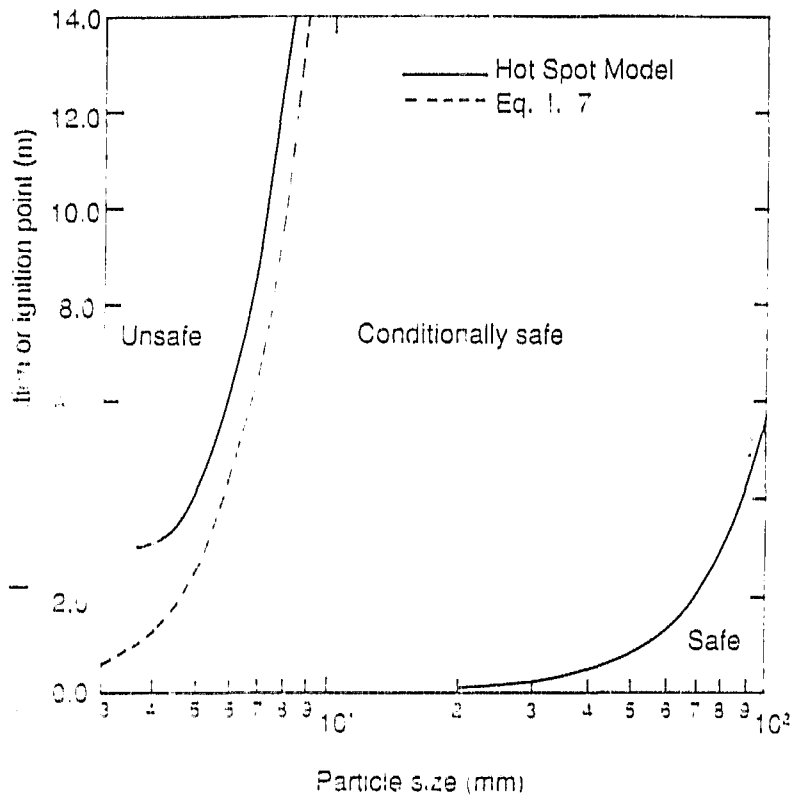

Figure 1.5 Ignition points calculated from the simplified three-dimensional model and Eq. (1.7) for the base case parameters

CHAPTER 2

NUMERICAL SOLUTION OF SMALL COAL STOCKPILE MODELS

2.1 Statement of problem and model formulation

This chapter is concerned with the numerical solution of more realistic models of spontaneous combustion than those developed by Brooks and Glasser,1986, Young et al.,1986 and Brooks et al.,1988b. The behaviour of small coal stockpiles is examined, and particular attention given to confirming the predictions of the one-dimensional model of Brooks and Glasser,1986 and developing and testing simple criteria for ignition points, particularly Eq. (1.7) (Brooks et al.,1988a). Models are considered for which the coal stockpiles have geometries similar to those that might be found in practice, and for which the natural convection flow patterns are predominantly unicellular. The models are restricted in this way because numerical solution of the model equations for stockpiles which show Benard-like convection cells requires a three-dimensional formulation and very fine discretization of the differential equations. Such a model would require more computer power than was available in this study. In Chapter 3 the question is addressed of how the interior of a coal bed may be modelled using a different approximate analysis.

A right frustum was chosen as being a suitable geometry for the numerical investigation of ignition points in small coal beds. The frustum closely approximates the shape of the coal stockpile that would be formed if the coal was thrown from a stacker and is very similar to the shape of instrumented test heaps that have been constructed at a coal mine in South Africa. If radial symmetry is assumed, the three-dimensional stockpile can be modelled with a two-dimensional mathematical formulation. It can be argued that the assumption of radial symmetry imposes a symmetry on the problem that is not felt in reality, however provided that the frustum is not so large that the flow pattern breaks down into Benard-like cells the assumption is probably good. For cases when the flow does show a cellular structure, if the diameter of the frustum is sufficiently large the toroidal shape of the outside Benard-like convection cells approximates two-dimensional roll cells. Such roll cells are known to be a stable planform in natural convection (Chandrasekhar,1961, Tveitereid,1977). The central cell can be considered to be an approximation to a hexagonal cell, and such cells are known to be

formed in porous media (Tveitereid,1977). This subject receives a thorough discussion in section 2.5. To make the simulations more general, the sloping edge of a large coal bed is modelled, by using Cartesian coordinates and assuming that the bed is infinitely long in one of the horizontal dimensions. As in the case of the frustum, the situation is considered where the flow pattern is predominantly unicellular. When the flow breaks down into cells in this edge model, the internal flow cells correspond to two-dimensional roll cells and thus have physical meaning. A comparison between this model and the frustum highlights the differences between the two situations and indicates how ignition points can be calculated both in small frustum-shaped stockpiles and at the edges of very large ones. A direct numerical solution of a truly three-dimensional model of a coal stockpile was not possible because of limitations on computer power. Such a study would almost certainly require array processing facilities which were not available for this work.

In addition to their added dimensionality, the models described in this chapter have fewer simplifying assumptions than those of Brooks and Glasser,1986, Young et al.,1986 and Brooks et al ,1988b. Reaction is considered to occur throughout the coal bed, rather than at a hot spot as considered by Young et al.,1986, and the rate of reaction is considered to be a function of both temperature and concentration, rather than being evaluated at an average temperature as was done by Brooks and Glasser,1986. No assumptions are made about special flow and heat transfer regions as was done by Brooks et al.,1988b, and molecular diffusion of oxygen was allowed for.

2.1.1 Model formulation

We commence the formulation of the model with a discussion of the assumptions made in the derivation of the governing equations. These assumptions have been thoroughly discussed and justified by Brooks,1986 and here only an overview is presented. The coal supply is assumed to be infinite because the time constant for complete coal oxidation is much larger than that for heat transfer. It is assumed that the reactant gas, which is air, and any product gases have the same physical properties and that the gas is incompressible. The velocities are known to be very low in coal beds justifying the use of the Darcy Law. In the Darcy Law, the permeability is calculated from the Blake-Kozeny equation (Bird et al.,1960). Because heat transfer is by far the slowest process occurring in the bed it is necessary to consider only the energy balance in unsteady-state form. In practice

it turns out to be extremely difficult to solve the model in unsteady-state form if this assumption is not made, as the governing equations are extremely stiff. It is assumed that the gas and solid are in thermal equilibrium and that effective continuum properties can be used. This continuum assumption has been frequently used in the literature e.g. Beukema et al.,1983, Viljoen et al.,1988, and is thoroughly discussed by Brooks,1986. (Of interest is the result of Chan and Banerjee,1981 in which they considered a horizontal porous layer of spherical glass beads saturated with water bounded by isothermal horizontal walls heated from below and with adiabatic vertical walls. The authors found that a model accounting for solid-fluid heat transfer gave better agreement with experimental results than did a continuum model). Inertial effects are neglected, as is the very small effect of viscous heating. The Boussinesq approximation is used so that buoyancy effects are included only in the body force term. Buoyancy effects are modelled by a thermal expansion coefficient approach which is different from that used by Brooks et al.,1988a. This does not really pose a problem as the two approximations are essentially the same for temperatures close to ambient which is where all solutions are sought. Moisture adsorption effects are neglected and according to the results of Schmal et al.,1985 this will have the effect of predicting higher reaction rates, thus giving conservative results.

The reaction rate is assumed to be linear with respect to oxygen partial pressure and reaction is assumed to occur only on the surface of the coal particles. The reaction rate expression is identical to Eq. (1.4). The coal particles are assumed to be spherical and of uniform size. This means that size segregation in the bed has not been considered. It is known that the segregation that occurs when non-uniformly sized material is thrown from a stacker makes coal beds more liable to spontaneous combustion. This is because the coal bed has a core of very fine reactive material, surrounded by an outer region of coarse material through which oxygen can easily pass to reach the reactive core. The energy liberated in this core due to the oxidation of the coal cannot readily be transported to the surface and dissipated to the atmosphere, because of the very good insulating properties of the surrounding coal layer. The finite element program which is used to solve the governing equations and is described in section 2.3 has the facility of being able to incorporate coal bed properties that are a function of position in the bed. In principle it would be possible to model the effect of particle size segregation. The effect of ageing is not included, but as it is known that the

reactivity of coal decreases with age it is expected that this will make the results conservative. Further discussion of the model derivation is given by Young,1985 and Brooks,1986.

The continuity equation and momentum, energy and species balance equations are:

Continuity equation

$$\nabla \cdot \rho \ \underset{\sim}{U} = 0 \tag{2.1}$$

Momentum balance

$$- \nabla P - \frac{\mu \underset{\sim}{U}}{\kappa} + \rho_a g (1 - \eta(T - T_a)) = 0 \tag{2.2}$$

Energy balance

$$(1 - \epsilon) \frac{\partial T}{\partial t} (\rho \ c_p)_s = k_e \nabla^2 T - (\rho \ c_p)_g \underset{\sim}{U} \cdot \nabla T + r_a (-\Delta H) \tag{2.3}$$

Concentration balance

$$0 = \epsilon D \nabla^2 C - \underset{\sim}{U} \cdot \nabla C - r_a \tag{2.4}$$

All symbols are defined in the nomenclature.

The model is completed by the addition of suitable boundary conditions. It is assumed that on the free surface of the coal bed the oxygen concentration will be ambient at points where air is flowing into the bed, while for points at which gas is flowing out of the bed there is zero gradient of concentration in the outward normal direction. Along the bottom of the stockpile it is assumed that the outward normal gradient of concentration is zero, and because only half of the frustum need be considered through symmetry considerations a similar condition is imposed on the bed centreline. The temperature boundary condition along the free surface of the bed is modelled by a heat transfer coefficient for regions of gas outflow and by a heat transfer coefficient and a term accounting for cooling due to inflow of ambient air for regions where the gas enters the bed. It is found in real coal beds that the temperature is almost ambient on the surface, and in the numerical simulations it has been found that the model with the above boundary conditions does in fact predict almost ambient conditions on the bed surface. Along the bottom of the bed it is assumed that the temperature is ambient as there is no available estimate of the heat transfer coefficient there. On the bed centreline there is no heat flux. The value of the heat transfer

coefficient on the free surface was fitted from experimental data (Anderson,1987). Because the model is to be written in terms of a stream function as discussed below, the specification of the flow boundary condition is left until the model has been presented in stream function form. The boundary conditions for the symmetrical half of the domain can be stated:

On the bed centreline (0,Z):

$$\frac{\partial T}{\partial n} = 0 \ , \ \frac{\partial C}{\partial n} = 0 \qquad (2.5a)$$

On the bottom surface:

$$T = T_a \ , \ \frac{\partial C}{\partial n} = 0 \qquad (2.5b)$$

On the free surface:

Outflow:
$$k_e \frac{\partial T}{\partial n} = -h \ (T - T_a) \ , \ \frac{\partial C}{\partial n} = 0 \qquad (2.5c)$$

Inflow:
$$k_e \frac{\partial T}{\partial n} = - \ (h + \rho_a \ v_n \ c_p) \ (T - T_a) \ , \ C = C_a \qquad (2.5d)$$

By defining suitable characteristic dimensions Eqs. (2.1)-(2.5) can be made dimensionless, which has many advantages. In dimensionless form the equations contain a number of dimensionless groups which are the natural parameters of the model and provide a means of comparison for different situations on the basis of dimensionless groups. In addition, if the problem is correctly scaled, the accuracy of the solution can be improved e.g. Markatos and Pericleous,1984, found that solution of the governing equations for a model of laminar and turbulent convection in a square cavity by a finite domain method in dimensionless form increased the accuracy by 3% compared to the dimensional solution. The scale analysis of Bejan, (Bejan,1981, Bejan and Khair,1985, Poulikakos and Bejan,1984) provides one method for the selection of suitable scaling factors. Dimensionless groups such as the Rayleigh number (Ra) or Peclet number (Pe) can also be used conveniently to classify various flow situations.

The following dimensionless variables were used:

$$r = \frac{r^*}{H} \qquad (2.6a)$$

$$z = \frac{Z}{H} \tag{2.6b}$$

$$u_r = U_r \,/\, (\alpha \,/\, H) \tag{2.6c}$$

$$u_z = U_z \,/\, (\alpha \,/\, H) \tag{2.6d}$$

$$\theta = (T - T_a) \,/\, T_a \tag{2.6e}$$

$$\Pi = \frac{P}{\alpha \mu \,/\, \kappa} + \frac{\rho g z}{\alpha \mu \,/\, \kappa} \tag{2.6f}$$

$$Y = \frac{C M \,/\, \rho_a}{Y_a'} \tag{2.6g}$$

Where H is the characteristic length of the coal bed defined as the height of the bed.

The dimensionless Darcy-Oberbeck-Boussinesq equations defining the model are:

$$\nabla \cdot \underline{u} = 0 \tag{2.7}$$

$$\nabla \Pi + \underline{u} - Ra \quad \theta \, \hat{z} = 0 \tag{2.8}$$

$$\varphi \frac{\partial \theta}{\partial \tau} + \underline{u} \cdot \nabla \theta = \nabla^2 \theta + \beta \varphi_h^2 \exp \left\{ \frac{\gamma \theta}{1 + \theta} \right\} Y \tag{2.9}$$

$$0 = Le \nabla^2 Y - \underline{u} \cdot \nabla Y - \varphi_h^2 \exp \left\{ \frac{\gamma \theta}{1 + \theta} \right\} Y \tag{2.10}$$

Eqs. (2.7)-(2.10) can be simplified even further by the introduction of a stream function ψ, which automatically satisfies the continuity equation:

$$v_r = \left(\frac{1}{r} \right)^c \frac{\partial \psi}{\partial z} \tag{2.11a}$$

$$v_z = - \left(\frac{1}{z} \right)^c \frac{\partial \psi}{\partial r} \tag{2.11b}$$

Where c = 0 for Cartesian coordinates

c = 1 for cylindrical coordinates

Taking the curl of the momentum balance equation eliminates pressure, and substitution of the stream function replaces the two components of velocity $\underline{u}$ by ψ. The stream function formulation is useful in that it allows easy flow visualisation and reduces the number of variables.

The dimensionless equations describing the processes occurring in the frustum-shaped coal bed, assuming radial symmetry, become:

Stream function equation:

$$r \frac{\partial}{\partial r}\left(\frac{1}{r}\frac{\partial \psi}{\partial r}\right) + \frac{\partial^2 \psi}{\partial z^2} = -r\,Ra\,\frac{\partial \theta}{\partial r} \qquad (2.12)$$

Energy balance:

$$\frac{1}{r}\frac{\partial \psi}{\partial z}\frac{\partial \theta}{\partial r} - \frac{1}{r}\frac{\partial \psi}{\partial r}\frac{\partial \theta}{\partial z} = \frac{1}{r}\frac{\partial}{\partial r}\left(r\frac{\partial \theta}{\partial r}\right) + \frac{\partial^2 \theta}{\partial z^2} + \beta\,\varphi_h^2 \exp\left(\frac{\gamma\,\theta}{1+\theta}\right) Y \qquad (2.13)$$

Oxygen mole fraction:

$$\frac{1}{r}\frac{\partial \psi}{\partial z}\frac{\partial Y}{\partial r} - \frac{1}{r}\frac{\partial \psi}{\partial r}\frac{\partial Y}{\partial z} = Le\left\{\frac{1}{r}\frac{\partial}{\partial r}\left(r\frac{\partial Y}{\partial r}\right) + \frac{\partial^2 Y}{\partial z^2}\right\} - \varphi_h^2 \exp\left(\frac{\gamma\,\theta}{1+\theta}\right) Y \qquad (2.14)$$

The dimensionless equations ...ie processes occurring in the trapezoidal-shaped coal bed, in ...mensional Cartesian coordinates become:

Stream function equation:

$$\frac{\partial^2 \psi}{\partial^2 r} + \frac{\partial^2 \psi}{\partial^2 z} = -\,Ra\,\frac{\partial \theta}{\partial r} \qquad (2.15)$$

Energy balance:

$$\frac{\partial \psi}{\partial z}\frac{\partial \theta}{\partial r} - \frac{\partial \psi}{\partial r}\frac{\partial \theta}{\partial z} = \frac{\partial^2 \theta}{\partial r^2} + \frac{\partial^2 \theta}{\partial z^2} + \beta\,\varphi_h^2 \exp\left(\frac{\gamma\,\theta}{1+\theta}\right) Y \qquad (2.16)$$

Oxygen mole fraction:

$$\frac{\partial \psi}{\partial z}\frac{\partial Y}{\partial r} - \frac{\partial \psi}{\partial r}\frac{\partial Y}{\partial z} = Le\left\{\frac{\partial^2 \theta}{\partial r^2} + \frac{\partial^2 Y}{\partial z^2}\right\} - \varphi_h^2 \exp\left(\frac{\gamma\,\theta}{1+\theta}\right) Y \qquad (2.17)$$

Taking the curl of the momentum balance equation eliminates pressure, and substitution of the stream function replaces the two components of velocity $\underline{u}$ by ψ. The stream function formulation is useful in that it allows easy flow visualisation and reduces the number of variables.

The dimensionless equations describing the processes occurring in the frustum-shaped coal bed, assuming radial symmetry, become:

Stream function equation:

$$r \frac{\partial}{\partial r}\left(\frac{1}{r}\frac{\partial \psi}{\partial r}\right) + \frac{\partial^2 \psi}{\partial z^2} = -r\ Ra\ \frac{\partial \theta}{\partial r} \qquad (2.12)$$

Energy balance:

$$\frac{1}{r}\frac{\partial \psi}{\partial z}\frac{\partial \theta}{\partial r} - \frac{1}{r}\frac{\partial \psi}{\partial r}\frac{\partial \theta}{\partial z} = \frac{1}{r}\frac{\partial}{\partial r}\left(r\frac{\partial \theta}{\partial r}\right) + \frac{\partial^2 \theta}{\partial z^2} + \beta\ \varphi_h^2 \exp\left(\frac{\gamma\ \theta}{1+\theta}\right) Y \qquad (2.13)$$

Oxygen mole fraction:

$$\frac{1}{r}\frac{\partial \psi}{\partial z}\frac{\partial Y}{\partial r} - \frac{1}{r}\frac{\partial \psi}{\partial r}\frac{\partial Y}{\partial z} = Le\left\{\frac{1}{r}\frac{\partial}{\partial r}\left(r\frac{\partial Y}{\partial r}\right) + \frac{\partial^2 Y}{\partial z^2}\right\} - \varphi_h^2 \exp\left(\frac{\gamma\ \theta}{1+\theta}\right) Y \qquad (2.14)$$

The dimensionless equations describing the processes occurring in the trapezoidal-shaped coal bed, in two-dimensional Cartesian coordinates become:

Stream function equation:

$$\frac{\partial^2 \psi}{\partial^2 r} + \frac{\partial^2 \psi}{\partial^2 z} = -\ Ra\ \frac{\partial \theta}{\partial r} \qquad (2.15)$$

Energy balance:

$$\frac{\partial \psi}{\partial z}\frac{\partial \theta}{\partial r} - \frac{\partial \psi}{\partial r}\frac{\partial \theta}{\partial z} = \frac{\partial^2 \theta}{\partial r^2} + \frac{\partial^2 \theta}{\partial z^2} + \beta\ \varphi_h^2 \exp\left(\frac{\gamma\ \theta}{1+\theta}\right) Y \qquad (2.16)$$

Oxygen mole fraction:

$$\frac{\partial \psi}{\partial z}\frac{\partial Y}{\partial r} - \frac{\partial \psi}{\partial r}\frac{\partial Y}{\partial z} = Le\left\{\frac{\partial^2 \theta}{\partial r^2} + \frac{\partial^2 Y}{\partial z^2}\right\} - \varphi_h^2 \exp\left(\frac{\gamma\ \theta}{1+\theta}\right) Y \qquad (2.17)$$

The model is completed by the addition of boundary conditions for Y, θ and ψ. The boundary conditions for oxygen concentration and temperature have already been discussed and can be stated immediately. The stream function ψ must be normal to the free surfaces and equal to an arbitrary constant along the bottom of the bed and on the bed centreline. The geometry of the frustum (or the sloping edge model) can be described in terms the characteristic length H and two geometric parameters A and B, which are defined in Eqs. (2.19g) and (2.19h) below. The boundary conditions may also be formally specified in terms of these geometric parameters, rather than in terms of outward normal derivatives. However the situation is more clearly understood from Figure 2.1, in which all the boundary conditions are

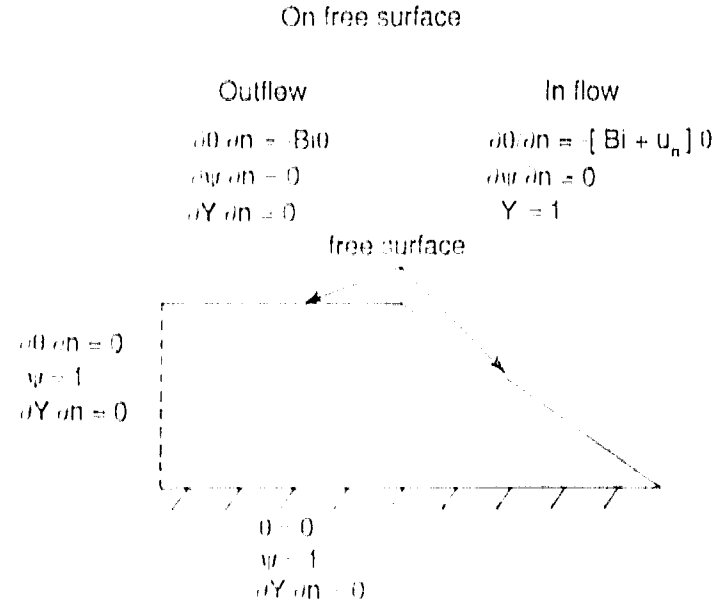

Figure 2.1 Boundary conditions and computational domain for the small stockpile model

shown. As an example of how the boundary conditions may be specified in terms of the geometric parameters the temperature boundary condition for regions of outflow is written in terms of A and B:

$$A \frac{\partial \theta}{\partial z} + B \frac{\partial \theta}{\partial r} = \left(A^2 + B^2 \right)^{0.5} Bi\ \theta \qquad (2.18)$$

For the region

$$R - AR \leq r \leq R$$

$$0 \leq z \leq BR$$

This boundary condition is derived in Appendix C.

It can be seen that the model contains the following 8 parameters

$$Le = \frac{\epsilon D \rho_a c_p}{k_e} \tag{2.19a}$$

$$\gamma = \frac{E}{R_g T_a} \tag{2.19b}$$

$$\beta = \frac{(-\Delta H)}{M T_a c_p} \tag{2.19c}$$

$$Bi = \frac{h H}{k_e} \tag{2.19d}$$

$$Ra = \frac{\rho_a^2 g c_p H D_p^2 \epsilon^3 T_a \eta}{150 \mu k_e (1 - \epsilon)^2} = Ra_L \eta T_a \tag{2.19e}$$

$$\varphi_h^2 = \frac{6 k_o \rho_a (1-\epsilon) H^2 c_p \exp(-\gamma)}{k_e D_p} \tag{2.19f}$$

$$A = \frac{R - R_{top}}{R} \tag{2.19g}$$

$$B = \frac{H}{R} \tag{2.19h}$$

Following the approach of Brooks et al.,1988a, it can be shown that the problem possesses 5 characteristic times, and that each of the parameters Ra, Bi, Le and φ_h^2 may be represented as the ratio of two of these characteristic times:

$$t_\lambda = \frac{H^2 \rho c_p}{k_e} \quad \text{time for conduction} \tag{2.20a}$$

$$t_c = \frac{\mu H}{\rho_a \kappa} \quad \text{time for convection} \tag{2.20b}$$

$$t_g = \frac{\rho D_p}{k(T_a) (1 - \epsilon) M} \quad \text{time for generation} \tag{2.20c}$$

$$t_r = \frac{\rho\, c_p\, H}{h} \quad \text{time for heat loss from surface} \qquad (2.20d)$$

$$t_d = \frac{H^2}{\epsilon\, \bar{D}} \quad \text{time for diffusion of species} \qquad (2.20e)$$

This allows one to write

$$Ra = \frac{t_\lambda\, \eta\, T_a}{t_c}\,, \quad Bi = \frac{t_\lambda}{t_c}\,, \quad \varphi_h^2 = \frac{t_\lambda}{t_g}\,, \quad Le = \frac{t_\lambda}{t_d} \qquad (2.20f)$$

Limiting behaviour of the model is obtained when one of the characteristic times is very much smaller or larger than the rest. In such cases it will be possible to simplify the model by neglecting some terms. Examination of the typical parameter values given in Appendix A shows that the characteristic time for thermal conduction, t_λ is very large, which implies that a typical coal bed is convection-dominated. For non-limiting cases, i.e. cases for which none of the terms can be neglected with respect to any of the others, only numerical solution of equations (2.7)-(2.10) is possible. Note that Ra defined by Eq. (2.19e) is slightly different to Ra_L used by Brooks et al.,1988a. This difference arises due to the different assumption on the buoyancy. Because the main interest lies in solutions to the equations in which the temperature rise is not great, the product $(\eta T_a) \approx 1.07$, and to the accuracy required by the practitioner it will be seen that this small difference will have no appreciable effect on the ignition criteria which will be developed.

2.2 Brief review of numerical methods for natural and forced convection problems

There is a paucity of literature on the modelling of spontaneous combustion, while there is extensive coverage given to modelling of combined natural convection and conduction in porous media. Some of this literature contains useful information on numerical solution techniques and there is also a wealth of literature devoted specifically to numerical techniques for the solution of such equations. Modelling of the processes occurring in a coal bed is a much more difficult task than simply modelling natural convection in a porous medium, because in addition to the usual problems of numerical stability and computational efficiency there are bifurcations in the solution space and severe stiffness problems. The problem is complicated by the presence of ignition points, and the complex

temporal and spatial structures that are known to occur in porous media with internal heat generation (Lennie et al.,1988, Kimura et al.,1987).

Convection problems such as those defined by Eqs. (2.7)-(2.10) are usually solved by either the finite difference method or the finite element method. There are other techniques available for the solution of non-linear elliptic partial differential equations, e.g. the method of lines, which was used by Brooks,1986 to solve his system of ordinary differential equations and spectral methods (Kimura et al.,1986). Such methods are more suited to idealised domains such as squares and circles or ones for which there exist mappings to simpler regions. The method of lines is attractive when compared to finite difference or finite element methods in that the computer storage requirements are generally much smaller, but the method is very difficult to apply for regions with comple geometry as would be encountered in modelling the spontaneous combustion of c al beds for example.

2.2.1 The finite difference method

The finite difference method is the most well-known method for the numerical solution of systems of elliptic or parabolic partial differ ntial equations. The essence of the method is to divide the computational domain into an array of grid points. At each grid point the differential operator is expressed by a difference formula in terms of the values of the field variables at neighbouring grid points. This results in a system of non-linear algebraic equations which must then be solved by some iterative method. Methods such as the ADI (alternating direction implicit) method result in a system of equations which forms a tridiagonal matrix, with great advantages in terms of storage and computational speed. In spite of the well-developed state of the finite difference method, there are several disadvantages to its use for the modelling of spontaneous combustion. In particular it is difficult to formulate finite difference schemes to allow for graded meshes. Such graded meshes may well be required in certain regions of the computational domain when there are very sharp gradients, e.g. the extremely steep gradients in oxygen concentration which occur in a boundary layer at the surface of a coal bed containing very small coal particles. The inclusion of complex boundary conditions, such as those shown in figure 2.1, is difficult with the finite difference method.

2.2.2 The finite element method

The finite element method is implemented by dividing the computational domain into a number of discrete elements and approximating the field variables within each element by low order polynomials termed the shape functions. The entire domain is modelled by combining the equations for each of the elements into a large system of simultaneous non-linear algebraic equations. This is better understood from a more formal mathematical description.

Consider a one-dimensional differential operator L(u) on [a,b]:

$$L(u) = 0 \tag{2.21}$$

The function u can be approximated in a weighted residual sense as:

$$u(x) \approx u^*(x) = \sum_{j=1}^{n} \varphi_j(x)\, c_j \tag{2.22}$$

The φ_j are continuous and satisfy the boundary conditions. In general substitution of (2.21) into (2.22) gives a non-zero residual R(x):

$$L(u^*) = R(x) \tag{2.23}$$

The Galerkin form of the weighted residual method requires that the weighted average of the residual vanish on the domain of the differential equations and that the weighting function be the same as the trial function:

$$\int_\Omega \varphi_j(x)\, R(x)\, dx = 0 \tag{2.24}$$

In the finite element method the domain Ω is divided into a number of subdomains termed elements, and the Galerkin process is applied to each of these elements. This process results in a matrix equation for each element:

$$K_e \underset{\sim}{u} - \underset{\sim}{F}_e = 0 \tag{2.25}$$

Where the subscript e refers to an element, K is the element stiffness matrix, and $\underset{\sim}{F}$ is the vector forcing function. In order to solve the problem on the entire domain each of the element matrix equations is combined in a single matrix equation:

$$K \underset{\sim}{u} = \underset{\sim}{F} \tag{2.26}$$

The system stiffness matrix K is generally banded. The finite element method is well-described in many texts, and further details

can be found in e.g. Norrie and De Vries,1983, Carey and Oden,1986 and Akin,1982.

2.2.3 Review of the literature

The brief review that follows gives an indication of some of the methods that have been used to model natural and forced convection. A review of this nature is obviously selective as the amount of material published in this field is enormous. The selection of a solution method for use in this study was based on this literature review.

McDonald, 1979, has presented an extensive review of the numerical considerations involved in combustion modelling, with particular reference to furnace applications. Many of the points discussed are of relevance to the modelling of spontaneous combustion in coal beds. McDonald considered that, of the two most popular numerical methods for the solution of combustion problems, finite difference methods were more advanced than finite element methods and that the matrix inversion problems resulting from a finite element method are in many cases identical to those arising from finite difference schemes. For systems of coupled non-linear equations, such as that defined by Eqs. (2.7)-(2.10), Picard iteration allows the equations to be treated independently but McDonald felt that many iterations may be required for large systems and that the block implicit approach may be preferable. In a discussion of the convergence properties of various algorithms McDonald demonstrated how "simple schemes" show poor convergence when compared to more advanced schemes (such as the alternating-direction implicit -ADI- method) when the mesh is increasingly refined. Such mesh refinement can be necessary to resolve the steep gradients that can occur in boundary layers, for example. However it was also shown that local mesh refinement can lead to a deterioration of performance of certain schemes when compared to their uniform mesh convergence properties. However, McDonald stated that it is usually possible to devise schemes to converge adequately on locally refined meshes.

It is known that in the one-dimensional convection-diffusion equation oscillatory solutions are obtained with second order finite difference approximations for cell Reynolds numbers (or Peclet numbers) greater than a critical value. This problem has been overcome in the past by the introduction of an artificial viscosity in a technique termed upwinding. The use of upwinding to improve the stability of schemes for the solution of the convection-diffusion equation has received

much attention as this is obviously a crucial point in convection modelling.

Spalding, 1972, developed a new finite difference scheme for the one-dimensional convection-diffusion equation. He showed that the conventional central difference formulation was considerably in error when compared to the exact solution for $|Pe| \geq 2$. The Peclet number Pe is defined

$$Pe = (c_p\ G\ L)/k_e$$

where G is the mass flow rate.

The conventional upwind formulation (one in which the fluid crossing an interface possesses a temperature equal to the temperature at the last grid point that the fluid crossed) is less accurate than the central difference formulation for $|Pe| \leq 2$. Spalding proposed two schemes. The first was a difference expression for temperature based on the exact solution for the one-dimensional equation (later referred to as exponential differencing). He also proposed a scheme which was a mixture of central differencing for Pe>2 and upwind differencing elsewhere. Runchal, 1972, examined this last scheme, central and upwind differencing for a model two-dimensional problem. He concluded that for Pe>2 only the Spalding and upwind schemes were stable and that the Spalding scheme was more accurate in this region. Young,1985 used Spalding differencing in a finite difference solution of his two-dimensional model of spontaneous combustion. Schulenberg and Muller,1984 used exponential differencing for the spatial derivatives in a study of porous medium convection. Shiralkar and Tien,1981 also used exponential differences in a finite difference solution of heat transfer in shallow enclosures.

Conventional upwinding has frequently been used in convection-diffusion modelling. Heinrich and Zienkiewicz,1977 described an upwinding scheme for the finite element method which they claimed to be accurate and to reduce oscillations for a number of test problems in which convection was dominant. However for an entry flow problem they imposed a boundary layer on the outlet flow (hence a region of large gradients) and then distributed a mesh with the largest elements at the outlet. This appears to be a self-defeating method. Prasad and Kulacki,1984, in a study of curvature effects on heat transfer, used a difference technique in which a grid was set up on the domain and the equations integrated over a finite area micro cell around each node. This method gives rise to upwind differences

for the convection terms. Markatos and Pericleous,1984 used a similar method to study turbulent and laminar natural convection in a cavity. Markatos and Pericleous considered that only mesh refinenment can detect the false difiusion introduced by upwinding, and that by obtaining grid-independent results false diffusion could be eliminated. Chan and Banerjee,1981 analysed three-dimensional natural convection in porous media using a marker-and-cell technique. The domain was discretized into cells of size ($\Delta x, \Delta y, \Delta z$) with centres (i,j,k). Chan and Banerjee used a method termed local error truncation to reduce diffusional truncation errors, and controlled the amount of upwinding after cancellation of low order diffusion truncation errors.

If significant flow gradients exist then the artificial viscosity introduced by upwinding may produce unwarranted numerical diffusion and it is not certain that from different initial guesses the same iteration path will lead to the same final solution (McDonald,1979). McDonald recommended the use of an artificial viscosity based on the rate of change of some gradient of flow scaled by the square or some higher power of the mesh to retain the formal order accuracy of the finite difference scheme and selectively damp the high frequency oscillations. Mesh refinement is an attractive alternative to upwinding but is subject to convergence problems and with the additional problem that the region requiring refinement is not known *a priori*. In general global mesh refinement may be prohibitively expensive and adaptive mesh refinement is a possible alternative.

Acharya and Patankar,1985, have described such an adaptive grid procedure for parabolic flows. In this technique the distribution of nodal points is adjusted in response to the computed solution. In this way regions in which there are large gradients or curvature effects are supplied with an abundance of nodal points. Carey and Plover,1983, have described a variable upwinding finite element formulation which can be used in conjunction with adaptive mesh refinement. They felt that use of a fixed upwinding parameter with mesh size reduction leads to convergence to a solution of the wrong problem. Carey and Plover felt that when local mesh refinement is used the upwinding parameter should be a function of the mesh size. Local mesh refinement was achieved by monitoring and reducing local residuals and introducing a local upwinding parameter that tended to zero as the mesh became increasingly refined. Gartling and Becker,1977 discuss rezoning in regions of sharp gradients for the finite element method.

Lillington and Shepherd,1978 discussed the effect of various boundary conditions and heat source profiles on the nature of solutions to the two-dimensional heat transport equation obtained by central difference approximations. Upwinding was felt to be inappropriate when recirculation was present because false diffusion resulting from the upwinding persists in this scheme. It was found that oscillations in solutions were dependent on the boundary conditions, the heat source profile and the parity of the mesh intervals. For fixed inlet and outlet conditions as $Pe \rightarrow \infty$ (i.e. as the problem becomes completely convection dominated) the solution was unbounded and oscillatory when the mesh parity was even. Lillington and Shepherd found a better approach was the specification of an inlet condition and neglection of diffusion at the outlet.

Smith,1980, performed a similar analysis to that of Lillington and Shepherd,1978 for upwind finite differences, central finite differences, linear finite elements and quadratic finite elements. He found that the first method was always stable while the latter three could all give oscillatory solutions depending on the mesh Peclet number, the boundary conditions, the source profile, the mesh parity and the numerical scheme. Smith concluded that oscillatory solutions could be avoided or reduced by the use of boundary conditions with specified outlet gradients (as opposed to a fixed temperature) and that finite element methods reduced or eliminated non-physical oscillations when compared to finite difference schemes. This is a strong argument for the use of the finite element method.

Gresho and Lee,1981, felt that *a priori* damping (i.e. upwinding) of solutions was inadvisable because oscillatory solutions provide a useful signal that the numerical scheme is not suitable for the physics of the problem at hand, in particular that the mesh size should be locally refined. They also stated that the use of upwinding can lead to the solution of a different problem.

Donea,1984, developed a method to improve the stability properties of a finite element method for convective transport problems. The time derivative was discretized by a Taylor expansion while the spatial derivative was left in continuous form. This equation was then approximated by conventional finite element methods. This technique was claimed to give more accurate and stable results, and did not produce unwanted dissipation, unlike upwinding. The method was applied to one or more space dimensions but development would be required for

application to combined convection-diffusion.

It seems that the finite element method is a good way of reducing the problems of numerical stability that are associated with solving convection-diffusion problems, and that by using the finite element method there is likely to be little need to use the so-called upwind method. There is strong evidence that the upwind method can lead to the solution of the wrong problem in certain cases, and it seems far better not to use the method if possible.

There is also some evidence that finite element methods are superior to finite difference methods in terms of computational speed. Havstad and Burns,1982 studied natural convection in a vertical annulus, and solved the governing equations using a finite difference method. Hickox and Gartling, 1985, also studied natural convection in a vertical, annular porous layer. Numerical solutions to the coupled dimensionless equations in pressure and temperature were obtained by a Galerkin finite element method. It is interesting that the equations were solved in primitive variable form rather than in terms of a stream function. (Gartling and Becker, 1976, state that the introduction of a stream function (or stream function and vorticity) which is done in finite difference schemes to avoid the need to satisfy the continuity equation is unnecessary in a finite element method). For temperature and pressure quadratic basis functions were used, while linear functions were used for the velocity field. A 10 x 20 mesh with eight-node quadrilateral elements was used. The steady-state solution was obtained by Picard iteration. The mesh was uniformly graded in the radial direction but graded vertically to accommodate the expected steep gradients near the upper and lower boundaries. The results obtained agreed well with those of Prasad and Kulacki, 1984 and Havstad and Burns, 1982 but the number of iterations required for convergence appeared to be considerably less than the number required by Havstad and Burns, 1982 who were limited by the cost of their numerical procedure. This result points to the possible superiority of finite element methods over finite difference methods in terms of computational speed.

Several works in the literature have considered natural convection with internal heat sources; these studies are the closest to the spontaneous combustion modelling considered in this thesis. Saatdjian and Caltagirone, 1980 studied natural convection in a porous layer under the influence of an exothermic decomposition reaction. They considered a two-dimensional porous medium saturated with a gas. As

the lower boundary temperature increased the matrix decomposed exothermically to give gaseous products considered to be the same as the saturating fluid. The decomposition reaction was considered to be a single reaction with Arrhenius temperature dependence. The equations were approximated by finite differences and solved using an algorithm in which both implicit and explicit procedures were used. Because explicit procedures were used the time step in the solution of the unsteady-state problem was limited to ensure numerical stability. The spatial discretization was performed on a 17 x 17 grid. Overall mass and energy balances showed that the temporal and spatial discretizations were reasonable.

Beukema et al.,1983, studied the influence of three-dimensional natural convection on cooling rates and temperature distributions in stored agricultural products. Heat generation was modelled as a uniform source term in the equation of energy. The system of three governing equations was reduced to one elliptic and one parabolic equation by the introduction of the vector potential and vorticity and the elimination of pressure. Heat transfer at the walls was described by overall heat transfer coefficients which accounted for the influence of both internal and external coefficients and conduction through the walls. Values for the heat transfer coefficients were obtained by a comparison of experimental and model results for different sets of values of the heat transfer coefficients. The use of heat transfer coefficients on the boundaries is of interest, as the most common approach in the literature is to specify either the boundary temperature or the temperature gradient along the outward normal to the boundary. The equations were approximated by finite difference discretizations with backward differences used for the time derivatives, central differences for the conduction terms and upwind differences used for the convection terms. This was done to ensure stability of the procedure. Beukema et al.,1983 did not mention the possibility of the introduction of artifical diffusion by the use of this technique. An unconditionally stable Crank-Nicholson scheme was chosen for the time integration. The iterative solution of the simultaneous equations was done by successive over-relaxation.

Handa et al.,1983 examined the spontaneous combustion of coal in a two-dimensional trapezoidal coal bed. The coal oxidation was modelled as a two-step process. Surprisingly the Darcy Law was not used in the momentum equations, and in the term accounting for viscous forces the viscosity of air was used, which is incorrect. The equations were solved using a finite difference scheme with upwind differencing for

the convective terms. The flow patterns in the trapezoid showed interesting development with time, although in one case two cells with the same direction of rotation were shown, a situation which is highly unlikely. For the particular set of parameters considered ignition was found to occur after approximately 50 days, and the temperature at ignition appeared to be ~50°C, which agrees with the results of Brooks and Glasser,1986 and with the results presented in section 2.5 of this work. The time to ignition was found to be a strong function of the activation energy.

Morita et al.,1986 modelled spontaneous combustion of coal in storage silos, and the model used was essentially the same as that used by Handa et al.,1983. The equations were solved using "the Decoupled method" and "the Quasi Implicit Difference Method was applied using the Upstream Difference Scheme". It is not clear exactly what this means because in the abstract the authors claim to have used the finite element method. The calculated results showed excellent agreement with experimentally measured temperature and concentration profiles.

Vasseur et al.,1984 considered two-dimensional natural convection with internal heat generation in concentric horizontal cylinders. In the small and large Rayleigh number limits, corresponding to a pseudo-conduction regime and a boundary layer regime respectively, the authors obtained analytical solutions. A numerical solution of the equations was also obtained with the equations approximated by finite differences. An alternating-direction-implicit (ADI) technique was used for the energy equation in which the spatial derivatives were represented by central differences and the time derivative by a forward difference. The equation in the stream function was solved by successive over-relaxation.

2.3 Description of the finite element program

The finite element method has some significant advantages over the finite difference method for the application required in this study. It appears that numerical oscillations can be reduced when compared with the finite difference method, and the method may also be faster than the finite difference method. Complex regions can be handled very easily and complex boundary conditions can be implemented easily, e.g. the "split" boundary conditions for inflow and outflow (figure 2.1). The shape and size of the elements can be manipulated to conform to regions of steep gradients in the field variables and it is very easy

to specify spatially-dependent properties of the continuum. This would be very useful in modelling the effects of size segregation, or the effect of coating the coal bed with a layer of reactive macerial or with a layer of unreactive material. To be weighed against these advantages is the fact that the mathematical sophistication of the technique is somewhat greater than that required by the finite difference method. The advantages of the finite element method for this study were felt to far outweigh this disavantage, and a finite element program which was based broadly on NAG software (NAG Finite Element Library,1982) was developed initially by Anderson, 1986. From conception the program was designed to solve general systems of linked non-linear partial differential equations with quite general boundary conditions. Further details of the program are given in Anderson and Bradshaw,1987.

The general class of problem soluble by the program is as follows:

$$M\ [\underline{\Phi}_t\ ,\underline{\Phi}] = K\ [\underline{\Phi}] \qquad (2.27)$$

Where M is an operator, operating linearly on the *first* time derivative of $\underline{\Phi}$. The left hand side of (2.27) takes the form of a linear sum of first order time-derivatives, whose individual coefficients may be nonlinear in spatial derivatives if necessary.

K is a general, nonlinear operator, operating on spatial derivatives of $\underline{\Phi}$ of any order below that of the shape functions employed. Application of Green's theorem reduces the order of the spatial derivatives, thus expanding the applicability range of any given shape function.

The current program implementation uses the Galerkin weighted residual method as described in section 2.2.2 although only minor changes would be necessary to change this to e.g. a collocation method.

The preliminary finite element analysis of the left and right hand sides of (2.27) is discussed in detail in many texts, e.g. Norrie and de Vries,1973. Assembly of right hand side contributions into a single matrix and a vector is discussed in detail by Anderson,1986 (see Appendix B). Assembly of left hand side contributions (into the matrix 'GYSM', the time-derivative multiplier) is done in a similar fashion

Brief Outline of Method of Solution

Finite element analysis of equation (2.27) yields:

$$SYSM(\underline{\Phi})\ \frac{\partial \underline{b}}{\partial t} = SYSK(\underline{\Phi})\underline{\Phi} + \underline{f}(\underline{x},\underline{\Phi}) \qquad (2.28)$$

Where **SYSM** and **SYSK** are matrices (both may depend on the dependent variable $\underline{\Phi}$ as shown)

$\underline{b}$ is the time dependent part of $\underline{\Phi}$ (where $\underline{\Phi} = \underline{N} \cdot \underline{b}$)
$\underline{N}$ are the shape functions, dependent only on $\underline{x}$
$\underline{f}$ is a vector

Details of the composition of the above matrices and vectors are discussed in detail by Anderson,1986.

For an unsteady-state solution, the system (2.28) is solved for $\partial \underline{b}/\partial t$ (right hand side evaluated at the current time value) using supplied initial conditions. The solution is then advanced in time by a multistep method or by Gear's method.

For a steady-state solution, the right hand side of (2.28) is equated to zero, and the resulting expression solved iteratively for $\underline{\Phi}$ until successive values satisfy a user-specified convergence criterion. Convergence is assumed when the average error for all three dependent variables is less than 10^{-3}. The average error is defined as the sum over all nodes of the absolute difference between successive iterates, normalized by the value of the old iterate, divided by the number of nodes. An alternative convergence criterion was also tested in which the maximum error was used instead of the average error. This made little difference to the results but increased run times considerably.

If the *coefficients* of the time derivatives do not depend on $\underline{\Phi}$ or t, (this can be seen by inspection) the user can set a flag which ensures that the matrix 'SYSM' is assembled and decomposed (into upper and lower triangular matrices) only *once* during unsteady simulations, right at the start. This has a dramatic effect on run times, since solution of (2.28) during successive time-marching steps requires only 'back-substitution' into the triangular matrices. As the total number of degrees of freedom in a problem increases, reduction of 'SYSM' rapidly begins to dominate overall solution time.

Other features of the program are an optional continuation method (De Villiers,1984) for the solution of non-linear problems in which convergence of the iterative procedure is difficult to obtain, the ability to solve a mixture of steady- and unsteady-state equations, the least-squares fitting of experimental data, great flexibility in the specification of boundary conditions and source terms and a wide choice of mesh element types with the option of crushing the mesh as desired. Relaxation can be implemented separately on any of the field variables.

Because of the key role that this program played in the modelling of spontaneous combustion in this study, a brief review is given of some of the sample problems that were used to test the accuracy and capabilities of the program. Many of the results have been checked against published data; the results and these checks are ommitted here for the sake of brevity but the report of Anderson and Bradshaw,1987 gives more details and is included in Appendix B.

Simulation of rivulet flow - a single, linear partial differential equation. This kind of analysis is relevant to the design of solid-fluid chemical reactors, such as 'trickle-beds'.

Simulation of steady thermal conduction in a composite medium - calculations of this sort are used to estimate thermal energy transfer in glass-fibre reinforced plastics and steel-concrete composites, for example.

Simulation of natural convection heat transfer in porous annulus - two linked nonlinear partial differential equations. Such calculations are used to evaluate the average Nusselt number for heat transfer through layers of insulation around steam pipes, and heat-leaks into cryogenic installations, for example. Many examples of this type of calculation may be found in the literature, see section 2.2.3.

Fitting measured temperature data to a model - least-squares estimation of parameters. The sum of squares of temperature prediction errors for some experimental measurements was minimised by variation of the Rayleigh number and a heat transfer coefficient. For experimental details and numerical results, see Anderson (1987). Fitted results predicted permeabilities (embedded in Ra) of the same order of magnitude as those estimated using known physical quantities (particle size, viscosity, etc.). This is how the heat transfer coefficient in section 2.1.1 was calculated.

The four problem types described above are merely representative of the range of problems soluble by the program.

A listing of the computer program is given in Appendix B, together with two reports (Anderson,1986 and Anderson and Bradshaw,1987) which give further details and outline implementation procedures.

2.4 Preliminary numerical investigations into the small stockpile model

Before proceeding to the calculation of ignition points for the small coal stockpile model it was felt desirable to examine the general behaviour of the model by comparison with results from the one-dimensional model, and to establish suitable parameters and a strategy for numerically calculating the ignition points. In Appendix A typical base case parameters are given. Of this set of parameters the practitioner has some control over the voidage ϵ and the particle size D_p. He also has control over the shape and size of the coal stockpile. Of the other parameters it is likely that only the pre-exponential factor k_o and the ambient temperature T_a will show much variation. The investigations in this study have accordingly been directed towards quantifying the effects of these parameters on ignition points in small coal beds. The majority of the experiments reported in this chapter were conducted for coal beds for which the sloping edge of the bed was at angle of 30° to the horizontal. It is found in practice that coal beds thrown from a stacker will form with an angle of between 30° and 40° to the horizontal. (Coal of high economic value is often stored in wind-rows, streamlined rows of carefully layered compacted material with a side angle of about 11° to the horizontal.)

2.4.1 Selection of finite element mesh

Schreiber and Keller,1983 have shown that poor spatial resolution in the solution of cavity driven flow can lead to spurious bifurcation points. It is especiallly important that this problem is averted in this work because the main aim is the location of limit points. The selection of a suitable finite element mesh can be seen to be vital. From the outset quadrilateral elements were chosen as it was felt that they were more convenient to work with than triangular elements from the point of view of mesh generation, although the finite element program allows the option of specifying triangular elements if desired. The elements were fitted to the trapezoidal shape of the

symmetrical half of the coal bed by means of a simple shrinking transformation. In selecting a suitable finite element mesh it is necessary to weigh up the inreased accuracy to be obtained from a mesh with many elements against the increased computer storage requirements and execution time that this will cause. When limited computer power is available the coarsest mesh which still yields acceptably accurate results is desired. Initial experimentation was performed with a mesh of 20 by 20 4-noded quadrilateral elements, which for the three independent variable model defined by Eqs. (2.12)-(2.14) or (2.15)-(2.17) gives 1200 degrees of freedom, i.e. 1200 non-linear algebraic equations to be solved iteratively. While this mesh gave acceptable results in terms of accuracy, the computational storage requirements (6 Mb on an IBM 3083 machine) and ignition point calculation times of several c.p.u hours each (several days of real time), meant that this mesh was too fine for general use.

Quadratic shape functions were felt to be better than linear ones, because for the same number of degrees of freedom, greater accuracy in the solution is possible with higher order shape functions. Smith,1980 made an investigation into the effect of boundary conditions and numerical schemes on the solution of the heat transport equation. He concluded that finite elements with quadratic shape functions offered the best way of avoiding the oscillatory solutions which plague this problem. This provided another point in favour of using quadratic shape functions. In Figure 2.2, the effect of different mesh types on the ignition particle size can be seen for the base case parameter set. For this experiment three different meshes have been used, 6 by 6 4-noded elements with linear shape functions, 3 by 3 8-noded elements with quadratic shape functions and 6 by 6 8-noded elements with quadratic shape functions. The numbers of nodes for these three meshes are respectively, 40, 49, 133, while the total number of degrees of freedom is found by multiplying the number of nodes by 3. It is immediately clear that the quadratic shape functions are superior in accuracy to the linear ones, and from the very small variation in the value of D_{pl} it can be assumed that the 6 by 6 mesh of 8-noded elements is adequate for the calcualtion of ignition points. Further refining the mesh was found to have a negligible effect on the results. All the results in the remainder of this chapter were obtained using this mesh. The finite element program in its present form in fact allows the user to specify a wide range of mesh types including 12-node quadrilateral elements.

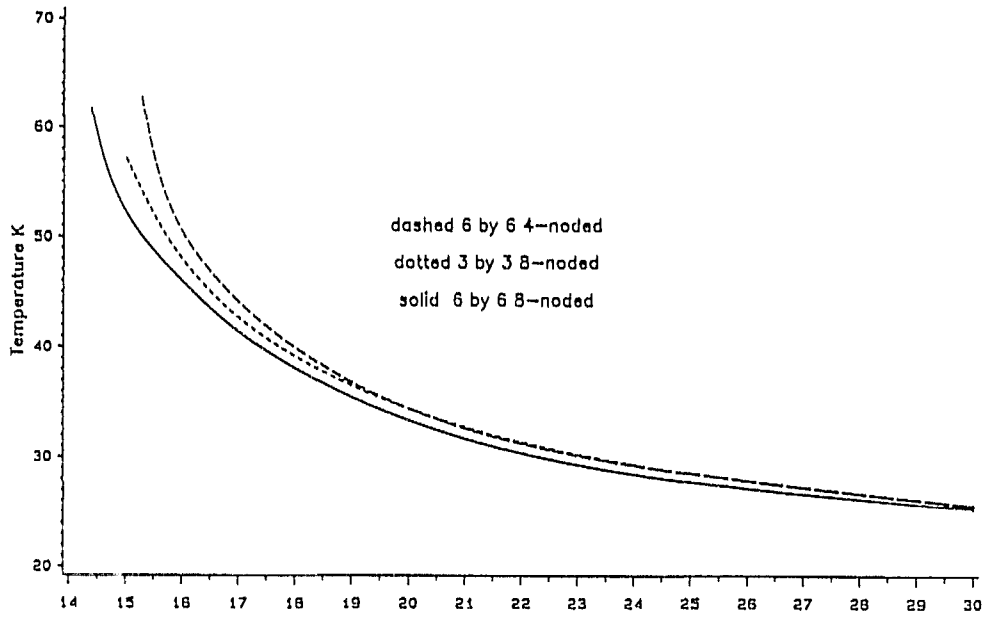

Figure 2.2 Effect of finite element mesh type on calculated ignition points in the frustum for A=0.577, B=0.333 and other parameters at base case values (Appendix A)

2.4.2 Choice of initial conditions and use of continuation

The results shown in figure 2.2 were obtained by calculating the maximum bed temperature at discrete values of particle size by iterating from an initial condition in the coal bed of ambient temperature and concentration and no flow. It was found that at a particular particle size the numerical scheme showed divergence, and for the 6 by 6 mesh of 8-noded elements, this occurred at a particle size of 14.5mm. Leaving aside for the moment the question of the validity of calling this particle size the ignition point, comparison with results given in section 2.5 for the same mesh and parameter set showed that the point of numerical breakdown found by using a simple continuation scheme occurred at a smaller particle size, 12mm. The reason that the continuation scheme gives a different (better) result can be explained as follows. Close to the point of numerical

breakdown, the conditions in the bed are far from the initial ambient, quiescent condition and it is known that obtaining good solutions to highly non-linear problems such as Eqs. (2.7)-(2.10) is strongly dependent on having good initial values. Hence, if the calculation to obtain steady-state conditions is made for a particle size of 12mm starting from an initial condition of ambient temperature and concentration and no flow, it would be expected that the calculation will not converge. This is exactly what has been observed in figure 2.2.

The continuation method is one way of ensuring that good initial guesses are avaliable at all stages of the computation. A thorough treatment of the continuation method is given by De Villiers,1984 and here only a very brief overview is given of the method as applied to this problem. If the steady-state calculation is commenced far from "ignition", there is little temperature rise in the bed, and correspondingly little flow and little consumption of oxygen. In this case the initial conditions are close enough to the steady-state solution to ensure convergence. If the particle size is then decreased slightly and the computation at this new particle size is started from the previous solution we can again ensure that the new solution is not far from the initial condition. This is the essence of how the continuation procedure is applied. Successively smaller steps in particle size are taken, and at each successive size the solution from the previous particle size is used as the initial condition. The decrement in particle size is chosen in such a way that the change in some measure of the solution (e.g. L_∞-norm) changes by approximately the same amount on each calculation step. From Figure 2.2 it can be seen that successively smaller steps in D_p will have to be taken to achieve this. In section 2.4.3 we discuss in more detail how ignition points can be obtained for the small coal bed using this continuation method.

2.4.3 Obtaining ignition points

One can locate ignition points either directly or by observing numerical breakdown of a continuation scheme as described in section 2.4.2. To calculate the ignition points directly one needs to locate the limit point of the system of algebraic equations which results from application of the finite element method to Eqs. (2.7)-(2.10). The system can be written:

$$f_i(\underline{x},p) = 0 \quad ,i=1,2,\ldots,n \tag{2.29}$$

where p is the bifurcation parameter. The condition for a real bifurcation point is:

$$\det(J) = 0 \tag{2.30}$$

where the elements of the Jacobian matrix are

$$\left\{ e_{ij} \right\} = \frac{\partial f_i}{\partial x_j} \quad ,i,j=1,2,\ldots\ldots,n \tag{2.31}$$

Equation (2.30) is equivalent to saying that zero is an eigenvalue of J, hence ignition will be indicated by an eigenvalue equal to zero Thus to locate the ignition point directly one must solve the system (2.29) and (2.30) simultaneously. There is of course the possibility that ignition is marked by a Hopf bifurcation, but only real bifurcation is considered in this work.

Such a direct calculation of limit points is not easy in practice for the very large systems of algebraic equations that result from using a numerical method such as the finite element method. The main problem is in the evaluation of the Jacobian J, because it is very difficult to obtain an analytical expression for the (e_{ij}) . This means that the elements of the Jacobian must be calculated numerically by perturbing the $f_i(\underset{\sim}{x},p)$ slightly and dividing the difference between the perturbed and unperturbed $f_i(\underset{\sim}{x},p)$ by the amount of the perturbation:

$$\frac{\partial f_i}{\partial x_j} \approx \frac{f_i(\underset{\sim}{x},p)\big|_{x_j+\Delta x_j} - f_i(\underset{\sim}{x},p) \;\big|\; x_j}{\Delta x_j} \tag{2.32}$$

This is not an accurate way to calculate the elements of J, and was found to give a singular Jacobian. It is also possible to locate limit points by using the method of arc length continuation (Ku cek and Marek,1983). In this method the arc length of the solution curve becomes a parameter of the system, and by using this arc length as the continuation parameter it is possible to proceed around limit points, something which is not possible using any other conventional scheme. Again the implementation of this method for the type of problem that we are considering is extremely difficult. Unless the elements of a Jacobia matrix similar to that in Eq. (2.30) can be obtained analytically, which is very difficult when the finite element method has been used, the elements of J must be calculated numerically as in Eq. (2.32). Unfortunately this is an extremely unreliable calculation and is fraught with scaling problems. Although it is

possible to scale temperature and concentration to ensure that the e_{ij} from these variables are of the same order of magnitude, scaling of the stream function is not really possible because it is the derivative of the stream function which is of importance. This lack of scaling leads to a matrix which is so ill-conditioned that any numerical routine to use the matrix fails because the matrix appears to be singular. For this reason all attempts to use arc length continuation on this problem proved unsuccessful. Arc length continuation has of course been used very successfully for simpler systems than the one considered here and further work in this area would perhaps yield fruitful results.

If one attempts to find D_{pi} by a continuation method (other than arc length continuation) or e.g. by Newton's method, the numerical scheme will break down at the ignition point (Kubicek and Marek,1983). If one can be sure that the point of numerical breakdown is in fact the limit point of the system of equations, then this simplistic method can be used to obtain ignition points. In Figure 2.3 the variation is shown of the maximum temperature with particle size in a frustum. The

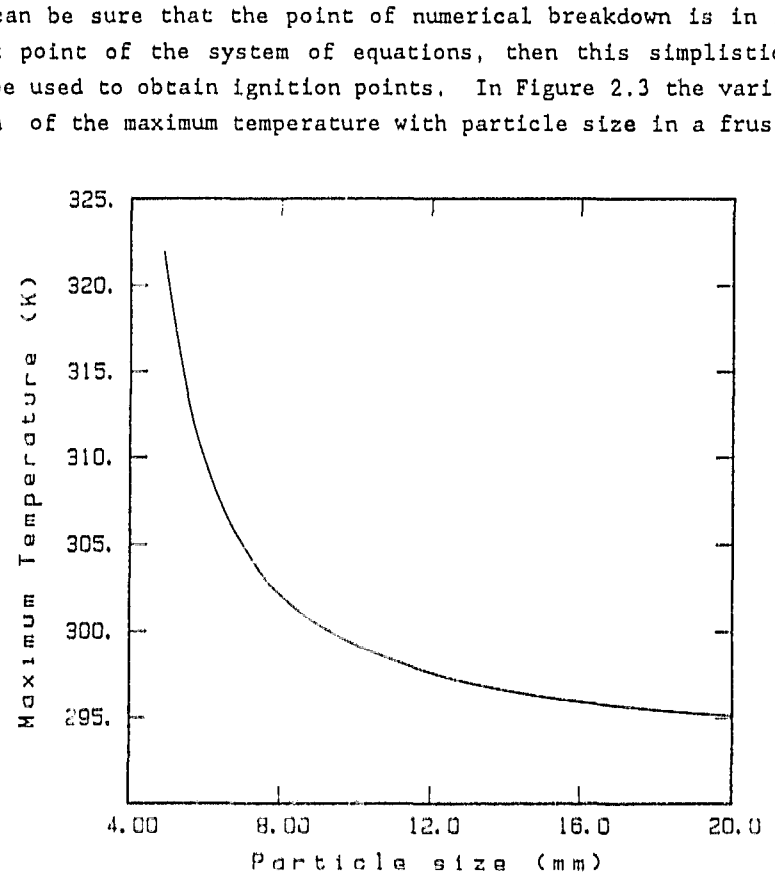

Figure 2.3 Variation of maximum bed temperature with particle size in the frustum for A=0.866, B=0.5, k_0=1 m/s and all other parameters at base case values (Appendix A)

results in Figure 2.3 were obtained using the simple continuation method described above, and using A=0.866, B=0.5, k_o=1 m/s with all other parameters at their base case values as given in Appendix A. In accordance with the results for the simpler models, one can observe what appears to be an ignition at a critical particle size. This particle size has been calculated by stepping down in particle size, using the continuation procedure of section 2.4.2, until the program fails to find a low temperature solution. While this does not prove that an ignition point has been found, the fact that the tangent is almost vertical, and the evidence from the simpler models, would seem to indicate that what we are observing is an ignition, and not a numerical artefact. This belief is also strengthened by the fact that utilizing a finer mesh does not change the position of the ignition. Because it is the determination of the point of ignition that is of interest, and not the conditions inside a burning bed, it is adequate merely to locate the ignition point. This is the technique that was used in this chapter to locate ignition points.

Because the calculation of ignition points using the continuation method requires a large amount of computer time, typically of the order of several c.p.u. hours for each calculation on an IBM 3083, this placed a limitation on the number cases which could be examined in the remainder of this chapter.

2.4.4 Examination of some general trends of the model

One of the important results predicted by the one-dimensional model is that for coal beds whose low-temperature steady-state solution lies on the extinguished branch, decreasing the voidage ϵ will increase D_{pi} (Brooks,1986). This result has been confirmed by Brooks et al.,1988b, for the simplified three-dimensional model. In figure 2.4 the results of a similar calculation for a two-dimensional cartesian coordinate stockpile edge are shown, verifying the behaviour of the simpler models. The geometric parameters defining this edge were A=0.866 B=0.5. All other parameters were at their base case values apart from the voidage ϵ.

From this result it can be seen that the *ad hoc* remedy for preventing spontaneous combustion of compacting the coal bed is in fact extremely dangerous if the bed consists of coal particles of size larger than D_{pi}. This is because compacting the bed increases the amount of reactive material per unit volume while decreasing the

permeability of the bed and thus hampering the cooling effect of the natural convection flow. For fine particles compacting the bed *would* be a good way of preventing spontaneous combustion. Obviously it is vitally important to know which kind of action the practitioner must take, and to do this the value of D_{pi} must be known.

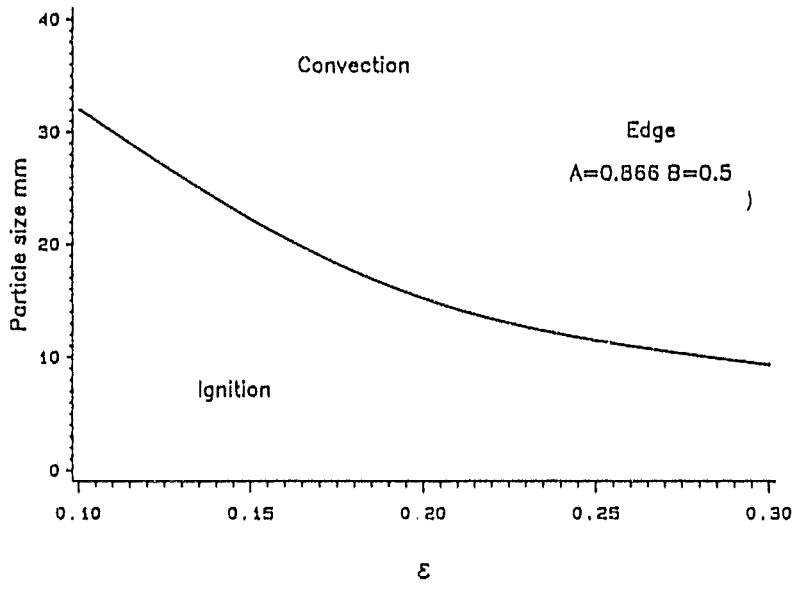

Figure 2.4 Locus of ignition points showing safe and unsafe regions as a function of bed voidage for A=0.866, B=0.5 and all other parameters at base case values (Appendix A)

As discussed in section 2.1.2 the value of the heat transfer coefficient, h, used in the temperature boundary condition, was fitted from experimental results (Anderson,1987). To investigate the effect that the value of the heat transfer coefficient has on ignition points, a calculation was made using three different values of h=0.5, 5, 50 $W/m^2/K$. The results are shown in figure 2.5, and it is apparent that the effect of h on D_{pi} is very small. Of interest is the result that the value of D_{pi} is at a minimum for h=0.5$W/m^2/K$. An explanation for this is that for small h, there exists a greater temperature driving force for flow than for large h, and the resulting strong convective flow helps reduce the temperature

in the bed. This is a small effect however, and the main conclusion is that the value of h, or equivalently the dimensionless parameter Bi, has little effect on the value of D_{pi}. For all calculations in this study the value used was that given in Appendix A, h=5 $W/m^2/K$, which was fitted from experimental data.

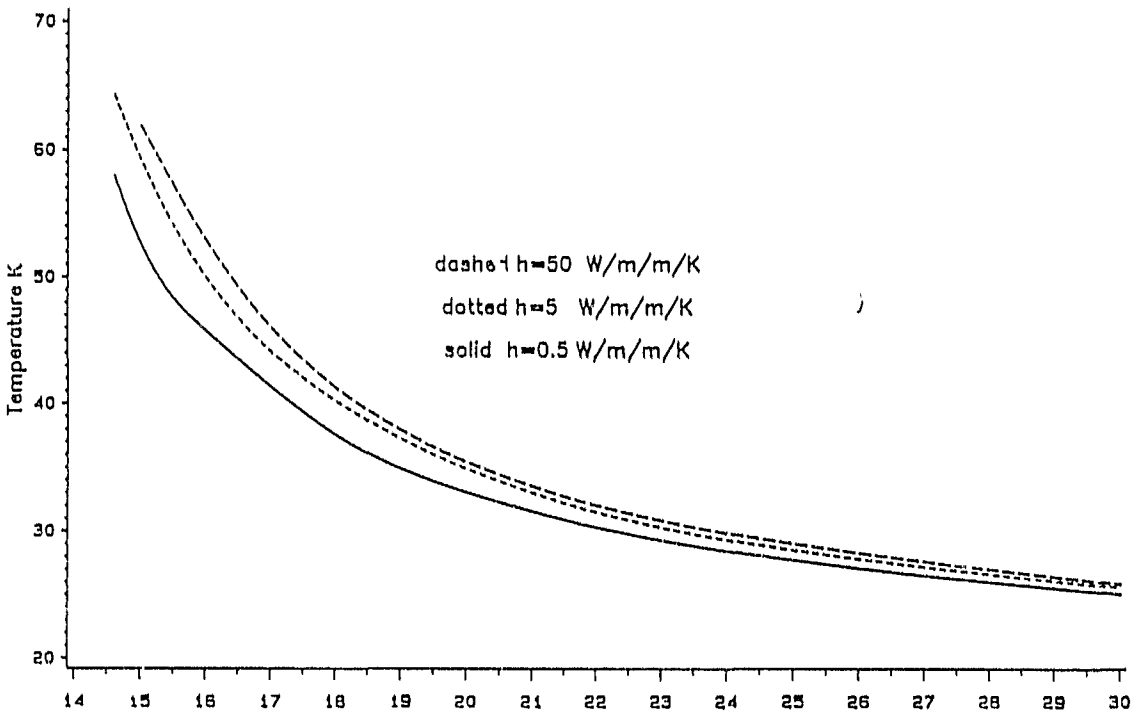

Figure 2.5 Effect of heat transfer coefficient on calculated ignition points in the frustum for A=0.577, B=0.333 and other parameters at base case values (Appendix A)

2.4.5 Unsteady-state solutions

If steady-state analyses indicate that a coal bed will ignite, one would like to know when this will happen. It may be that some beds which will eventually ignite if left for long enough will do so only after many years. If the stockpile is to be dismantled before this time then the coal can be safely stockpiled. Ideally one would like a simple expression for the time to ignition for a stockpile in terms of measurable parameters, in the same way as was done for the ignition point particle size criterion, Eq. (1.7). Unfortunately no such

simple, reliable expression has yet been developed, and the unsteady-state modelling of spontaneous combustion is not a well-researched field.

Brooks,1986 examined the unsteady-state behaviour of a one-dimensional coal bed. He found that at the ignition temperature there was an extremely rapid increase in bed temperature with time. Schmal et al.,1985 considered an unsteady-state model of a one-dimensional coal bed, but neglected natural convection. In order to use the results of Schmal et al. one would have to pick a maximum permissible temperature (at which ignition is considered to have commenced) and then calculate what natural convection flowrate thi corresponded to. By comparison with the imposed velocity one woul then be able to estimate the time to reach this maximum temperatur .

Gijbels and Bruining,1982 attempted to derive a relationship for the time to ignition for underground coal stores. Unfortunately their analysis was incorrect as they took the Laplace transform of an unbounded function. Viljoen et al.,1988 have presented a method for determining whether a bed of reactive porous material will ignite or be stabilised by a natural convection flow. The essence of the method lies in comparing the growth time for a small convective perturbation to the bed, to the growth time for the conduction only solution. If the perturbation to the bed is not large enough then natural convection will not build up quickly enough to prevent the bed from exploding. The technique rests on the assumption that if the convective perturbation grows to the same size as the conduction solution in a time that is less than the time taken for thermal explosion (for a bed in which there is no convection), then the bed is safe. This assumption needs verification. The method is not suitable at present for use by the practitioner, as it requires specification of the size of the imposed perturbation, which is an abstract concept in terms of coal beds. Further work in this direction may produce a result that is more directly applicable to the coal stockpiling situation.

It is more difficult to obtain unsteady-state solutions to equations (2.7)-(2.10) than to solve the steady-state problem. Examination of the terms multiplying the time derivatives of the energy equation and the concentration equations, φ=900 and ϵ=0.3 respectively, shows them to differ in size by many orders of magnitude, meaning that the problem is so stiff that even stiff equation integrators such as Gear's method are unlikely to be adequate. The alternative is to

solve the equations as a mixture of steady and unsteady-state equations with only the energy equation written in unsteady-state form. Solution of the equations in this form adds an additional complication in that it is very difficult to decide for how long the unsteady-state equation can be integrated before the steady-state equations must be solved, prior to integrating the unsteady-state equation in time once more. Decoupling equations in this manner can lead to problems as severe as solving the original system (McDonald,1979). In an attempt to obtain unsteady-state solutions, this mixed-form decoupled approach was used, but the computations were extremely slow and divergent. This is unfortunate because the unsteady-state behaviour can be very useful. Some beds that will burn in the steady-state do so only after an extremely long time, and it may be that the bed will have been used before high temperature burning commences.

2.4.6 Solutions on the ignited branch

As discussed in section 1.3, there exists a region of particle sizes on the ignited branch for which the maximum steady state temperature rise is acceptably low. This happens because of the very low flowrates and high reactivities in beds of fine coal, which means that the oxygen is consumed on the surface of the bed where the temperature rise is easily dissipated to the surroundings. Calculation of these solutions is difficult, because the physical system has now developed a boundary layer in which extremely steep gradients of concentration occur. To resolve such gradients numerically is difficult and in spite of using very fine meshes close to the boundary we were unable to obtain any solutions on the ignited branch. It appears that a better method would be to write a two-region model, with one set of equations describing heat transfer in the interior of the bed assuming that no reaction takes place as there is no oxygen present, and the other set describing the behaviour in the thin boundary layer where all the reaction is assumed to take place. Although this was attempted it proved to be much more difficult than envisaged and still remains an area for further investigation.

2.5 Ignition points in small stockpiles and stockpile edges

2.5.1 Ignition points in frusta

In this section ignition points are calculated for frusta which resemble instrumented coal heaps at a coal mine in South Africa. The test heaps, each made up of different size fractions and equipped with thermocouples and oxygen probes, were approximately 90m in diameter and 17m high with a side angle of about 30°. The frusta which were examined in this section were of similar dimensions. The ignition point particle sizes for these frusta were calculated using the continuation procedure described in sections 2.4.2 and 2.4.3. The method is summarised again briefly. Starting from ambient conditions at some particle size for which very little temperature rise is expected, steady-state conditions in the coal bed are calculated for a decreasing series of particle sizes, using the result from the previous larger particle size as the starting condition for the next smaller size. The step size used was such that the value of D_{pi} was found to within at least 1mm. The j^{th} particle size in the stepping sequence is given by:

$$D_{p_j} = D_{p_{max}} - \left(D_{p_{max}} - D_{p_{min}} \right) \sin \left[\frac{\pi}{2} \frac{(j - 1)}{(N - 1)} \right] \qquad (2.33)$$

Where $D_{p\ max} >> D_{pi}$, $D_{p\ min} < D_{pi}$ and N is the number of terms in the stepping series, typically 30.

This relationship spaces points more closely at smaller particle sizes; if the measure in the change in the solution with particle size is taken to be indicated by the maximum temperature, a suitable L_∞-norm, it can be seen from figure 2.3 that successively smaller steps in D_p must be taken to keep the change in the solution approximately constant.

It is found that at a certain particle size the computational procedure diverges, because the argument of the exponential function in the temperature equation exceeds the allowed range of the computer arithmetic. At this point it is assumed that the steady-state solution to Eqs. (2.7)-(2.10) would be a high temperature burning solution, i.e. the bed has ignited, and the numerical procedure cannot be expected to find such a solution using the continuation method described section 2.4.2. The particle size immediately before this divergence occurs is taken to be the ignition point particle size

D_{pi}. It is also found in some cases that the computations fail to converge according to the convergence criteria, but do not diverge. This situation is discussed in more detail in section 2.5.3. It appears that these cases represent either periodic (or possibly chaotic) convection, which is known to exist for porous medium convection driven by internal sources (Lennie et al.,1988, Viljoen et al.,1989, Kordylewski and Krajewski, 1984).

2.5.1.1 Ignition points in frustum-shaped coal beds with one convection cell

In figures 2.6 a-c typical streamlines, isotherms and concentration contours are shown for a frustum at ignition. In this case the base radius of the frustum was 45m, the height 15m and the side angle 30°. The geometric parameters were thus A=0.577, B=0.333. The other parameters were at their base case values (Appendix A) except for the pre-exponential factor k_o=1 m/s.

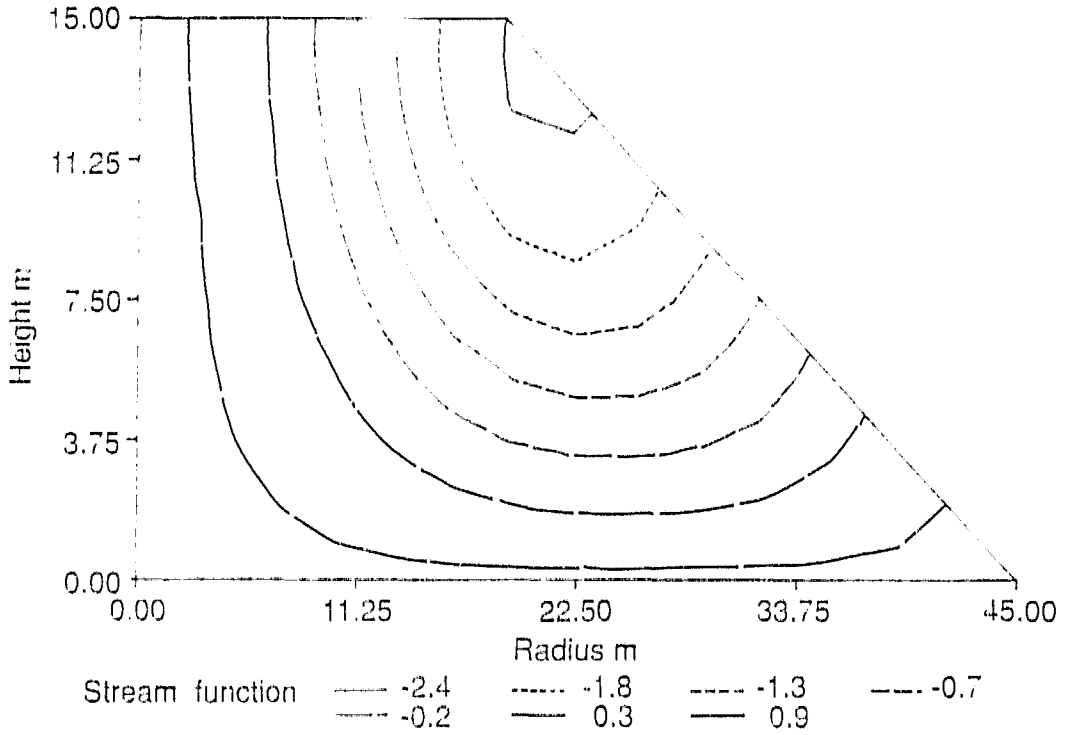

Figure 2.6a Typical streamlines in a frustum for A=0.577, B=0.333, k_o=1 m/s other parameters at base case values

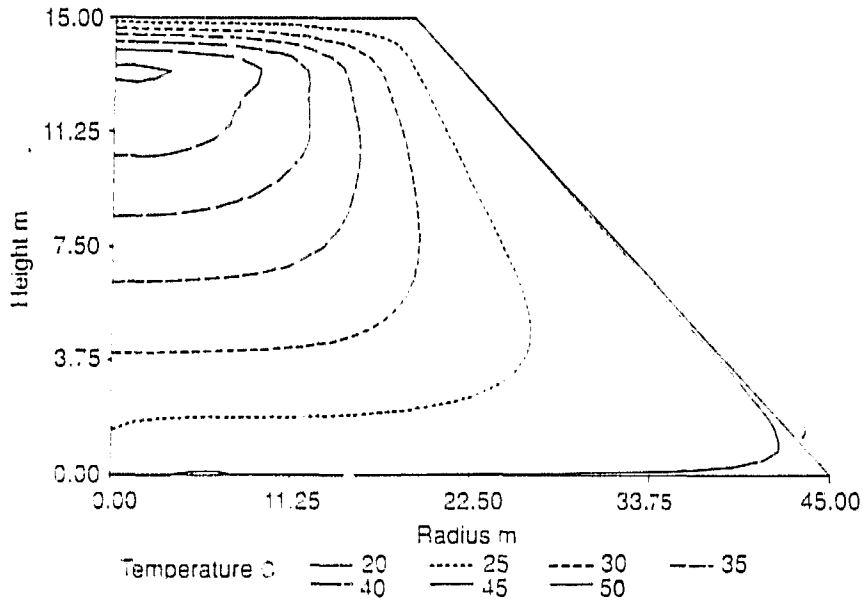

Figure 2.6b Typical isotherms in a frustum for A=0.577, B=0.333, k_o=1 m/s other parameters at base case values

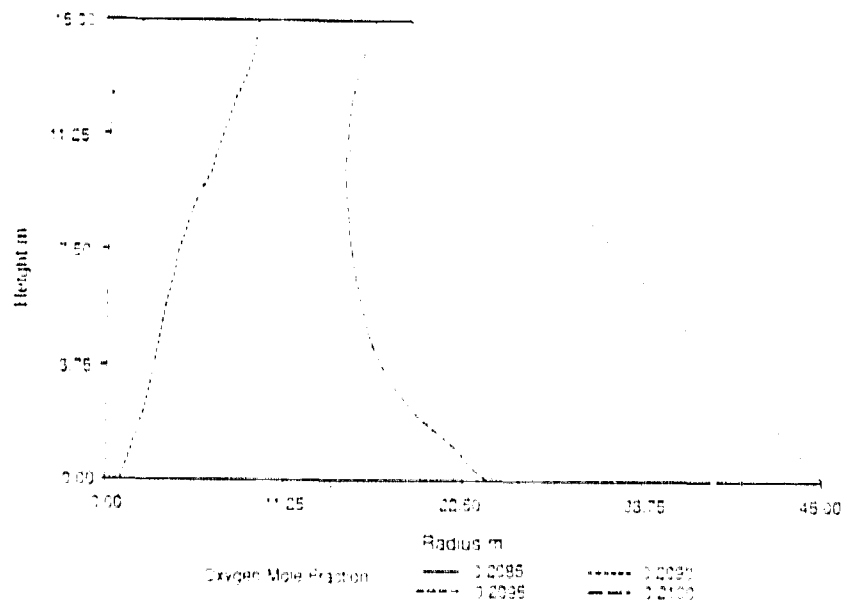

Figure 2.6c Typical concentration contours in a frustum for A=0.577, B=0.333, k_o=1 m/s other parameters at base case values

It can be seen that the flow pattern is unicellular, with all the air entering on the sloping surface and leaving through the flat upper surface. Inspection of figure 2.6 shows that the temperatures on the surface of the bed are close to ambient, and that the consumption of oxygen is extremely low. Such results are typical of those obtained on the extinguished branch of solutions, i.e. solutions for particle sizes greater than D_{pi}. The maximum temperature in the bed is found on the centreline of the bed, approximately 1.5 m below the surface. In real coal beds it has been found that the surface temperature of the bed may be ambient while a metre under the surface the bed is red hot. The assumptions made in deriving Eq. (1.7), i.e. ambient temperature at the ends of the bed and a zero order reaction, would also have been reasonable for the results shown in figure 2.6.

It is found that for frusta which are somewhat flatter than that shown in figure 2.6, the flow pattern breaks down into a number of convection cells. The question of when this occurs and the implications that it has for the determination of ignition points are discussed in more detail in section 2.5.1.2.

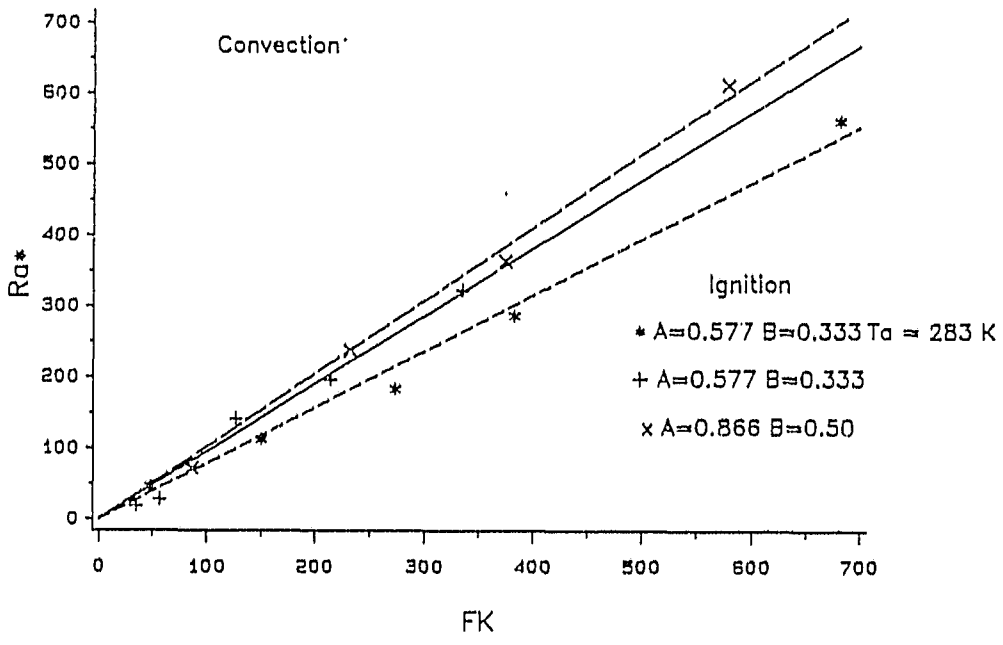

Figure 2.7 Locus of ignition points for the frustum with one circulation pattern for parameters in Table 2.1

Shown in figure 2.7 are the loci of ignition points for different frusta which exhibited only one circulation pattern. Two different frusta were examined, both with a side angle of 30°, height 15m but with base radii 30 and 45m. These frusta can be characterised by the parameters A and B, as indicated on the figure. The frustum with base radius 45m was also modelled with an ambient temperature of 283K, to assess the effect of ambient temperature on the ignition point and to test how well the simple criterion Eq. (1.7) modelled the effect of ambient temperature. The results in figure 2.7 were obtained for a range of pre-exponential factors, k_o, between 0.5 and 50 m s^{-1}.

parameter	bed 1	bed 2	bed 3
γ	23.89	23.89	24.73
β	7.42	7.42	7.676
Le	0.0353	0.0353	0.0353
A	0.577	0.866	0.577
B	0.333	0.500	0.333
Bi	1125	750	1125
R (m)	45	30	45

Table 2.1 Parameter values used in calculation of ignition points in figures 2.7 and 2.14

The results have been plotted as the modified Rayleigh number Ra^* as a function of the Frank-Kamenetskii parameter FK. Elementary geometry has been used to write the values for Ra^* and FK as if the characteristic length was the length of the diagonal from the toe of the frustum to the centreline of the bed at the upper surface. The loci of ignition points divide the parameter space into safe and unsafe regions. Straight lines have been fitted through the data. Ra^* and FK are not natural parameters of Eqs. (2.7)-(2.10), but arise when the so-called positive exponential approximation is used (Frank-Kamentskii,1969). This is discussed in section 3.3, but for the purposes of this section we note that it is unnecessary to make this approximation for a numerical solution. It is however very useful, and perfectly reasonable, to present the results in this form, because it allows direct comparison with the simple ignition criterion of Brooks et al.,1988a (Eq. (1.7)). In that expression the locus of ignition points was described by:

$$Ra_L^* = FK \tag{2.34}$$

The parameters are defined:

$$Ra^*_L = \frac{Ra_L}{\gamma} \tag{2.35}$$

$$FK = \beta\ \gamma\ \varphi_h^2 \tag{2.36}$$

It can be seen that Eqs. (2.7)-(2.10) could also be written in terms of Ra^* and FK.

From figure 2.7 it can be seen that the numerically-calculated ignition points lie on a curve with the functional form:

$$Ra^* = f\ (A,B)\ \frac{\sqrt{B^2 + 1}}{B}\ FK \tag{2.37}$$

The slope $f_1(A,B)$ reflects the dependence of the ignition points on the shape of the frustum. Ra^* is seen to be a weak function of the geometry (A,B), and for the purposes of the practitioner the slope could be considered to be 1. As was discussed in section 2.2.1, Ra^* differs from Ra^*_L by the factor ηT_a=1.07. It is quite clear that to the accuracy with which $f_1(A,B)$ is assumed = 1, Ra^* can be assumed to be equal to Ra^*_L. This means that the locus of ignition points for the frustum is described by the same equation as for the one-dimensional model if one uses the diagonal length as the characteristic length. Such a length is felt to give a crude measure of an "average streamline", and to be a reasonable characterisation of the size of the bed. The term $\sqrt{(B^2+1)}/B$ in Eq. (2.37) merely converts the dimensionless parameters, which are defined in terms of the height of the bed, into a parameter set in which the diagonal is the characteristic length. This means that if Ra^* and FK had been defined in terms of the diagonal length and not the height of the bed, then Eq. (2.37) would have had exactly the same form as Eq. (2.34). The fact that the ignition point loci in figure 2.7 have approximately the form of Eq. (2.34) indicates that the choice of length scale was reasonable. It has been found that using the height or the surface to volume ratio of the bed did not give such good agreement with the simple relationship Eq. (2.34). (Lin and Akins,1986 found that a suitable length scale for natural convection in enclosures was given by the product of the volume to surface area ratio and a dimensionality parameter). In figure 2.8 a similar set of results to that presented in figure 2.7 is given, but using the base radius of

the frustum as the characteristic length. This figure shows that the base radius is perhaps a better characteristic length as the curves for two different frusta fall almost exactly on each other. However, using the base radius has less physical justification than using the length of the diagonal, but for the results in figure 2.8 the length of the base radius is perhaps closer to the average streamline.

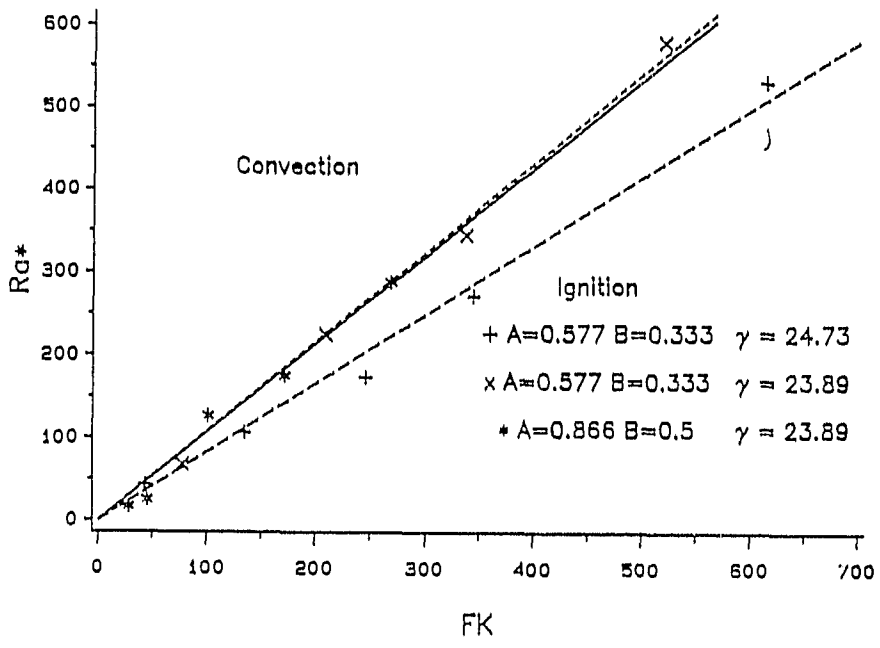

Figure 2.8 Locus of ignition points for the frustum with one circulation pattern and base radius as characteristic length for parameters in Table 2.1

From figures 2.7 and 2.8 it appears that the simple criterion for ignition points, Eq. (2.37) does not entirely adequately account for the effect of ambient temperature on ignition points. However, Eq. (2.37) is conservative for the case when T_a=283 K, i.e. it predicts ignition at a larger particle size than occurs in practice.

From figure 2.9 it can be seen that characterising the size of the frustum by the length of the longest streamline and using this length

in Eq. (2.37) results in the simple criterion predicting a conservative value for D_{pi}.

In considering the results of figures 2.7-2.9 it must be borne in mind that the value of D_{pi} has not been found exactly for any given value of k_o. This means that in figures 2.7-2.9 the value of Ra^* could be smaller and the value of FK could be larger than the indicated ignition point, although in all cases the value of D_{pi} was found to within at least 1mm.

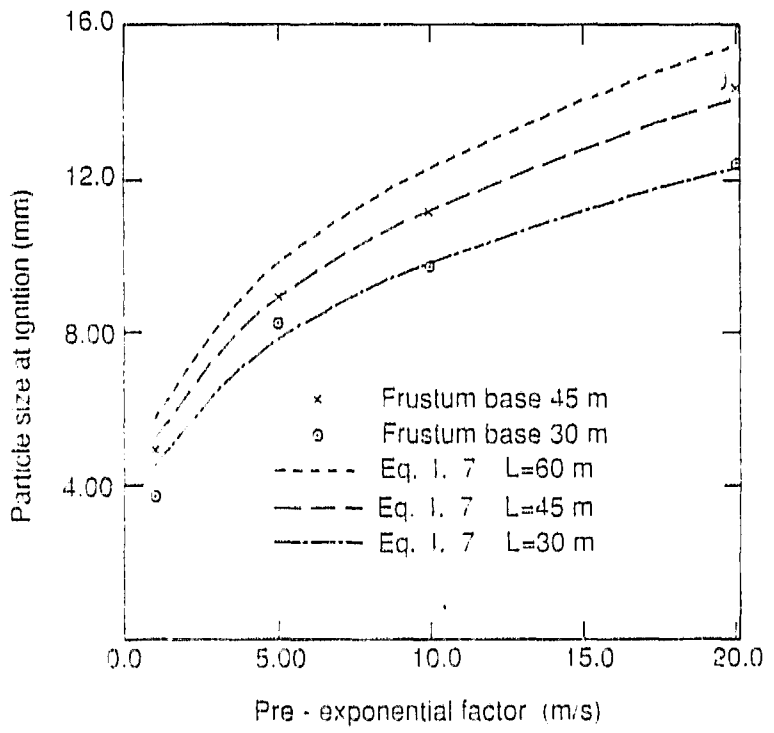

Figure 2.9 Locus of ignition points for the frustum with only one convection cell, and showing the effect of different length scales for the parameters in Table 2.1

Of interest is the result shown in figure 2.10, in which the maximum temperature in the frustum is plotted as a function of the particle size normalized by the ignition particle size. This has been done for the two different sizes of frusta in table 2.1 and for a range of

pre-exponential factors 1-50 m s^{-1}. To within the accuracy that the ignition points have been found it can be seen that all the points lie on one curve, which indicates that D_{pi} is strongly characteristic of the system. It did not prove possible to determine from first principles the form of the curve in figure 2.10, however it would be possible to fit the data empirically, and by using Eq. (2.37) for the value of D_{pi}, to obtain an expression for the maximum temperature in the coal bed as a function of easily measurable parameters.

Thus, for frusta which show one circulation pattern it has been shown that the locus of ignition points is well-described by Eq. (2.37), which is the same as was derived for the simplified one-dimensional model if the diagonal is taken as the characteristic length. This is an extremely useful result because it means that the practitioner can very easily calculate the minimum particle size for safe stockpiling for a coal bed of given size and coal reactivity, or alternatively the maximum bed size for a coal of given particle size and reactivity.

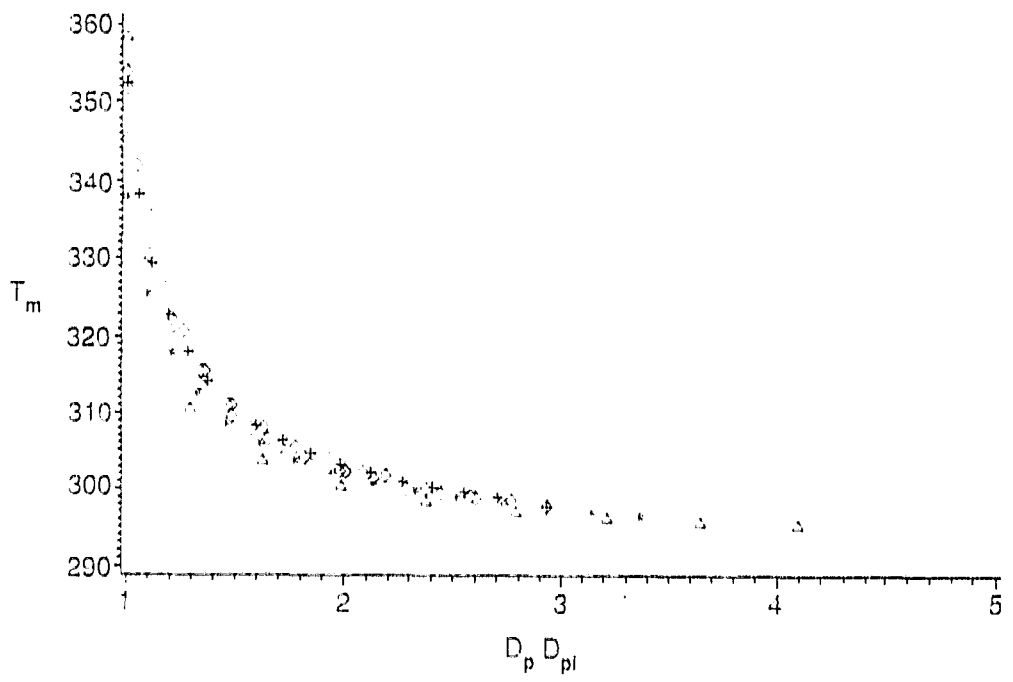

Figure 2.10 Maximum temperature in the coal bed as a function of reduced particle size for frusta of Table 2.1 and k_o 1-50 m/s

2.5.1.2 Ignition points in frusta which show multiple convection cells

When a frustum is made flatter and wider than the ones examined in the previous section, the flow pattern breaks down into a number of Benard-like convection cells. This can be seen in figure 2.11, which shows streamlines and isotherms for a frustum of base radius 30m and height 5m. There are two internal cells visible, i.e. convection cells in which the flow enters and leaves the bed solely through the upper surface, and an edge cell, which resembles the circulation pattern shown in figure 2.6 for the case where the frustum had a unicellular flow. This result is typical of all those obtained when the flow pattern shows Benard-like cells both for frusta and edge models discussed in section 2.5.2. The typical features are: an odd number of cells, the maximum temperature at ignition on the bed

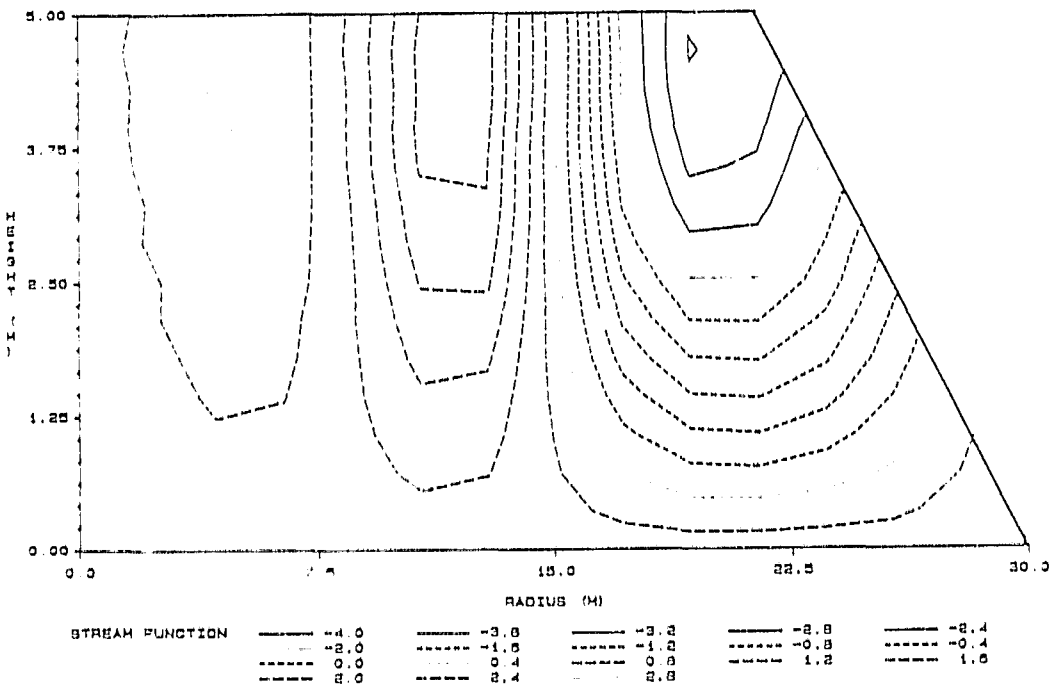

Figure 2.11a Typical streamlines in a frustum showing multiple convection cells for A=0.288, B=0.166 and other parameters at base case values

centreline, the width of the internal cells equal, and equal to the

width of the outflow region for the edge cell. A cell has been defined as the smallest adiabatic cell, i.e. the width is measured from the point of inflow to the point of outflow. Although the assumptions of a zero order reaction and ambient surface temperatures would also have been reasonable for the case shown in figure 2.11, one would expect that Eq. (2.37) would no longer describe the locus of ignition points. This is particularly the case because the point in the bed showing the highest temperature at ignition is close to the surface and on the centreline of the bed. Oxygen is supplied to this hot-spot by a two-dimensional roll cell, and the flow in this roll cell has turned through 180°. This is a situation very different from that modelled by the one-dimensional model.

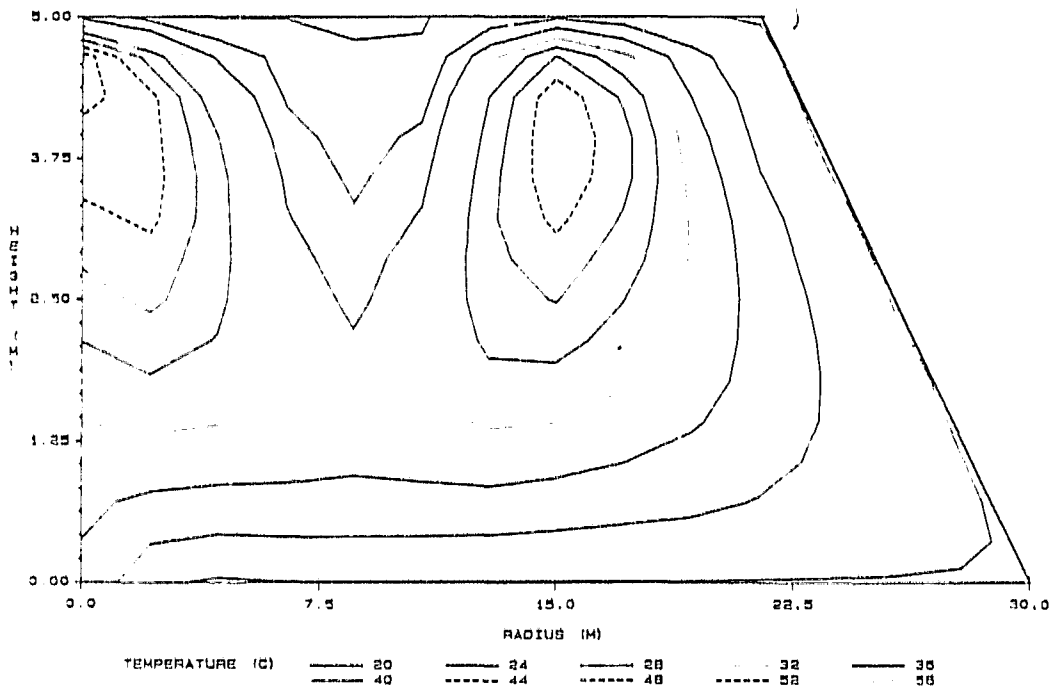

Figure 2.11b Isotherms in a frustum showing multiple convection cells for A=0.288, B=0.166 and other parameters at base case values

The weakness of assuming radial symmetry now also becomes apparent, as it is very unlikely that the toroidal convection cells predicted by the model would be found in reality. Of course if the radius of curvature of the toroidal cells is very large then the cells resemble two-dimensional roll cells, which occur in practice. This still

leaves the problem of the centre cell which could be considered to approximate a hexagonal cell of the kind that are known to form in porous media (Tveitereid,1977). While recognising that this imposition of symmetry is not very satisfactory, it is still of interest to consider frusta which show multiple convection cells and to compare the results obtained in this geometry with those obtained for a more realistic edge model described in section 2.5.2.

In figure 2.12 the loci of ignition points are shown for three different frusta all with the three convection cell pattern. In this case the results have been plotted as $\sqrt{Ra^*}$ as a function of FK^*, and it can be seen that this functional form appears to describe the results reasonably well. The characteristic length used in figure 2.12 was the diagonal length of the edge cell. The parameter FK^* does not depend on particle size and is defined as follows:

$$FK^* = FK \sqrt{Ra^*} \qquad (2.38)$$

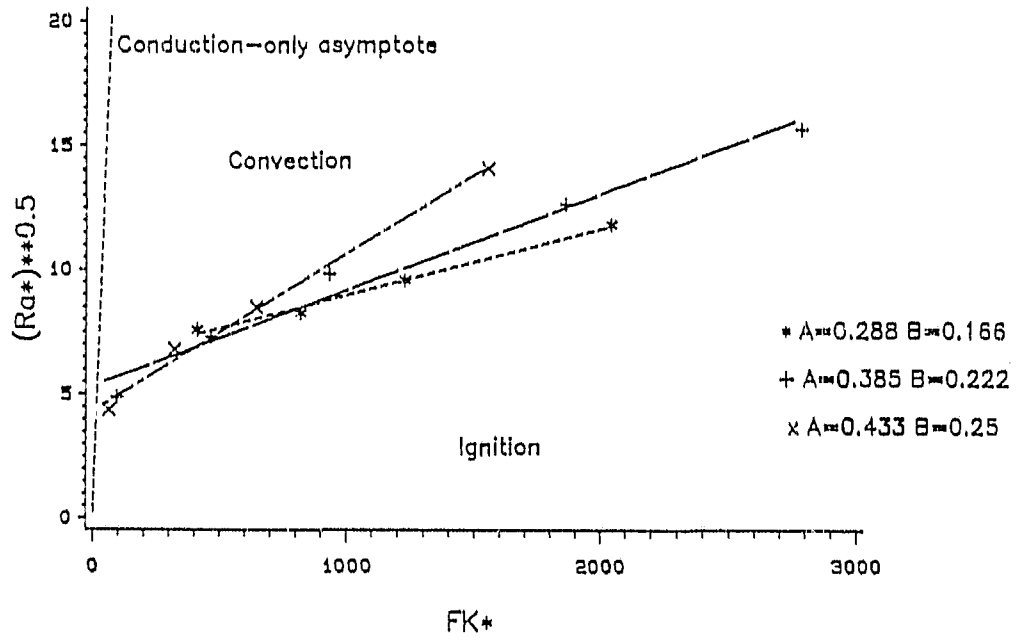

Figure 2.12 Locus of ignition points for frusta showing multiple convection cells for parameters in Table 2.2

parameter	bed 1	bed 2	bed 3
γ	23.89	23.89	23.89
β	7.42	7.42	7.426
Le	0.0353	0.0353	0.0353
A	0.288	0.385	0.433
Γ	0.166	0.222	0.250
Bi	750	1125	1000
R (m)	30	45	40

Table 2.2 Parameter values used in calculation of ignition points in figures 2.12 and 2.15

From figure 2.12 it appears that the ignition point locus can be described by a relationship of the form:

$$\sqrt{Ra}^* = f_2\,(A,B)\;FK^* + 5 \qquad (2.39)$$

where $f_2\,(A,B)$ is a function of the frustum geometry and $\sqrt{Ra}^*>5$.

It was found that the correct length scale appeared to be the diagonal of the edge cell. By elementary geometry and using the characteristic features of the Benard-like cells, it is possible to express this length in terms of the height of the bed, provided that one knows the side angle of the bed. Because all the computations of sections 2.5.1 and 2.5.2 were made for a side angle of 30°, it is found that the locus of ignition points can be described by:

$$FK \approx \frac{200}{\left[1 + (\sqrt{3}+0.75)^2\right]}\left(1 - \frac{5}{\sqrt{Ra}^*}\right) = 27.9\left(1 - \frac{5}{\sqrt{Ra}^*}\right) \qquad (2.40)$$

The slope of the curves in figure 2.12 is $\approx 1/200$. The denominator represents the length scale correction, and $\sqrt{Ra}^*>5$.

It is significant that a different functional form for the locus of ignition points has been obtained for the case where multiple convection cells are present. The fact that the flow turns around in the roll cells means that the predominant mechanism in the bed is no longer the same as that when only a single convection cell (the edge cell) is found.

In figure 2.13 the loci of ignition points have been plotted as

Ra^* vs FK, as was done for the frusta which showed only one convection cell, but using the diagonal as the length scale. It can be seen that the locus of ignition points in this case is not well-described by a relationship of the form of Eq. (2.37). Although we know that the assumption of radial symmetry is poor for the frusta which show Benard-like cells, we have been able to show that the ignition points fall on a curve described by Eq. (2.40). This is a useful result, and complements the earlier expression for frusta with only one flow cell.

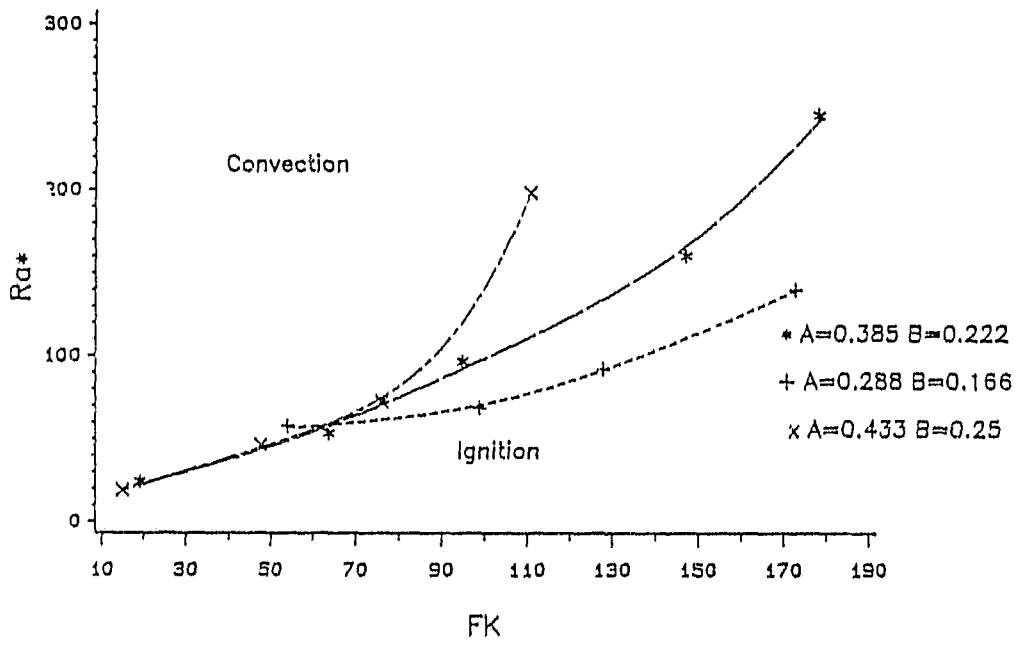

Figure 2.13 Locus of ignition points for frusta with multiple convection cells showing incorrect functional form for parameters in Table 2..

2.5.2 Ignition points at edges of large coal stockpiles

To make the analysis of ignition points in coal beds more general it is necessary to look at a two-dimensional cartesian model, assuming that the bed is infinitely long in one horizontal direction. In this

way it is possible to consider the edges of large coal stockpiles and to look more closely at the situations where the flow breaks up into cells. This can be achieved because each of the convection cells is adiabatic and there is no flow between cells. Thus by considering only an edge cell, it is possible to examine the effects that will be present at the edge of a large coal bed. By looking at the situation when multiple cells are present it is possible to draw empirical conclusions as to how large a coal bed must be before the flow breaks down into Benard-like cells, and which ignition point criterion to use in that case. In this section a two-dimensional formulation is used, asssuming that the coal beds are infinitely long in one of the horizontal directions. This slightly restrictive assumption was necessary because the vast amount of computer power that would be required to solve the three-dimensional model was not avaliable. The coal beds are assumed to have a trapezoidal cross section at the edge.

2.5.2.1 Ignition points at edges showing one convection cell

In figure 2.14 the loci of ignition points are shown for the edge

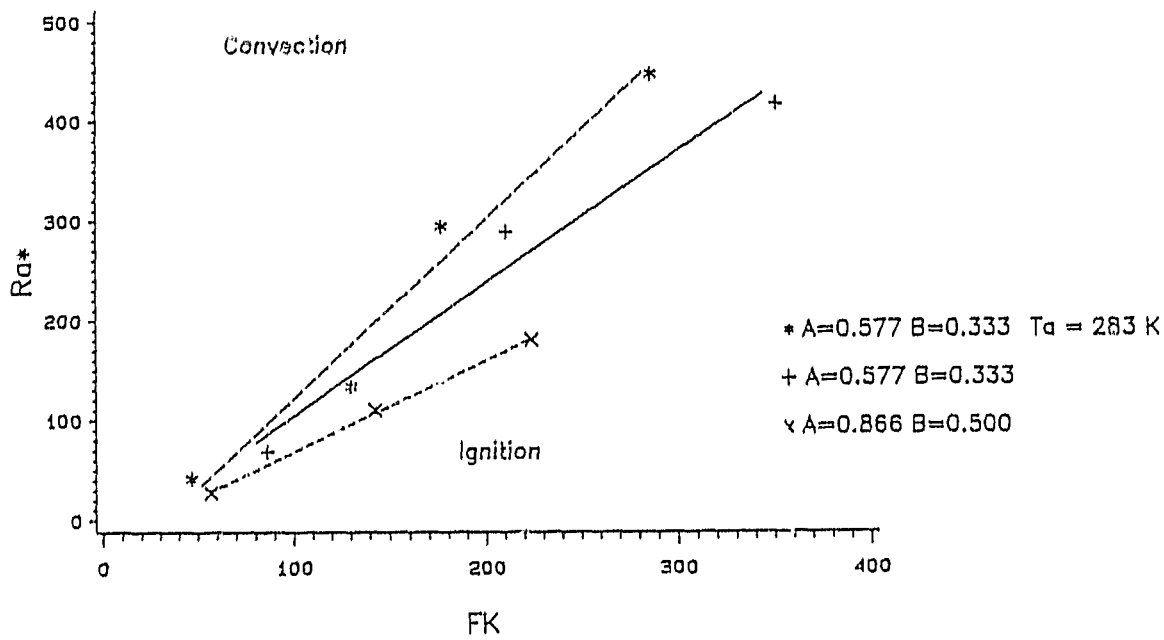

Figure 2.14 Locus of ignition points for the edge model with a single convection cell for parameters in Table 2.1

model in which only one convection cell was present. The geometries used were the same as those described in section 2.5.1 and detailed in table 2.1, although of course a two-dimensional cartesian formulation was used. For this case it appears that the ignition points are described by an equation of the form:

$$Ra^* = f_3(A,B) \frac{\sqrt{B^2 + 1}}{B} FK \qquad (2.41)$$

where $f_3(A,B)$ is a function of the edge geometry, and ≈1.

The curve for the edge with A=0.577, B=0.333, T_a=293K most closely fits Eq. (2.34). The function $f_3(A,B)$ has a small effect on the ignition points and although the form of $f_3(A,B)$ is different to $f_1(A,B)$, and has a larger effect on ignition points than $f_1(A,B)$ in Eq. (2.37), for the purposes of the practitioner it seems that the ignition points in coal beds which show only one circulation pattern can be adequately described by Eq. (2.37). Thus either for frusta or two-dimensional edges, if there is only a single convection cell present the locus of ignition points is described to the accuracy required by the practitioner by Eq. (2.37). In the next section the question of when multiple convection cells occur is discussed.

2.5.2.2 Ignition points at edges with multiple convection cells

When the flow pattern shows multiple convection cells in this edge model, the internal cells that are formed have more physical meaning than those in the frusta. These internal cells in the case of the edge model are in fact two-dimensional roll cells, which are known to be stable in natural convection in porous media (Tveitereid,1977). In figure 2.15 ignition points are shown for the edge model where multiple convection cells are present. The results have been plotted the same way as for the frustum (figure 2.12) and using the same set of parameters as given in table 2.2. It appears that the locus of ignition points in this case is again well-described by an equation of the form:

$$\sqrt{Ra^*} = f_4(A,B)\ FK^* + 5 \qquad (2.42a)$$

This expression can be written more compactly as:

$$FK \approx \frac{130}{\left[1 + (\sqrt{3} + 0.75)^2\right]} \left\{1 - \frac{5}{\sqrt{Ra^*}}\right\} = 18.15 \left\{1 - \frac{5}{\sqrt{Ra^*}}\right\} \qquad (2.42b)$$

The constant 130 represents the inverse of the slope of the curves in figure 2.15, while the denominator is the factor to correct the length scale, as was discussed for Eqs. (2.39)-(2.41), i.e. the correct length scale for this problem is the diagonal length of the edge cell, but FK is defined in terms of the height of the bed. The diagonal length of the edge cell can easily be expressed in terms of the height of the bed, which is the purpose of the denomimator in Eq. (2.42b). Eqs. (2.42a-b) are valid for $\sqrt{Ra^*}>5$.

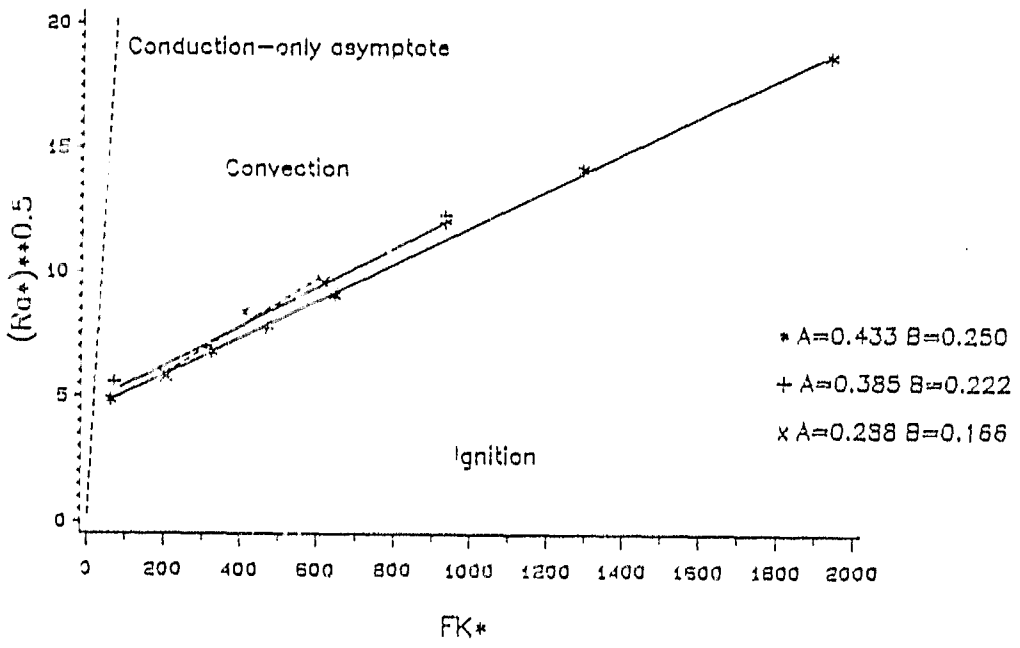

Figure 2.15 Loci of ignition points for the edge mode with multiple convection cells for parameters in Table 2.2

It is very significant that the functional form of the expression for the locus of ignition points is the same for both frusta and at edges, as this is strongly indicative that this form does indeed describe the

locus of ignition points for coal stockpiles of trapezoidal cross-section with multiple Benard-like cells.

It is also significant that the asymptotic form of the equation describing the locus of ignition points as Ra becomes large is of the same functional form as the expression for thermal explosion in a bed in which conduction is the only form of heat transfer (i.e. FK=constant, see section 3.3). This is also the form of the conduction asymptotes of both the Dirichlet and general one-dimensional models of Brooks et al.,1988a. In the Dirichlet model it was assumed that the temperature at both ends of the bed was ambient and that the consumption of oxygen could be neglected. For that model the ignition point locus was described by Eq. (1.7) (Eq. (2.34)), while the conduction asymptote was given by FK=3.514. This is known as the thermal explosion limit as will be discussed in section 3.3. In the general model the same convection and conduction asymptotes were found as the Biot number became large. For an even simpler model called the lumped thermal model, in which it was assumed that the bed temperature was uniform, the convection asymptote was given by Ra_L^*=0.541 FK, while the conduction asymptote was given by FK/Bi=0.736. Thus it can be seen that even for the poor assumption of the lumped thermal model the form of the convection and conduction asymptotes is maintained, even though the constants are different. In this regard one can note that the results of Schmal et al.,1985 indicate that allowing for moisture effects has the effect of making the bed temperature more uniform. If this is the case then the assumption of the lumped thermal model may not be as poor as first appears. Thus, although convection most certainly occurs in this edge with multiple cells, the fact that the flow must turn through 180° and is therefore relatively slow means that the locus of ignition points is described by a conduction asymptote-type expression.

As in the case of frusta it was found that when multiple cells formed there was always an odd number of cells, and that the ignition occurred at the hot spot on the centre line of the bed. The streamlines and isotherms shown in figure 2.16 are typical. In this particular case they were obtained for a domain of width 40m and height 10m with a side angle 30°. As can be seen the internal cells are of equal width, and this width is approximately equal to the width of the outflow region for the edge cell.

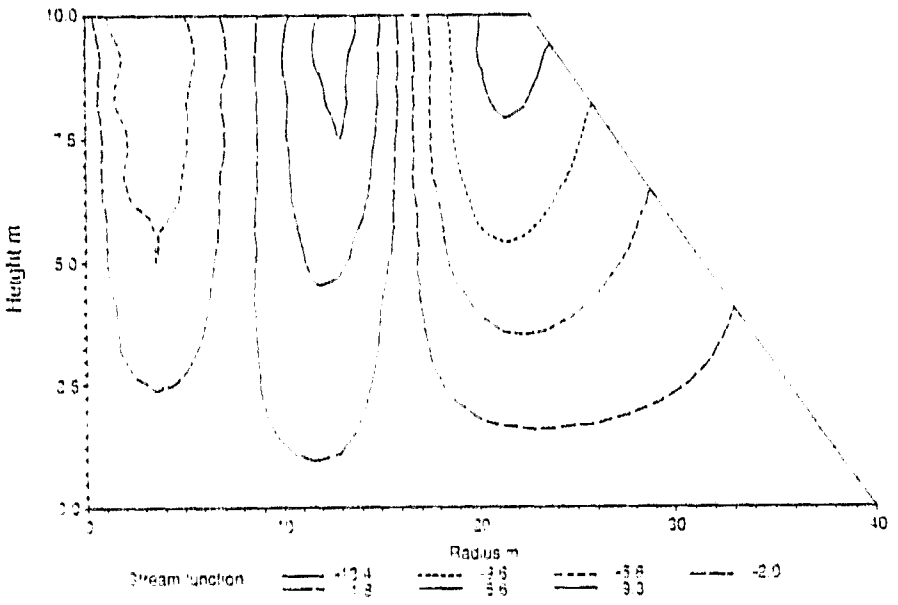

Figure 2.16a Streamlines in the edge model with multiple flow cells for bed 3, Table 2.2

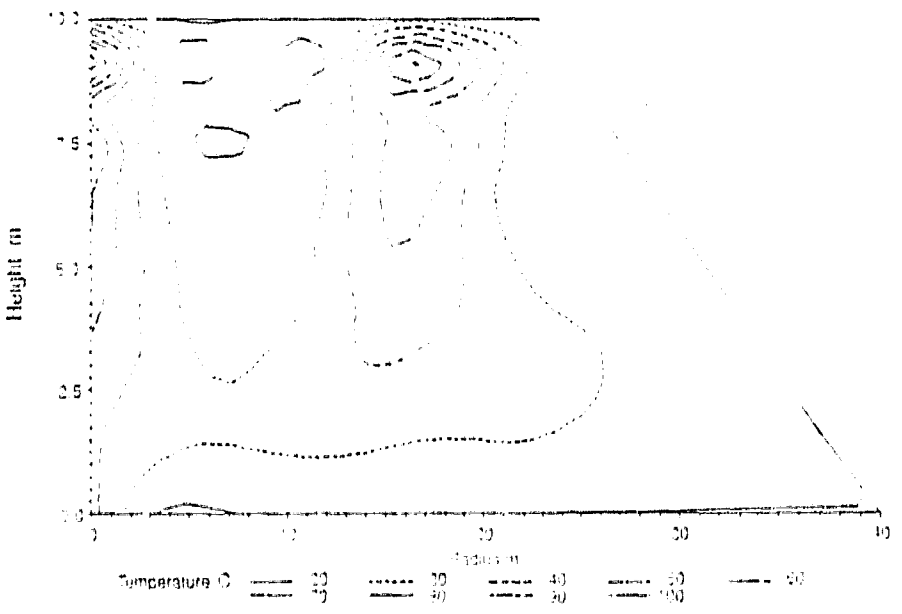

Figure 2.16b Isotherms in the edge model with multiple flow cells for bed 3, Table 2.2

In order to establish more clearly the condition for which the flow pattern shows multiple convection cells, the width of the edge in figure 2.16 was reduced until the convection cells coalesced. The pre-exponential factor used was k_o=10 m/s. The results of this computation are shown in figure 2.17, in which the number of cells has

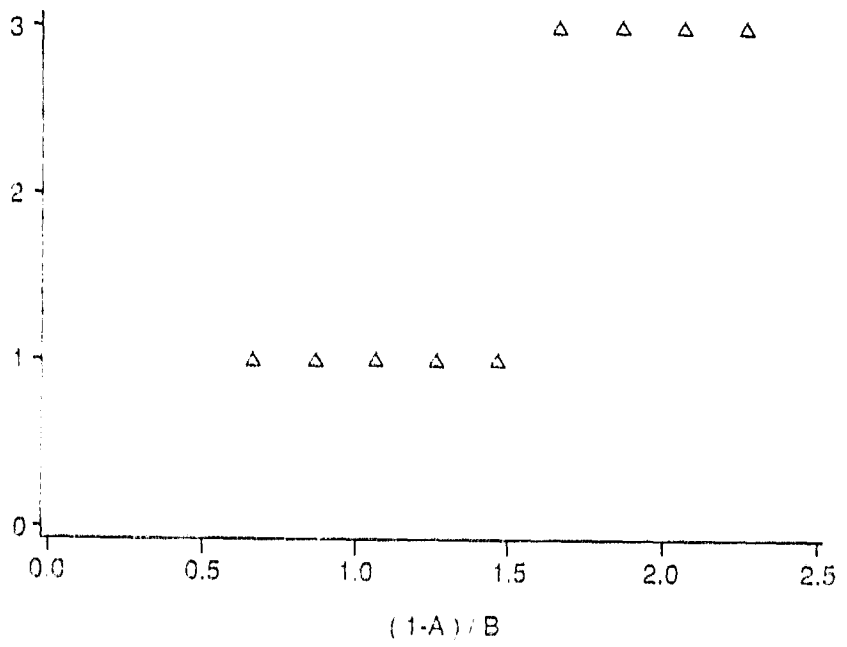

Figure 2.17 The formation of multiple convection cells in the edge model for bed 3, Table 2.2 base case parameters

been plotted as a function of the ratio of the width of the upper flat surface to the height of the edge. The ratio has been expressed in terms of the geometric parameters A and B, i.e. (1-A)/B. It can be seen that only an odd number of cells was found, a result that was also found for all frusta and edges which showed multiple cells. The transition between 1 and 3 cells occurred at (1-A)/B=1.5 and examination of figure 2.16 shows that the hot spot separation is also given by 1.5 times the height of the edge. This empirical result was

found to be valid for most cases that showed multiple cells. The size of the internal cells is such that they are each approximately of width H/2, and this is a result that is confirmed in Chapter 3 of this thesis, when the interior of large coal beds is examined analytically.

Using this empirical result it is possible to predict when multiple flow cells will form in a coal bed of trapezoidal cross section, and if such cells are formed, what their approximate size will be. In this way the length of the diagonal of the edge cell can be calculated and by using Eq. (2.42) the locus of ignition points can be calculated. This very simple empirical criterion was used in Eqs. (2.40) and (2.42b) to correct the length scale and the resulting simple relationships for the locus of ignition points can be used by the practitioner to determine the critical parameters for safe stockpiling for coal beds which show multiple flow cells.

2.5.3 Ignition points in edges with only sloping surfaces

Stockpiled coal is often stored in "wind-rows", carefully compacted beds of crushed coal with a very shallow side angle to minimise the effect of wind pressure. It was felt to be of interest to examine ignition points for coal beds with shallow side angles. Analysis of the edge model was made which contained only a sloping surface, and for which the angle to the horizontal was 15°. This geometry resembles the edge of wind-rows beds. It was found that this type of edge model gave convergence problems as the reactivity of the coal was increased, indicating that periodic convection is likely to be found in such cases. The results of this investigation are given in table 2.3.

A	B	γ	β	Le	R (m)	$\varphi^2_{h_i}$	Ra_1
0.995	0.266	23.89	7.42	0.0353	45	0.040	247.6
0.995	0.266	23.89	7.42	0.0353	45	0.0875	1313.6

Table 2.3 Results of ignition point calculations for the sloping edge model

From so few results it is difficult to draw any firm conclusions about the behaviour of this type of bed. In the cases which gave converged

solutions, the flow pattern showed a single edge cell, with most of the flow leaving the bed through the 0.2m wide flat part at the top of the bed on the centreline. This flat portion was included because quadrilateral elements were used in the finite element program. As the reactivity of the coal was increased it appeared that the convection became periodic. To study this type of behaviour, unsteady-state solutions are required.

2.6 Numerical investigation into convection cell size in coal beds

In order to gain further insight into the formation of convection cells in coal beds, numerical experiments on an open-topped box were carried out, with the aims of finding stable cell sizes and also calculating ignition points in convection cells. It was felt that such an investigation would provide some insight into the preferred size of the internal cells To perform this investigation, a box, impermeable on the bottom and sides and adiabatic on the sides was examined. The boundary conditions on such a box are the same as the conditions on the boundaries of the adiabatic internal cells observed in sections 2.5.1.2 and 2.5.2.2. The boundary conditions for the top surface were the same as for the edge and frustum models, while on the inmpermable walls of the box the normal derivative of concentration was equal to zero. The boundary conditions may be stated:

The geometric parameters are A=0, B=H/R

$$\text{On } (z, 0), (z, 1): \frac{\partial Y}{\partial n} = \frac{\partial \theta}{\partial n} = 0, \ \psi = 1 \qquad (2.43a)$$

$$\text{On } (r,0): \frac{\partial Y}{\partial n} = \theta = 0, \ \psi = 1 \qquad (2.43b)$$

$$\text{On } (r,BR): \text{inflow } \ Y = Y_a, \ \frac{\partial \theta}{\partial n} = -(Bi + u_n)\ \theta, \ \frac{\partial \psi}{\partial n} = 0 \qquad (2.43c)$$

$$\text{outflow } \frac{\partial Y}{\partial n} = 0, \ \frac{\partial \theta}{\partial n} = -Bi\ \theta, \ \frac{\partial \psi}{\partial n} = 0 \qquad (2.43d)$$

It should not be expected that this analysis will predict exactly the situation in an infinite or laterally-unbounded coal bed, as it is known that the presence of side walls influences the results even when the computational domain is large (Joseph,1976). However it does provide a useful insight into the formation of convection cells.

2.6.1 Cell size selection in the open-topped box

In this section we are concerned with finding, by numerical

experiment, the stable roll cell size in the open-topped box, rather than calculating ignition points. Coals of two different reactivities were examined and the steady-state convection patterns were calculated for a number of different Rayleigh numbers and aspect ratios, using different sized boxes for the two different coals. These calculations were performed both for a zero order reaction and a first order reaction. It was found that the zero order reaction in some cases indicated ignition where this was not indicated for the first order reaction. It was felt that it was the zero order reaction approximation which was in error. An explanation for this is as follows. The iterative calculation used to obtain the steady-state solution can be considered as some indeterminate time-marching procedure, i.e. the iteration generally proceeds forward in time. Early on in the calculation the flow rates in the bed are very small, as is the temperature rise. In this situation it is known that the consumption of oxygen is significant. This has the effect of limiting the temperature rise at places where the reaction rate starts to speed up. As time progresses, the flow rates become larger and the consumption of oxygen decreases until at steady-state it has been shown (sections 2.5.1. and 2.5.2) that the consumption of oxygen is negligible. However, when the approximation of a zero order reaction has been made, early in the calculation there is no limitation of the temperature rise caused by lack of oxygen, and the bed proceeds to ignition much more rapidly than should really occur. For this reason it was felt that the first order reaction was more reasonable, and the results of the calculations using a zero order reaction were discarded.

The results of the calculations are presented in figures 2.18 and 2.19, which show the number of roll cells for different aspect ratios and values of Ra/B. It can be seen that for some cases no stable solution could be found. Inspection of the results for these cases showed that the convection appeared to be periodic, with the cell sizes and numbers changing continuously during the course of the iteration. Such a result has been found by many authors e.g. Viljoen et al.,1989.

From figure 2.18 it can be seen that small cells are favoured by large values of Ra and small aspect ratios, i.e. very flat coal beds. This result was also found by Gatica et al.,1987. From figure 2.19 there appears to be a fairly large region in which there was no stable steady-state solution; this region was on the boundary of stability of one and two cells. It is difficult to draw conclusions as to stable

cell sizes in these simulations, particularly as it is known that the initial condition affects the steady-state solution when a number of different flow planforms are possible stable solutions. However, it seems that no roll cells form which have an aspect ratio less than 0.4 This means that long flat cells are not likely to be a stable flow pattern.

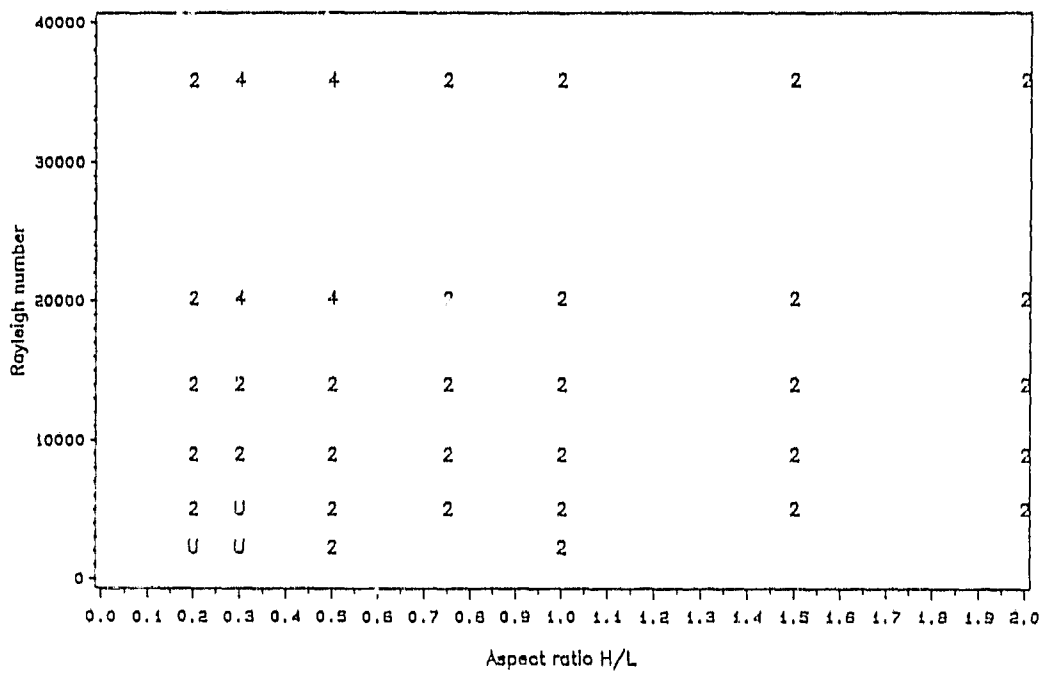

Figure 2.18 Stable roll cells in the open-topped box for base case reactivity coal. 2 - two roll cells, 4 - four roll cells, u - unstable solution.

2.6.2 Ignition point calculations in the open-topped box

Ignition points in the open-topped box were calculated using the continuation procedure described in section 2.4.2. The calculation was performed for different sized boxes and several pre-exponential factors. The idea behind this analysis was to find the stable roll cell size at ignition, and to relate this to the correct choice of characteristic length to be used in the criteria for ignition. This

was important because the results of section 2.6.1 did not provide any real information on the preferred roll cell size, except that long, flat cells are not formed and oscillatory convection occurred.

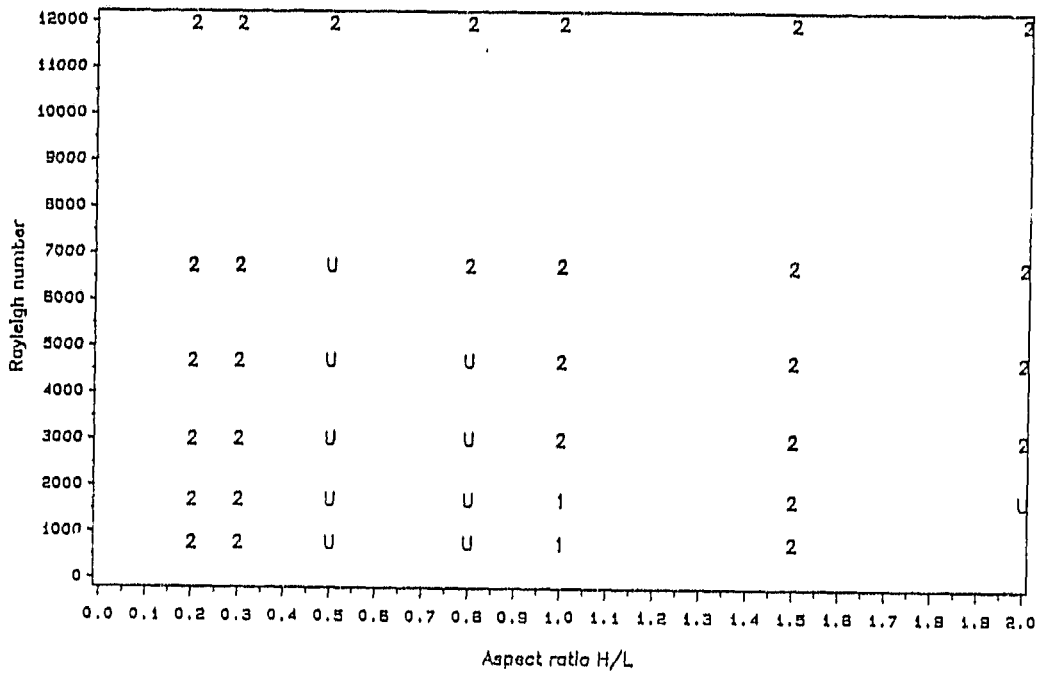

Figure 2.19 Stable roll cells in the open-topped box for a low reactivity coal. 2 - two cells, 4 - four cells, u- no stable solution.

The analysis of the results was unfortunately complicated by the fact that the boxes which showed multiple flow cells generally had cells of uneven size, making it very difficult to draw conclusions about the relationship between cell size and ignition point particle size. It was also found that a number of cases had no stable solution, but did not show numerical breakdown. This is the same phenomenon as discussed in section 2.6.1 and it seems likely that for these cases the convection is either periodic or possibly chaotic. This situation is found most frequently for boxes of small aspect ratio, in which it would be expected that a large number of convection cells would be formed. The results of the calculations are presented in table 2.4.

Aspect ratio B of box	Number of cells	Ra_i	$\varphi^2_{h_i}$	D_{pi} (mm)	k_o (m/s)	L (m)
1.0	2	2083.5	0.243	9.65	10	15
0.5	4	1528.5	0.050	11.70	10	30
0.333	4	2178.5	0.015	17.09	10	45
2.0	1	2573.8	0.616	7.585	5	7.5
1.0	2	1286.0	0.154	7.585	5	15
0.666	2	936.1	0.066	7.92	5	22.5
0.5	4	3053.2	0.018	16.52	5	30
0.333	4	617.0	0.014	9.10	5	45

Table 2.4 Ignition point calculations for the open-topped box

From the results in table 2.4 it can be seen that the preferred cell size appears to be one with an aspect ratio of 2, i.e the cell is half as wide as the height of the box and the hot-spot separation is equal to the height. This is a result of great interest, as it can be compared with the cell size found by an analytical technique described in Chapter 3.

2.7 Concluding remarks

In this chapter a numerical investigation has been made into the ignition behaviour of small coal stockpiles and the edges of very large ones. It appears that the particle size at ignition in this situation can be calculated from a simple algebraic expression, to within the limits of accuracy required by the practitioner in industry. For coal stockpiles which show only one natural convection pattern, the following expression describes the locus of ignition points both in frusta and on the edges of very large beds of trapezoidal cross section:

$$Ra^* = \frac{\sqrt{B^2 + 1}}{B} FK \qquad (2.44)$$

In terms of physical parameters, to avo'd ignition the particle size D_p must be such that:

$$D_p > D_{pi} = \left(\frac{1-\epsilon}{\epsilon} \right) \left[\frac{900\ \gamma^2\ \beta\ \mu\ k_o\ \exp(-\gamma)\ H\ \sqrt{B^2 + 1}}{\eta\ T_a\ g\ \rho_a\ B} \right]^{1/3} \qquad (2.45)$$

This is a similar relationship for the particle size at ignition as was derived for a simplified one dimensional model, Eq.(1.7) (Brooks et al.,1988a). It has been found that if the length of the diagonal from the toe of the stockpile to the centreline at the upper surface of the stockpile is used as the length in Eqs. (2.44)-(2.45) then Eq. (2.45) becomes identical to Eq. (1.7). It appears that this length in some way approximates the length of an "average streamline", and that good agreement between the one-dimensional model and the frusta or edge model is achieved because the one-dimensional model is modelling in some sense this "average streamline".

It was found that as the coal beds were made flatter and longer, multiple convection cells formed. By experimentation, convection cells were found to form when the length of the flat upper surface of the layer was greater than 1.5 times the height of the layer. The horizontal separation of two adjacent hot-spots in the stockpile was found to be equal to 1-1.5 times height of the layer. In terms of the geometric parameters A and B defined in Eqs. (2.19g)-(2.19h), the condition for the formation of multiple cells may be expressed:

$$\frac{(1 - A)}{B} > 1.5 \qquad (2.46)$$

When the stockpile shows multiple convection cells Eq. (2.44) no longer describes the locus of ignition points, and the following criterion should be used:

$$FK = b \left(1 - \frac{5}{\sqrt{Ra^*}} \right) \qquad (2.47)$$

Where,

for frusta: $b = 27.9$ (2.48)

for edges: $b = 18.15$ (2.49)

In the limit as the Rayleigh number becomes very large the particle size must be such that:

$$D_p > D_{pi} = \frac{\beta \gamma 6 k_o \rho_a (1 - \epsilon) H^2 c_p \exp(-\gamma)}{b \quad k_e} \qquad (2.50)$$

The constant b includes a correction to convert from the diagonal length of the edge cell to the height of the bed. The appropriate length scale when multiple cells form appears to be the length of the diagonal of the edge cell. Because the stockpiles always show an odd number of cells, the widths of the internal cells and the outflow region of the edge cell are always equal, and the hot-spot separation is 1-1.5 times the height of the stockpile, it is possible to predict *a priori* approximately what this diagonal length will be. It can be seen that the functional forms of the two ignition point criteria Eqs. (2.44) and (2.47) are quite different, indicating that the fundamental behaviour of the beds in each of these two cases is governed by a completely different mechanism. It was expected that Eq. (2.44) would not predict ignition points in the multiple cell case, because the internal convection cells experience a flow turn-around, and this is clearly a very different situation to that modelled by the one-dimensional chimney. In the limit as Ra becomes very large Eq. (2.47) is of the same form as the thermal explosion limit or the conduction asymptote for the one-dimensional models, indicating the importance of conduction when cells form.

We are now in a position to predict ignition point particle sizes in small coal stockpiles from simple algebraic expressions which can easily be used by the practitioner in industry. In the next chapter a method is developed of finding ignition points in the interior of large coal stockpiles using an approximate analysis.

CHAPTER 3

IGNITION POINTS IN VERY LARGE COAL STOCKPILES

3.1 Introduction

In this chapter an infinite layer of coal is considered, and by using an approximate analysis the two- and three-dimensional convective planforms are examined and ignition points calculated for a zero order reaction for the interior of a coal bed. This complements the work of Chapter 2, in which small coal stockpiles or the edges of large ones were examined, and completes the analysis of ignition points in coal stockpiles. In section 3.2 the model is discussed. In section 3.3 the conduction only solution is examined as a worst case solution and the thermal explosion limits are calculated using a method that can be used to obtain ignition points for the conduction-convection problem. The determination of the onset of convection is discussed in section 3.4. The convection planforms are examined in section 3.5 and in section 3.6 it is shown how ignition points may be obtained for the infinite layer model, and a simple relationship is presented for the particle size at ignition. A method for determining the stability of the steady-state convection planforms is described in section 3.7.

Related to the modelling of spontaneous combustion is the classical theory of thermal explosions and particularly the recent work which has been done on the effect of natural convection on thermal explosion, in which it has been shown that natural convection stabilises the reaction and increases the value of the critical Frank-Kamenetskii parameter (FK, defined in the nomenclature) for explosion. Most of this work has considered two-dimensional convection using approximate analyses. Jones,1973 calculated marginal stability curves for the onset of convection in a confined exothermically-reacting fluid, assuming the reaction to be of zero order. He showed that for small Rayleigh numbers it was possible to proceed directly to explosion without convection ever becoming significant. Merzhanov and Shtessel,1973 examined the effect of natural convection on the thermal explosion of liquids and showed that sufficiently vigorous natural convection could stabilise the system. Kordylewski and Krajewski,1984 used a numerical technique to study the effect of natural convection on the ignition of a porous material with a zero order chemical reaction. They showed that the critical condition for ignition was shifted to higher temperatures than for the

pure conduction case, and they also found evidence for the existence of oscillatory convection at high Rayleigh numbers. They postulated that this form of convection was similar to turbulence and that the improvement of heat transfer due to turbulence indicated that for sufficiently high Rayleigh numbers ignition could be prevented. Viljoen and Hlavacek,1987 used a continuation method to trace the branches of stability for a zero order porous medium exothermic reaction in a rectangular cavity. They used a low-order Galerkin method and showed that natural convection has the effect of stabilising the system. The thermal explosion limit was calculated using a polynomial approximation to the exponential temperature dependence. For the convecting system they found a Hopf bifurcation at a larger critical parameter value than for the thermal explosion limit, beyond which they could find no solutions. It was presumed that explosion occurred beyond this point. Viljoen et al.,1988 calculated induction times for the onset of natural convection and for thermal explosion for a zero order reaction in a porous medium. If the induction time for the onset of natural convection is shorter than that for thermal explosion, natural convection can stabilise the bed. This is of interest in the storage of coal as it may be the case that the time to spontaneous combustion is longer than the required stockpiling time.

In addition to the considerable volume of work on the stability of fluid motions (e.g. Joseph,1976) some work has been done on the stability of systems with internal heat generation, considering the stability of different flow planforms, and conditions for the onset of natural convection. Roberts,1967 used a mean-field approximation to study three-dimensional convection patterns in a fluid with uniform internal heat generation. He found that two-dimensional rolls were stable for all Rayleigh numbers (Ra) and that down-hexagons were stable for a limited range of Rayleigh numbers. Tveitereid and Palm,1976 examined the same problem and found that down-hexagons were the stable planform for a limited range of Rayleigh numbers and that rolls were not a stable planform. The discrepancy is probably due to the approximations used by Roberts,1967. Tveitereid,1977 considered a similar problem in a porous layer with impermeable horizontal surfaces and found stable rolls and down-hexagons for a limited range of Rayleigh numbers, while up-hexagons were unstable for all Ra. Steinberg and Brand,1983 examined the instabilities in a porous layer with a binary mixture with a fast chemical reaction. The medium was heated either from above or below and the authors found that stationary or oscillatory instabilities appeared depending on the sign

and magnitude of the heat of reaction.

In a series of papers Gatica et al.,1987a, 1987b, 1988 considered the stability of chemically reacting systems for both forced flow and natural convection in porous media. In their 1987b paper they considered non-linearly stratified fluids and showed that at the onset of convection the local convection cells could be better represented by local eigenfunctions than by global ones. They showed that for large aspect ratios (width/height) FK had a stabilising effect while the opposite was true for small aspect ratios. As expected, smaller wave number perturbations were found more likely to survive as the aspect ratio was decreased. Their 1988 paper examined both forced flow and closed cavity natural convection with chemical reaction. Strong convection was found to favour the formation of small convection cells. Viljoen et al.,1989 considered a porous medium in a cavity with a catalytic surface and showed the existence of oscillatory convection for certain conditions. They also showed that the onset of convection could be marked by oscillatory instabilities.

3.2 Model formulation

The model used in this chapter is derived using the same assumptions as were discussed in Chapter 2. The computational domain differs, as do the associated boundary conditions. We consider a laterally-unbounded layer of coal of uniform thickness which approximates the interior of a large coal bed, and allows assumption of spatially-periodic solutions.

The dimensionless Darcy-Oberbeck-Boussinesq equations defining the model are:

$$\nabla \cdot \underline{u} = 0 \tag{3.1}$$

$$\nabla \Pi + \underline{u} - Ra\ \theta\ \hat{z} = 0 \tag{3.2}$$

$$\varphi \frac{\partial \theta}{\partial \tau} + \underline{u} \cdot \nabla \theta = \nabla^2 \theta + \beta \varphi_h^2 \exp\left\{\frac{\gamma \theta}{1+\theta}\right\}(1+T) \tag{3.3}$$

$$0 = Le\ \nabla^2 T - \underline{u} \cdot \nabla T - \varphi_h^2 \exp\left\{\frac{\gamma \theta}{1+\theta}\right\}(1+T) \tag{3.4}$$

The dimensionless variables are defined in the nomenclature and typical values of the parameters are given in Appendix A. From Eqs.

(3.1) and (3.2) one can show that there is no vertical component of vorticity, hence the velocity $\underline{u}$ is poloidal and can be replaced by the scalar potential χ (Joseph,1976)(see Appendix H):

$$\underline{u} = \underline{\delta}\,\chi = \left(\frac{\partial^2}{\partial x \partial z}, \frac{\partial^2}{\partial y \partial z}, - \nabla_1^2 \right) \chi \qquad (3.5)$$

where ∇_1^2 is the horizontal Laplacian.

Taking the curl of the momentum equations to eliminate pressure gives:

$$\nabla^2 \chi = - Ra\ \theta \qquad (3.6)$$

$$\varphi \frac{\partial \theta}{\partial \tau} + \underline{\delta}\chi \cdot \nabla \theta = \nabla^2 \theta + \beta\, \varphi_h^2 \exp \left\{ \frac{\gamma \theta}{1 + \theta} \right\} (1 + T) \qquad (3.7)$$

$$0 = Le\ \nabla^2 T - \underline{\delta}\chi \cdot \nabla\ T - \varphi_h^2 \exp \left\{ \frac{\gamma \theta}{1 + \theta} \right\} (1 + T) \qquad (3.8)$$

For the zero order reaction model one need retain only Eqs. (3.6) and (3.7) with T equal to zero. The coal layer is bounded below by an impermeable, perfectly-conducting plane while the upper surface is permeable and also at ambient temperature. This is known to be a reasonable assumption for real coal beds. For the oxygen concentration boundary condition one can assume that good backmixing occurs on the upper surface of the bed so that the concentration is ambient there, with no flux on the lower surface. Note that Schmal et al.,1985 found that the outlet oxygen boundary condition had little effect on the temperature profiles in their one-dimensional model. The boundary conditions are:

$$- \nabla_1^2 \chi\ (0) = \theta\ (0) = \frac{\partial T}{\partial z}(0) = 0 \qquad (3.9a)$$

$$- \frac{\partial}{\partial z} \left(\nabla_1^2 \chi\ (1) \right) = \theta\ (1) = T\ (1) = 0 \qquad (3.9b)$$

3.2.1 Simplification of the model

Since the activation energy in the system is usually large (typically $\approx$60kJ mol^{-1} K^{-1}) and the temperature rise small (<40°C) for solutions on the extinguished branch, one can replace the Arrhenius temperature dependence by the approximation introduced by Frank-Kamenetskii,1969 in thermal explosion theory:

$$\frac{E}{R\,T} \approx \frac{E}{R\,T_a} - \frac{E}{R\,T_a} \left(\frac{T - T_a}{T} \right) \qquad (3.10)$$

to write:

$$w = \gamma\ \theta \tag{3.11}$$

In terms of the new variable w the model now becomes:

$$\nabla^2\ \chi = -\ Ra^*w \tag{3.12}$$

$$\varphi\ \frac{\partial\ w}{\partial\ \tau}\ +\ \underline{\delta}\chi\cdot\ \nabla\ w = \nabla^{\ 2}w + \frac{FK^*}{\sqrt{Ra^*}} e^{\ w}(\ 1 + T\ ) \tag{3.13}$$

$$0 = Le\ \nabla^2\ T\ -\ \underline{\delta}\chi\cdot\ \nabla\ T\ -\ \frac{FK^*}{\gamma\ \beta\ \sqrt{Ra^*}} e^{\ w}(\ 1 + T\ ) \tag{3.14}$$

where

$$FK^* = \beta\ \Delta\ \sqrt{\gamma} \tag{3 15}$$

$$\Delta = \varphi_h^2\ \sqrt{Ra} \tag{3.16}$$

$$Ra^* = \frac{Ra}{\gamma} \tag{3.17}$$

The temperature boundary condition becomes:

$$w(0) = w(1) = 0 \tag{3.18}$$

Because one is primarily interested in calculating ignition points in the infinite layer, it will be assumed that the reaction is of zero order. This assumption is known to be good at ignition (Chapter 2, Viljoen et al.,1988) and the validity of the assumption was checked for the results in section 3.6.

3.3 Conduction-only solution

In the classical thermal explosion theory it can be shown that solutions to the conduction-only problem exist only for values of FK less than FK_{crit}, where FK_{crit} depends on the geometry of the system. The effect of natural convection is to shift the thermal ignition point to higher temperatures and to increase the value of FK_{crit} compared to the pure conduction case. In terms of the coal bed this means that the ignition point is shifted to a smaller particle size, giving a larger range of safe stockpiling sizes. One can thus consider the pure conduction solution to be a worst case solution. The conduction-only solution is also applicable when the induction time for convection is longer than the time to thermal explosion. Normally one might expect that in a real coal bed there would always be perturbations to the bed sufficiently large that a conduction-only solution could not exist. However, it may be the case

that the perturbations to the coal bed are not in the region of attraction of the convective solution. Simply put, the perturbations may be so small that before any appreciable flow develops in the bed a thermal explosion situation has been reached. It can be shown that when conduction is the only heat transfer mechanism in a coal bed thermal explosion will occur for $\delta=3.514$ (see e.g. Frank-Kamenetskii (1969)) . The associated temperature will be low, ~308K. Viljoen et al. 1988 have shown that if the induction time for natural convection is longer than the time for thermal explosion then thermal explosion will occur in the material concerned.

One can calculate the thermal explosion limit for the conduction-only case numerically, using both a collocation method and the Galerkin method. Thermal explosion is indicated by the breakdown of the numerical method and for a zero order reaction one can check the explosion limit by comparison with the known analytical solution. This is instructive because when considering the conduction-convection problem it is not possible to obtain an analytical expression for the ignition point, while use of the breakdown of the computational scheme to indicate ignition is easy and has previously been shown to be effective in Chapter 2. For the conduction-convection problem it is possible to calculate ignition points directly or by using an arc-length continuation scheme, however both these methods become more difficult to apply as the complexity of the model increases.

The conduction-only equation for the zero order reaction is:

$$\frac{d^2w_c}{dz^2} + FK\, e^{w_c} = 0 \;,\; w_c(0) = w_c(1) = 0 \qquad (3.19)$$

Equation (3.19) was solved using orthogonal collocation and ignition was indicated by divergence of the computations. In later sections where the Galerkin method is used to solve the conduction-convection problem one has to expand the exponential function of temperature as a polynomial. It is useful to see the effect of this approximation on the thermal explosion limit and accordingly the following equation is solved in which the temperature exponential has been expanded as a second order polynomial about $w_c=0$:

$$\frac{d^2w_c}{dz^2} + FK\left(1 + w_c + \frac{w_c^2}{2}\right) = 0 \;,\; w_c(0) = w_c(1) = 0 \qquad (3.20)$$

For comparison purposes equation (3.20) was also solved by a Galerkin method. The Galerkin method provides a convenient means of solving

boundary value problems, and the essence of the method is given below. Further details are given in many texts e.g. Kantorovich and Krylov,1964.

Consider a system of two linked differential equations in terms of u(x,y,z) and v(x,y,z) on the domain D. This system may be represented by the differential operators

$$L_1(u,v) = 0 \tag{3.21a}$$

$$L_2(u,v) = 0 \tag{3.21b}$$

The solutions are approximated by

$$u^*(x,y,z) = \sum_{i=1}^{n} c_{1i}\, \varphi_{1i}(x,y,z) \tag{3.22a}$$

$$v^*(x,y,z) = \sum_{i=1}^{n} c_{2i}\, \varphi_{2i}(x,y,z) \tag{3.22b}$$

$\varphi_{1i}(x,y,z), \varphi_{2i}(x,y,z)$, i=1,2,...,n satisfy the boundary conditions. The c_{1i}, c_{2i} are the undetermined coefficients. For (u^*,v^*) to be an exact solution to the problem, i.e. for:

$$L_1(u^*,v^*) = 0 \tag{3.23a}$$

$$L_2(u^*,v^*) = 0 \tag{3.23b}$$

it is required that $L_1(u^*,v^*)$ be orthogonal to the complete set of functions φ_{1i}, i=1,2,...,n,.... and that $L_2(u^*,v^*)$ be orthogonal to the complete set of functions φ_{2i}, i=1,2,...,n,.... However we have an incomplete set with c_i, i=1,2,..n. Thus only n orthogonality conditions can be satisfied:

$$0 = \iiint_D L_1(u^*(x,y,z),v^*(x,y,z))\, \varphi_{1i}(x,y,z)\, dxdydz =$$

$$\iiint_D L_1\left(\sum_{j=1}^{n} c_{1i}\varphi_{1i}(x,y,z)\ ,\ \sum_{j=1}^{n} c_{2i}\varphi_{2i}(x,y,z)\right) \varphi_{1i}(x,y,z)\, dxdydz \tag{3.24a}$$

$$0 = \iiint_D L_2(u^*(x,y,z),v^*(x,y,z))\ \varphi_{2i}(x,y,z)\ dxdydz =$$

$$\iiint_D L_2\left(\sum_{j=1}^{n} c_{1i}\varphi_{1i}(x,y,z)\ ,\ \sum_{j=1}^{n} c_{2i}\varphi_{2i}(x,y,z)\right)\ \varphi_{2i}(x,y,z)\ dxdydz \qquad (3.24b)$$

From Eqs (3.24a)-(3.24b) the coefficients c_{1i}, c_{2i} can be determined and hence from Eqs. (3.22a)-(3.22b) the approximate solution to the original problem (Eqs. (3.21a)-(3.21b)) can be recovered.

To solve Eq. (3.20) using the Galerkin method, the conduction-only equation with a quadratic approximation to the temperature exponential, solutions are sought of the form:

$$w = \sum_{n=1}^{\infty} A_n \sin(n\pi z) \qquad (3.25)$$

Substitution of (3.25) into (3.20), multiplication by the particular value and integration over the layer yields the following infinite set of algebraic equations:

$$-\frac{m^2\pi^2}{2} A_m + FK\left\{\frac{1-(-1)^m}{m\pi} + \frac{A_m}{2} + \frac{1}{2}\sum_{n,p} A_n A_p \int_0^1 \sin(p\pi z)\right.$$

$$\left. X\ \sin(m\pi z)\sin(n\pi z)\,dz\right\} = 0 \qquad (3.26)$$

The series can be truncated at some suitable point. The resulting set of non-linear equations was solved using the NAG routine C05NBF, which uses a modification of Powell's Method. The integral in Eq. (3.26) was evaluated numerically.

The results of the thermal explosion limit calculations are summarised in table 3.1.

Eqn	solution method	number of collocation points	Order of polynomial	Number of Galerkin terms	FK_c
3.19	collocation	15	9	-	3.5139
	"	15	7	-	3.5140
	"	15	11	-	3.5139
3.20	"	15	11	-	3.9979
	"	15	7	-	3.9979
3.20	Galerkin	-	-	25	4.0200

Table 3.1. Values of the critical Frank-Kamenetskii parameter for the conduction-only model with zero order reaction.

The value of FK_{crit}=3.514 for the solution of (3.19) agrees exactly with the analytical solution, while FK_{crit} for the approximate equation (3.20) is larger, FK_{crit}=3.9979. This compares with the work of Viljoen and Hlavacek,1987 in which it was found that FK_{crit}=3.995. It would be expected that FK_{crit} for Eq. (3.20) would be larger than for Eq. (3.19) as the source term in (3.20) is less strongly temperature dependent. However the quadratic approximation still retains the thermal explosion. The high order Galerkin method gives a result comparable to the collocation method for the solution of Eq. (3.20). The approximate model Eq. (3.20) shows a larger value of FK_{crit}, which means that the approximation is not conservative, i.e. it predicts ignition at a smaller particle size than does the rigorous model. This point must be borne in mind in later sections as it is possible that the analysis of the conduction-convection problem will also not be conservative. It seems that the breakdown of the numerical method gives a reliable indication of the presence of the ignition point. This is encouraging for the convection situation where direct methods of locating the ignition point become more difficult and breakdown of a numerical scheme can readily be used as a guide to the presence of a bifurcation point.

3.4 Onset of convection

The temperature profile set up when a porous layer is heated either from below or internally depends on the value of Ra. Below a critical value of Ra (Ra_{crit}) conduction is the only form of heat transfer while beyond Ra_{crit} convection commences and modifies the the heat transfer and temperature profile. This is the porous medium analogue

of the classical Rayleigh-Benard problem. Any lateral temperature gradient in a coal bed in which conduction is the only form of transport will immediately give rise to convection. As there will inevitably be such gradients in a real coal bed it is reasonable to assume that convection will always be present. However it is of interest to calculate the onset of convection because the wave number at which convection commences gives an indication of the size of convection cell which is likely to be first formed. In what follows the neutral stability curve for the onset of monotonic convection is calculated by assuming that the principle of the exchange of stabilities holds. Viljoen et al.,1989 have shown that the onset of oscillatory convection can in fact precede steady convection under certain conditions for a first order chemical reaction.

At the onset of convection the convection solution (χ, w) is approximated by:

$$\chi = \delta\ \tilde{\chi}_1 + \delta^2\ \tilde{\chi}_2 + \ldots\ldots \tag{3.27}$$

$$w = w_c + \delta\ \tilde{w}_1 + \delta^2\ \tilde{w}_2 + \ldots. \tag{3.28}$$

where the subscript c represents the conduction solution and the parameter δ is assumed to be small enough to allow a linear theory to be formulated. The conduction solution is known to exist only f $FK<FK_{crit}$.

Substitution of Eqs. (3.27) and (3.28) into Eqs. (3.12) and (3.13) and retaining only terms of order δ yields

$$\nabla^2\ \tilde{\chi}_1 = -\ Ra^*\ \tilde{w}_1 \tag{3.29}$$

$$\varphi \frac{\partial\ \tilde{w}_1}{\partial\ \tau} = \nabla^2\ \tilde{w}_1 + \nabla_1^2\ \tilde{\chi}_1 \frac{d\ w_c}{d\ z} + \frac{FK^*}{\sqrt{Ra}^*}(\ \tilde{w}_1 + \tilde{w}_1\ w_c) \tag{3.30}$$

Solutions of the form

$$\tilde{w}_1 = G \exp\left\{ i (k x + l y) \right\} \sin (\pi z) \exp (\sigma \tau) \quad (3.31)$$

$$\tilde{x}_1 = G \exp\left\{ i (k x + l y) \right\} F (a , z) \exp (\sigma \tau) \quad (3.32)$$

are sought.

The form of F(a,z) is found by substituting (3.31) and (3.32) into (3.29) and solving the resulting ordinary differential equation. The form of F(a,z) is given in Appendix D. This is the approach followed by Tveitereid,1977. Eqs. (3.31) and (3.32) are a first order truncation of a Fourier-type series where it has been assumed that a first order truncation will adequately represent the small convection perturbations to the basic solution. The conduction solution is approximated by an n-term series, Eq. (3.25) as it is expected that the solution will be conduction-dominated. Only monotonic convection is considered and accordingly $\sigma=\sigma_r+i\sigma_i=0$. Application of the Galerkin method gives the following dispersion relation:

$$0 = -\frac{a^2+\pi^2}{2} - a^2 \sum_n n \pi A \int_0^1 F (a , z) \cos (n \pi z) \sin (\pi z) dz + \frac{FK^*}{\sqrt{Ra^*}} \left(\frac{1}{2} + \frac{A_1}{2} \right) \quad (3.33)$$

The sytem has been parameterized so that Ra^* is the only parameter which is a function of particle size. The point of the onset of convection is given by $\min(Ra^*,a)$ on the neutral stability curve of Ra^* as a function of a. The neutral stability curve for $FK^*=50$ is shown in figure 3.1.

It can be seen that the curve rises extremely rapidly for $0.5>a>4$, and that the value of the minimum wave number is at $a\approx1.6$. A typical family of neutral stability curves is presented for $FK^*=50$, 70, 80 in figure 3.2.

It is expected that the range of stable wave numbers will lie close to the minimum value of a and so figures 3.1 and 3.2 give a useful indication of where one should seek solutions to the convection-conduction problem. Tveitereid,1977 found that the range of stable wave numbers for a porous layer with internal heat generation was quite small, and close to the minimum wave number at

the onset of convection.

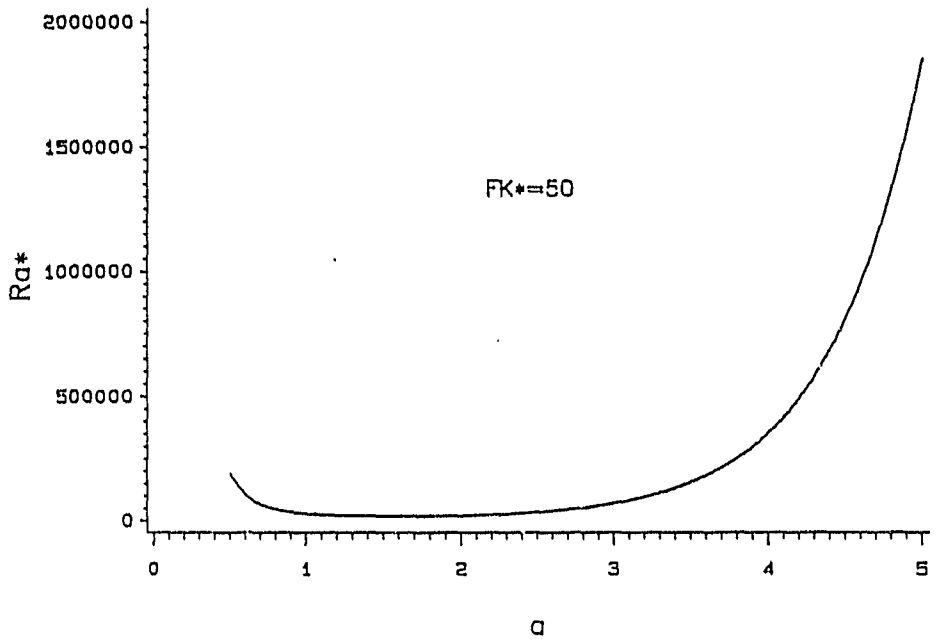

Figure 3.1 Neutral stability curve for the onset of monotonic convection for $FK^*=50$

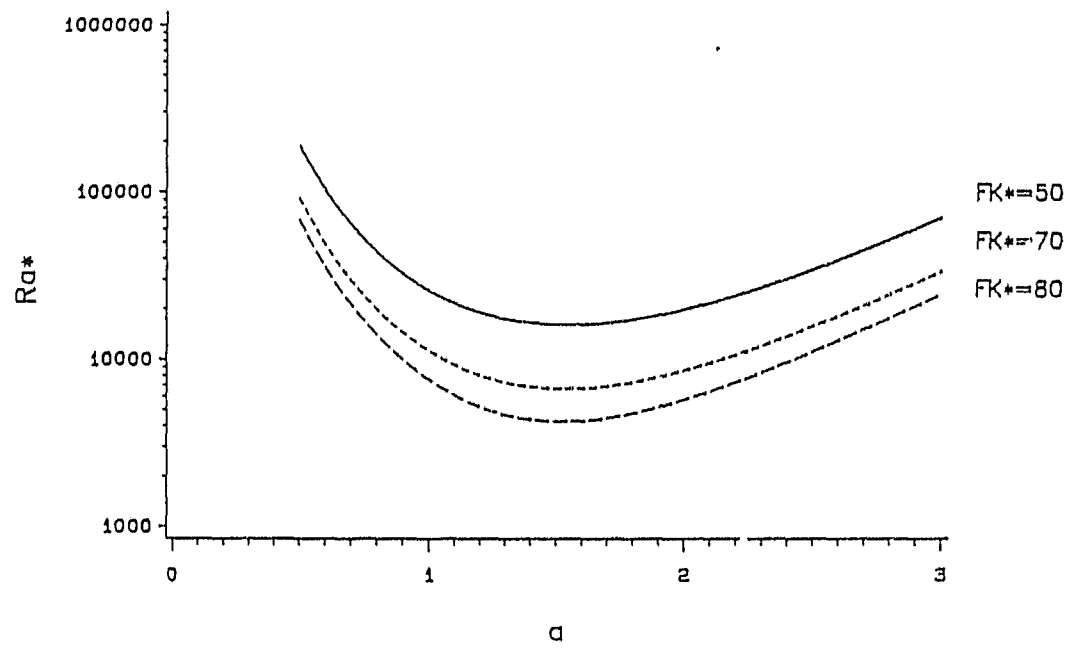

Figure 3.2 Neutral stability curves for the onset of montonic convection showing dependence on FK^* for $FK^*=50$, 70, 80

The neutral stability curve cannot exist for values of FK* greater than the thermal explosion limit. One can also calculate the thermal explosion limit by using a continuation procedure at a fixed wave number to calculate Ra^* for the onset of convection. The thermal explosion limit is indicated by breakdown of the numerical method. FK^* is used as the continuation parameter. The results of such a calculation can be seen in figure 3.3 , where the neutral stability curve appears as the almost vertical line terminating just above the thermal explosion limit curve that was calculated using the exact value FK=3.51.

For the parameter set used in figure 3.3 the numerical scheme indicated thermal explosion at FK^*=100. Although the curve does not exactly intersect the thermal explosion limit curve, at the point that the continuation scheme broke down the tangent of the neutral stability curve was almost vertical and steepening, which indicates that FK^* at the explosion point had been found within the limits of accuracy of the numerical scheme. As expected Ra^* at the explosion point is not found very accurately.

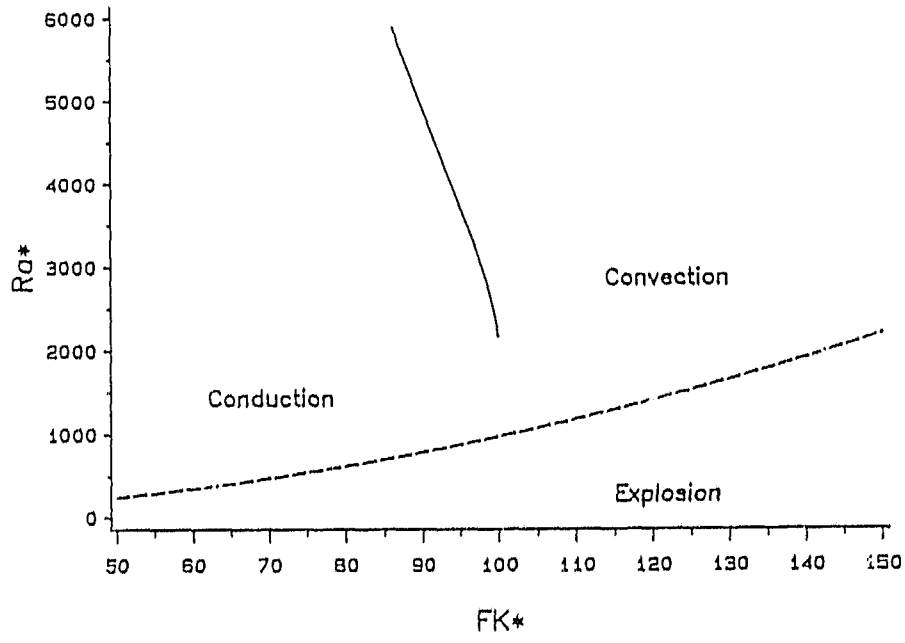

Figure 3.3 Neutral stability curve and thermal explosion limit for the infinite layer with a=1

3.5 Steady and unsteady-state convection patterns

The main interest in these results lies in the steady and unsteady-state convection patterns and the determination of ignition points. Steady and unsteady-state convection patterns were obtained for the zero order model closely following the approach of Tveitereid,1977. The Galerkin method is used to transform the set of partial differential equations (3.12)-(3.13) into either an infinite set of algebraic equations for the steady-state case or an infinite set of ordinary differential equations for the unsteady-state problem. A brief description of how this was done is given in Appendix D. Solution of a suitably truncated set of these equations allows one to recover the temperature and velocity profiles in the coal layer.

Solutions of the form:

$$w = \sum_{h} \sum_{p,q} B_{pqh} \exp\left\{ i(pkx + qly) \right\} \sin(\pi hz) \qquad (3.34)$$

$$\chi = \sum_{h} \sum_{p,q} B_{pqh} \exp\left\{ i(pkx + qly) \right\} F_h(\lambda,z) \qquad (3.35)$$

are sought,

where:

$$\lambda^2 = (pk)^2 + (ql)^2 \qquad (3.36)$$

in which k and l are the x- and y-components of the wave number a.

The limits on the integer summation indices are:

$$-\infty < (p,q) < \infty \; ; \; 1 \leq h < \infty \qquad (3.37)$$

The form of $F_h(\lambda,z)$ is found by substituting (3.36) and (3.37) into (3.12) and solving the resulting ordinary differential equation. $F_h(\lambda,z)$ is given in Appendix D.

To obtain the system of algebraic equations, Eqs. (3.34)-(3.35) are substituted into (3.13), the equation multiplied by its weighting function and integrated over the layer. This results in an infinite set of equations in the coefficients B_{rsg}. As discussed in section 3.3 the exponential function of temperature is approximated by a second order Taylor expansion about w=0, which it is expected will under-estimate the reaction rate dependence on temperature. In steady-state form the infinite set of equations is:

$$0 = -\frac{1}{2} B_{rsg} (g^2\pi^2 + \nu^2) - \sum_{h,f} \sum_{\substack{p+t=r \\ q+u=s}} B_{pqh} B_{tuf} \left\{ \lambda^2 b(f,g,h,\lambda) - (ptk^2 + qul^2) a(f,g,h,\lambda) \right\} + \frac{FK^*}{\sqrt{Ra^*}} \left\{ \frac{1}{2} B_{rsg} + \frac{(1 - (-1)^g)}{g\pi} \Big|_{r=s=0} + \sum_{h,f} \sum_{\substack{p+t=r \\ q+u=s}} \left[\frac{1}{2} B_{pqh} B_{tuf} c(f,g,h) \right] \right\} \quad (3.38)$$

where:

$$\nu^2 = (rk)^2 + (sl)^2 \quad (3.39)$$

The integrals $a(f,g,h,\lambda)$, $b(f,g,h,\lambda)$ and $c(f,g,h)$ are given in Appendix D. In order to limit the solutions of this set of equations to those which one would expect are physically reasonable, the infinite set is truncated such that modes for which:

$$g^2 + \frac{3}{4} r^2 + \frac{1}{4} s^2 > \Lambda^2 + 1 \quad (3.40)$$

are neglected, where Λ is an integer truncation number. This is the form of truncation used by Tveitereid,1977 and Tveitereid and Palm,1976. The components of the wave number satisfy:

$$k^2 + l^2 = 4 l^2 = a^2 \quad (3.41)$$

Only real coefficients where:

$$B_{rsg} = B_{-r-sg} = B_{r-sg} = B_{-rsg} \quad (3.42)$$

are considered.

These restrictions allow hexagons, rolls and squares to be planforms as these are the most likely solutions (Tveitereid,1977, Tveitereid and Palm,1976) and it is known that these are physically reasonable solutions (Chandrasekhar,1961, White,1988, Busse and Frick,1985).

Steady-state solutions were obtained using the NAG routine C05NBF, which uses a modification of Powell's Method. The integrals $a(f,g,h,\lambda)$, $b(f,g,h,\lambda)$ and $c(f,g,h)$ were evaluated numerically, and the results were checked against an alternative form of the computer program in which the integrals were expressed analytically. The

results were identical. A listing of the computer program is given in Appendix E.

Figures 3.4a and 3.4b show a horizontal section of the infinite coal layer at half the height of the layer. The down-hexagonal planform can be clearly seen, with the principle vertices of the hexagons at the centres of the triangular-shaped blobs.

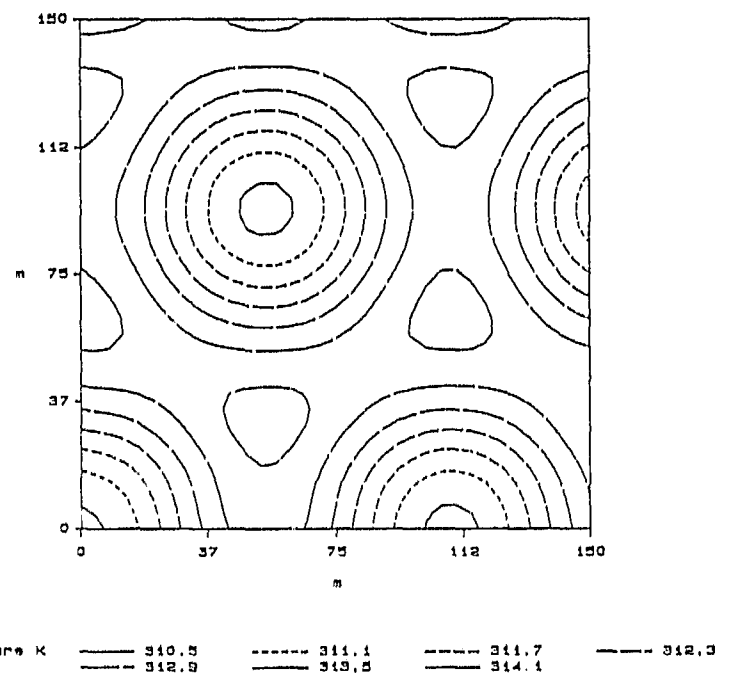

Figure 3.4a Horizontal section of the coal layer at half-height showing isotherms with a=1, τ=90, FK=10.37

The planform in figure 3.4 was obtained by solving Eq. (3.39) in unsteady-state form. The left-hand side of the equation was replaced by $\varphi\partial w/\partial\tau$. The initial condition was a mild up-hexagon planform. (An up-hexagon is defibed as one in which the flow rises at the centre of the centre of the cell when viewed from above). It was found that using an up-hexagonal initial perturbation gave a down-hexagonal pattern after some time, indicating that the up-hexagons are not stable to perturbations while down-hexagons are. The results for figure 3.4 were obtained with a truncation number of 2, which gives 26 terms. It was found that the computational effort increased

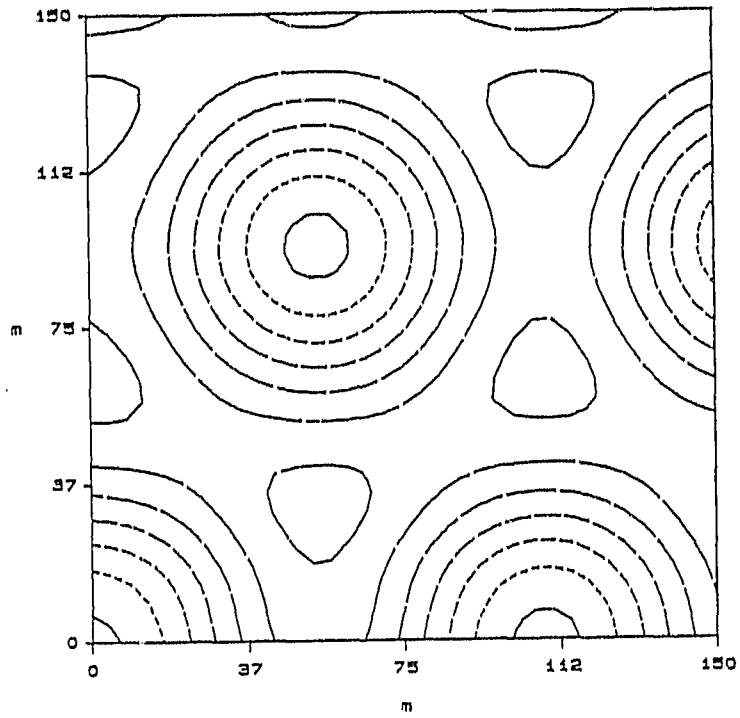

Figure 3.4b Horizontal section of the coal layer at half-height showing contours of equal vertical velocity with a=1, τ=90, FK=10.37

dramatically with increasing truncation number, restricting most of the calculations to Λ=2. It was found that Λ=1 was not a satisfactory truncation, as it gave rise to spurious oscillations. Down-hexagons appeared to be a stable planform, as solving both the steady- and unsteady-state problem with an initial perturbation of down-hexagons resulted in a final steady pattern of down-hexagons. An initial pattern of rolls did not show any change to a hexagonal pattern during the time of integration, indicating the stability of rolls to small perturbations. Ideally the stability of the steady-state solutions should be established by examining the temporal behaviour of a perturbation to the steady-state solution. Although such a stability analysis was attempted it was found that the determination of the eigenvalues was insufficiently accurate to yield any useful information (see section 3.7). The tentative conclusion that rolls and down-hexagons are the stable planforms in this system is supported

by the results of Tveitereid,1977.

The results of unsteady-state and steady-state calculations have been compared and it has been found that provided one is far from ignition the two methods give the same answer in the limit as the integration time becomes large. In most cases the steady state is reached only after many years. Close to ignition the results show poorer agreement, with the unsteady-state calculation showing explosion when the steady-state calculation does not. The reason for this is probably that the zero order reaction approximation is not good during the early stages of the flow and temperature development in the unsteady-state calculation. Early on the flow rates are very small, and one would expect oxygen consumption to be significant and thus limit the temperature rise. However, with the zero order approximation there is no oxygen limitation at low flow rates and hence the temperature can rise more rapidly, leading to explosion. The steady-state calculation does not suffer from this problem, presumably because the correspondence between iteration steps and real time is not such that high oxygen consumption is required early on in the calculation.

3.6 Ignition points in the interior of the stockpile

One can determine the ignition points in the layer either directly or by observing numerical breakdown of a continuation scheme as described in section 3.3. To calculate the ignition points directly one needs to locate the limit point of the system of algebraic equations (3.38). The system can be written:

$$f_i(\underline{x},p) = 0 \quad ,i=1,2,\ldots,n \tag{3.43}$$

where p is the bifurcation parameter. The condition for a real bifurcation point is:

$$\det(J) = 0 \tag{3.44}$$

where the elements of the Jacobian matrix are:

$$\left\{ e_{ij} \right\} = \frac{\partial f_i}{\partial x_j} \quad ,i,j=1,2,\ldots\ldots,n \tag{3.45}$$

Equation (3.44) is equivalent to saying that zero is an eigenvalue of J, hence ignition will be indicated by an eigenvalue equal to zero. Thus to locate the ignition point directly one must solve the system (3.43) and (3.44) simultaneously. There is of course the possibility

that ignition is marked by a Hopf bifurcation, but only real bifurcation is considered in this work.

In the indirect method of ignition point calculation continuation in the bifurcation parameter (e.g FK^* for a fixed Ra^*) is used until divergence of the method indicates that the ignition point has been found. In this work that was the approach followed as it was found that the eigenvalue calculation was unreliable and apt to give bifurcation points for non-physical conditions. For some cases the determinant of the Jacobian J was calculated analytically at the point located by the indirect method, and it was found that det(J) was in fact extremely close to zero, indicating that this simplistic method does give a good estimate of the ignition poin'

In figure 3.5 the locus of ignition points is shown for seven different sizes of roll cell, calculated by the continuation method for the zero order reaction.

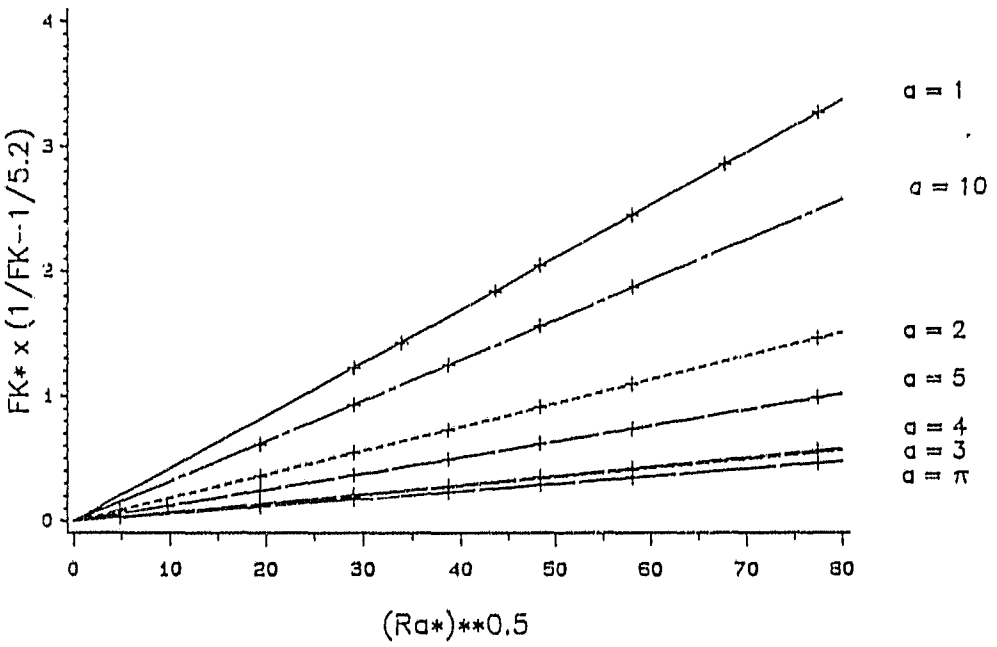

Figure 3.5 Locus of ignition points for various sizes of roll cell

The results were obtained for a truncation number Λ=2. It was found

that the locus of ignition points was described, to within the accuracy of the calculation, by $FK^*/\sqrt{Ra^*}=FK_1=$constant, FK_1 being a function of the wave number. In figure 3.5 the ignition loci have been plotted as $FK^*(1/FK_1-1/5.2)$ versus $\sqrt{Ra^*}$. This has been done so that the curves for different wave numbers can be distinguished while still showing the functional dependence. The height of the layer has been used as the characteristic length. Of interest was the result for a=1, the largest roll cell examined, where it was found that for $FK^*<60$ the system proceeds directly to thermal explosion. Such a result was also found by Jones,1973 and can be expected if the induction time for the onset of convection is greater than that for thermal explosion. This situation is likely to arise in coal beds of small particle size if the roll cell size i very large. Note also that the curves go through a minimum slope for $a=\pi$, suggesting that there might be some significance for this cell size.

As expected the presence of convection shifts the thermal explosion limit to a higher critical value. The functional dependence of FK_1 for a single wave number $a=\pi$ is shown in figure 3.6. The validity of the zero order reaction assumption was checked and it was found that at ignition the consumption of oxygen was extremely low.

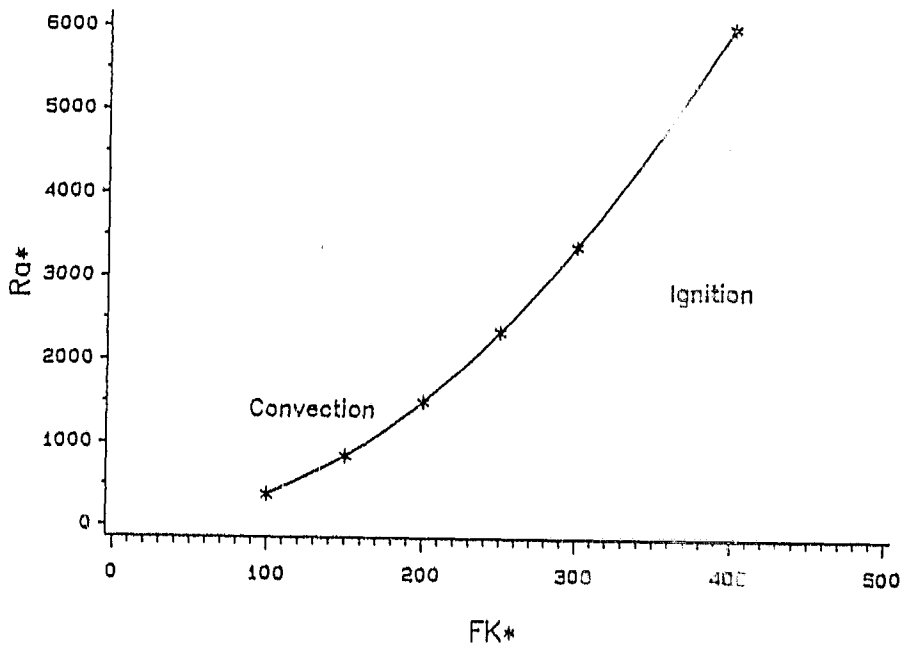

Figure 3.6 Locus of ignition points for roll cells with a=π

In figure 3.7 the locus of ignition points as a function of cell size is shown.

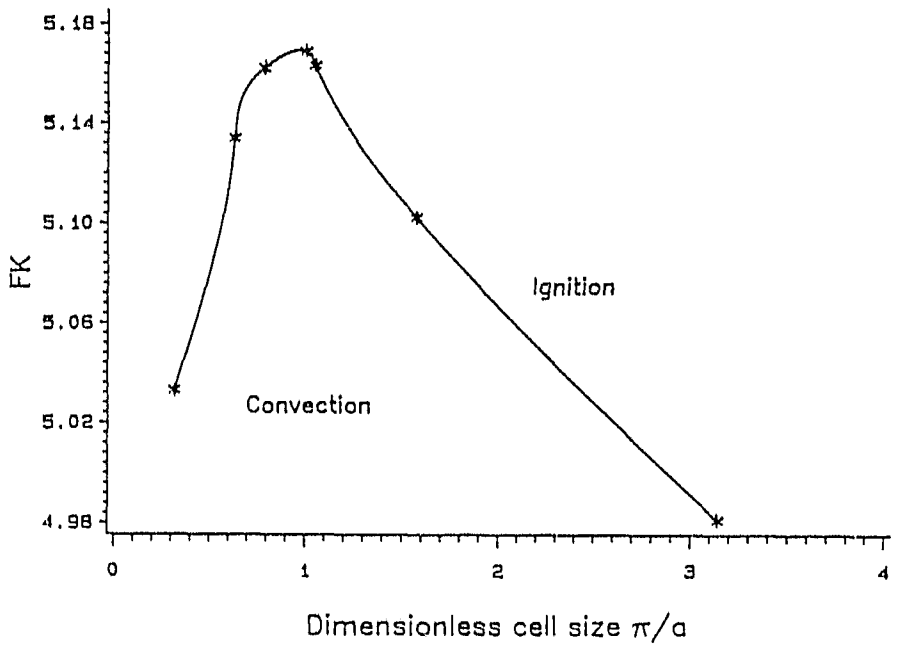

Figure 3.7 Locus of ignition points for roll cells as a function of roll cell size

One can see that there is a "best" cell size, i.e. one for which the value of FK_i is largest. This behaviour was not predicted from the ignition criterion of Brooks et al.,1988a, as in that expression:

$$Ra_L^* = FK \tag{3.46}$$

and so the ignition particle size was proportional to the cube root of the bed length, and D_{pi} should decrease montonically with decreasing bed length L. In Chapter 2 it was found that for frustum-shaped coal beds or bed edges showing only one flow cell Eq. (3.46) was able to predict satisfactorily ignition points if the length of the diagonal was used as the bed length scale L. The flow pattern in that situation was dominated by flow in through the sloping surface, while the present situation is very different in that all the flow enters and leaves through the upper surface of the infinite layer. The "best" cell size phenomenon can be explained as follows. For very

large roll cells, the average streamline is long and slow, and convection is not very strong. This means that FK_i at ignition will not be increased very much above the thermal explosion value. As the cell size is decreased somewhat the convection becomes stronger, and the stabilising effect of this strong convective flow increases FK_i compared to the large cell size case. If the cell size is decreased even more, so that the roll cell is very narrow, the flow must then turn around very sharply. This requirement has the effect of slowing down the flow so that the convection is now not as strong as for a medium cell size. Examination of the velocity profiles for different roll cell sizes showed that this reasoning is likely to be correct.

From figure 3.7 it can be seen that the variation of FK_i with cell size is small, and that for the purposes of the practitioner FK_i can be considered to be a constant. The cell size for which FK_i attains its maximum value is $a=\pi$, which corresponds to a flow pattern in which two adjacent hot spots are at a horizontal seperation equal to the height of the layer. This can be seen in figure 3.8, where the isotherms in the layer are shown for $a=\pi$ at ignition. This is an important result, as it confirms the results of sections 2.5.2.2 and 2.5.2 in which it was found that the preferred width of the internal cells was half the height of the bed, and that the hot-spot separation was 1-1.5 times the height of the bed.

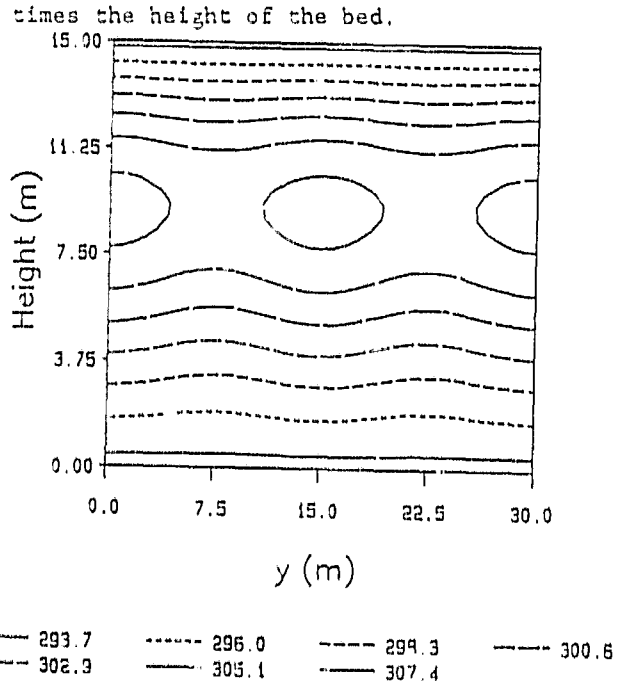

Isotherms in K

Figure 3.8 Isotherms at ignition for $a=\pi$ and FK=5.167

It seems likely that such a cell will form preferentially in the layer and that it is reasonable to express the ignition criterion as:

$$FK_i = 5.17 \tag{3.47}$$

In terms of more familiar variables, a stockpile is safe provided that

$$D_p > D_{pi} = \frac{\beta \gamma 6 k_o \rho_a (1 - \epsilon) H^2 c_p \exp(-\gamma)}{5.17 k_e} \tag{3.48}$$

One can compare this result to Eq. (3.49), which is the criterion of Brooks et al.,1988a expressed in similiar variables:

$$D_p > D_{pi} = \left(\frac{1 - \epsilon}{\epsilon}\right)\left[\frac{150 \gamma^2 \beta \mu 6 k_o \exp(-\gamma) L}{g \rho_a}\right]^{1/3} \tag{3.49}$$

The functional dependence of D_{pi} on the coal bed parameters is seen to be quite different for the two criteria. The implication of this is that Eq. (3.46) gives a good description of the ignition point locus for a coal bed in which the natural convection flow does not experience a flow direction reversal, but is inadequate for the description of the interior of the coal bed. For the interior of the bed Eq. (3.47) should be used to determine ignition points. The question of when multiple flow cells form in a coal bed has been partly addressed in Chapter 2. Eq. (3.47) has the same functional form as the asymptotic forms of Eqs. (2.40) and (2.42b) as Ra became very large, the expressions which were found to describe the locus of ignition points in stockpiles of trapezoidal cross section when multiple convection cells were present. This is a very significant result and gives a strong indication that the form of the expression is of the right kind. Note that the length scale in the two situations is different, being the height of the layer for the infinite layer model and the length of the diagonal of the edge cell for the trapezoidal stockpiles described by Eqs. (2.42b). However the constants have been corrected so that the two equations may be compared directly. The reasons for the differences between the constants are discussed in section 4.3.

It is also of interest to compare the equation describing the locus of ignition points, Eq. (3.47), with the result of Viljoen and

Hlavacek,1987. For a zero order reaction in an exothermically-reacting porous medium in a cavity they found a Hopf bifurcation at FK=5.2 beyond which they could find no solutions. It was presumed that explosion occurred beyond this point.

Ignition points for the hexagonal planform have not been calculated, but one would not expect that the result would be very different to that for roll cells. The fact that it has been shown that roll cell size has only a second order effect on ignition, and the result of Tveitereid,1977 in which it was found that the Nusselt number in a porous layer with internal heat generation was essentially independent of flow planform, both indicate that hexagons are unlikely to give a different ignition criterion to that found for roll cells. It would be of interest to calculate ignition points using a higher order truncation than has been done. The probable effect of this would be to move the position of the maximum temperature in the bed closer to the surface and to increase the value of this maximum. The possibility that ignition has been found at a slightly lower maximum bed temperature than would occur in reality means that Eq. (3.47) is probably a conservative criterion, in that it predicts ignition at a larger particle size than occurs in practice. The increase in the computational effort required to examine higher order truncations would be considerable.

3.7 Stability of steady-state solutions

As mentioned in section 3.5 it is desirable to test the stability of the steady-state solutions. In this section a method is described, based on the approach of Kimura et al.,1987, for examining the stability of the steady-state solutions to small perturbations. It was found that the numerical routines used to evaluate the eigenvalues required in this method were very unreliable. We consider small perturbations to the steady-state Fourier coefficients and assume that the perturbations are sufficiently small to allow a linear theory to be formulated. The perturbations have an exponential time dependence.

We write:

$$B_{pqh} = B^{(o)}_{pqh} + \delta_{pqh} \exp(\sigma_{pqh}\, \tau) \qquad (3.50)$$

Where:

$$\sigma = \sigma_r + i\,\sigma_i \tag{3.51}$$

$$\zeta_{pqh} = \delta_{pqh}\exp(\sigma_{pqh}\,\tau) \tag{3.52}$$

The $B^{(o)}_{pqh}$ are the steady-state coefficients. The trial function are obtained by substituting Eq. (3.50) into Eqs. (3.34)-(3.35) to give:

$$w = \sum_h \sum_{p,q} \left(B^{(o)}_{pqh} + \zeta_{pqh} \right) \exp\left\{ i(pkx + qly) \right\} \sin(\pi hz) \tag{3.53}$$

$$\chi = \sum_h \sum_{p,q} \left(B^{(o)}_{pqh} + \zeta_{pqh} \right) \exp\left\{ i(pkx + qly) \right\} F_h(\lambda,z) \tag{3.54}$$

The form of $F_h(\lambda,z)$ is found in the same way as in section 3.5. Eqs. (3.53)-(3.54) are then substituted into Eq. (3.12) and the Galerkin method applied. This yields the following infinite set of equations in the ζ_{pqh}:

$$\frac{\varphi}{2}\dot{\zeta}_{rsg} = -\frac{1}{2}\,\zeta_{rsg}\,(g^2\pi^2 + \nu^2) - \sum_{h,f} \sum_{\substack{p+t=r \\ q+u=s}} \left(\zeta_{tuf} B^{(o)}_{pqh} + \zeta_{pqh} B^{(o)}_{tuf} \right) X$$

$$\left\{ \lambda^2\, b(f,g,h,\lambda) - \pi^2\,(ptk^2 + qul^2)\, a(f,g,h,\lambda) \right\} + \frac{FK^*}{\sqrt{Ra^*}} \left\{ \frac{1}{2}\,\zeta_{rsg} \right.$$

$$\left. + \sum_{h,f} \sum_{\substack{p+t=r \\ q+u=s}} \left[\frac{1}{2} \left(\zeta_{tuf} B^{(o)}_{pqh} + \zeta_{pqh} B^{(o)}_{tuf} \right) c(f,g,h) \right] \right\} \tag{3.55}$$

where:

$$\nu^2 = (rk)^2 + (sl)^2 \tag{3.56}$$

The integrals $a(f,g,h,\lambda)$-$c(f,g,h)$, which were evaluated numerically, are given in Appendix D. Noting that:

$$\dot{\zeta}_{rsg} = \sigma_{rsg}\,\zeta_{rsg} \tag{3.57}$$

enables us to write the left-hand side of Eq. (3.55) as:

$$\frac{\varphi}{2}\,\sigma_{rsg}\zeta_{rsg} \tag{3.58}$$

Thus it can be seen that the system represented by Eq. (3.55) when suitably truncated is an eigenvalue problem of the form:

$$\sigma \underline{\zeta} = A \underline{\zeta} \tag{3.59}$$

The behaviour of the eigenvalues σ determines the stability of the steady-state solutions. If any of the eigenvalues has a positive real part, then that steady-state solution is not stable to the small perturbation , as the perturbation will grow in time. If all the real parts of the eigenvalues are negative, then the solution is stable. If the real part of one of the eigenvalues is zero and the imaginary part non-zero then the solution is oscillatory.

As discussed in section 3.5, it was found that the commercial routines that were used to calculate the eigenvalues were very unreliable and unfortunately this method could not be used to determine the stability of the steady-state solutions.

3.8 Conclusion

Using a Galerkin method, natural convection planforms in an infinite layer of coal have been obtained, and it was found that down-hexagons and roll cells were the only planforms that were stable in time. A simple continuation scheme was used to calculate ignition points in the layer for a number of different roll cell sizes. From these calculations it was possible to present a simple criterion for the ignition point particle size in the interior of a large coal bed which can be used by the practitioner to determine safe stockpiling procedures. The functional form of this criterion is similar to the one found in Chapter 2 by numerical experiment for coal stockpiles which the natural convection flow showed multiple convection cells as the Rayleigh number became very large. Because ignition points were found to occur at much larger Rayleigh numbers (for the same coal reactivity) in the infinite layer, no investigations were made on the form of the ignition point criterion for very small values of Ra to see if the criterion for the infinite layer had exactly the form as was found in Chapter 2. Thus, while we are fairly confident of the form of the ignition criterion for multiple cells for large Ra, the functional form must still be verified for small Ra. In Appendix E details are given of how the analysis of this chapter could be extended to the case of a first order reaction.

CHAPTER 4

IMPLICATIONS FOR THE MODELLING OF SPONTANEOUS COMBUSTION

It has been seen that all the models of spontaneous combustion discussed in this thesis, from the one-dimensional chimney and the simplified three-dimensional model in Chapter 1, through to the two and three-dimensional models of Chapters 2 and 3, all show steady-state multiplicity. It is this multiplicity that gives rise to the problems experienced by the practitioner: under certain conditions the coal stockpile may be at a low temperature steady-state (close to ambient temperature), while at the same set of conditions the coal bed may be burning at a temperature of many hundreds of degrees. The situation is complicated by the fact that coal stockpiles which are "safe" may be safe for two different reasons, as was discussed in section 1.3. The precautions and stockpiling procedures to be taken depend on correctly identifying the region in which the stockpile lies in terms of figure 1.2. The essential feature as far as the practitioner is concerned is to ensure that the coal bed is not in the situation where only a high temperature burning solution exists. It is thus vitally important to be able to identify the parameter values for which high and low temperature solutions exist.

For coals commonly found in practice, a plot of maximum bed temperature as a function of particle size has the form shown in figure 1.2. There are other variants to this bifurcation diagram, as discussed by Brooks et al.,1988a, but these are found less frequently and for rather narrow ranges of parameters. Inspection of the curve in figure 1.2 showed that the two points of real interest were the ignition point D_{pi}, and the point at which the maximum temperature on the ignited branch of solutions ceased to be acceptably low D_{pc}. If one were to set an upper limit on the acceptable temperature on this branch of solutions, e.g. T=350K, then one could give a definition for "safe" coal stockpiles. As it has been shown that the maximum temperature at ignition is also of the order of 350K, it would appear that such a definition could be:

Stockpiles are safe with T≤350K if:

$$0 < D_p < D_{pc} \text{ and } D_p > D_{pi} \qquad (4.1)$$

Stockpiles are unsafe if:

$$D_{pc} < D_p < D_{pi} \qquad (4.2)$$

D_{pc} is the particle size on the ignited branch of solutions for which the bed temperature is at the specified maximum. Classifying a bed as safe if $D_p<D_{pc}$ needs qualification. The particle size D_{pc} can be predicted from the lumped thermal model of Brooks et al.,1988a once the maximum temperature has been set (Glasser and Bradshaw,1989). Because of the assumptions that were made in the derivation of that model, the exact value of D_{pc} may be in error, although the expression used to predict it is likely to be of the correct form. However, this is not a very good storage criterion, because in time the bed in this situation will become less safe if left untended. The temperature rise for this type of bed was low because fine, reactive particles consume all the oxygen close to the surface of the bed from where the energy generated can easily be dissipated to the surroundings. In time this outer layer of coal will become completely oxidised and cease to scavenge the oxygen close to the surface. Oxygen will then be able to penetrate deeper into the bed, from where, because of the high resistance to flow of these small particles, the heat cannot be removed by natural convection. Thus the bed will become less safe as time progresses. It may be the case that the bed will have been dismantled before this happens, but as there is as yet no easily applied criterion for safe stockpiling times, it would appear to be far better to consider such a bed as inherently unsafe. It was for this reason that the work in this thesis was directed rather towards identifying ignition points than the point D_{pc}.

In the preceding two chapters two different methods were used to analyse different stockpile situations; a numerical method was used to examine small coal stockpiles and an approximate analysis was used to investigate the behaviour of very large coal beds. From these analyses simple criteria were developed which can be used by the practitioner in industry to determine the ignition point for a given coal stockpile. In this chapter the results from the two methods are discussed in order to give an overview of how to predict the ignition point in a coal stockpile.

4.1 The small stockpile model

In Chapter 2 a numerical method was used to examine small coal stockpiles and to determine when a stockpile can be considered to be

small. It was found that for certain sizes of frusta or edges of large stockpiles the natural convection flow showed only one circulation pattern. All the flow was found to enter the bed through the sloping surface and to exit through the upper surface. In this case the locus of ignition points was well-described by the following equation:

$$Ra^* = \frac{\sqrt{B^2 + 1}}{B} \quad FK \qquad (4.3)$$

The appropriate length scale for such beds has been found to be the length of the diagonal from the toe of the edge or frustum, to the upper surface at the centreline of the frustum or the inner boundary of the edge region. If this length was to be used in Eq. (4.3), then the term involving the geometric parameter B would fall away and Eq. (4.3) would be exactly the same as the relationship derived for the locus of ignition points for a one-dimensional model (Brooks et al.,1988a), which indicates that the one-dimensional chimney can be seen to resemble the small frustum or the edge of a large coal stockpile where there is only one flow cell. Criteria of this form were found by Brooks et al.,1988a to describe the ignition points of other simplified one-dimensional models. If the right hand side of Eq. (4.3) is multiplied by a constant, then for a lumped thermal model (uniform bed temperature) the constant is = 0.541, while for a plug-flow model, a model with the ends of the bed at ambient temperature and the general model the constant = 1. These results give confidence that the form of Eq. (4.3) is indeed correct.

Eq. (4.3) is a simple algebraic expression which may easily be written in terms of physical parameters that are more readily understood by the practitioner. It is possible to restate the relationship as a criterion for choosing the particle size to prevent ignition in the bed:

$$D_p > D_{pi} = \left(\frac{1 - \epsilon}{\epsilon} \right) \left[\frac{150\ \gamma^2\ \beta\ \mu\ 6\ k_o\ \exp(-\gamma)\ H \sqrt{B^2 + 1}}{\eta\ T_a\ g\ \rho_a\ B} \right]^{1/3} \qquad (4.4)$$

It can be seen that each of the parameters appearing in Eq. (4.4) is easily measurable, and hence it is a simple matter to predict the minimum particle size that is allowed for a particular coal stockpile in order to prevent spontaneous combustion. This is a very powerful piece of information for the coal mining industry.

The practitioner has control over only the parameters ϵ and H, while the rest are properties of the coal and cannot be altered. Eq. (4.4) shows that compaction of a bed which lies on the extinguished branch of solutions ($D_p > D_{pi}$) will increase the required minimum particle size for prevention of ignition. This result is contrary to intuition but can be explained if one remembers that the bed is safe because natural convection removes the heat generated by the chemisorption reaction. Compacting the bed hinders natural convection and so reduces the capacity for heat removal, making the bed less safe. Eq. (4.4) shows that the smaller the bed the safer it will be, however the bed length appears to the one third power, so the dependence is not very great. One can see that the ambient temperature has a large effect on the particle size at ignition; coal beds are safer if the ambient temperature is low.

In order to be able to use Eq. (4.3) it is necessary to know that all the flow enters the bed through the sloping surface and exits through the upper surface. If this is not the case then Eq. (4.3) is no longer a good description of the locus of ignition points in the coal bed. This would be expected, as it is known that Eq. (4.3) describes the behaviour of a chimney: the chimney is clearly very different to a bed in which the flow pattern is anything other than grossly straight. From numerical experiment it was found that as the edges or frusta were made longer and flatter the flow pattern showed Benard-like convection cells, internal cells for which the flow enters and leaves the bed through the upper surface, i.e. the flow turns around through 180°. It was found that this occurred when:

$$\frac{1 - A}{B} > 1.5 \qquad (4.5)$$

Eq. (4.5), written in terms of the geometric parameters A and B, means that Benard-like cells will form if the length of the upper surface of the bed is greater than 1.5 times the height of the bed. It was found that these roll cells exhibited several characteristic features. Only an odd number of cells was formed, and the width of the internal roll cells was equal and also equal to the width of the outflow region of the edge cell. The horizontal separation of adjacent hot-spots was approximately 1-1.5 times the height of the layer. From these characteristics and using Eq. (4.5) it is possible to make a prediction about when multiple cells will form in a coal stockpile with a trapezoidal cross-section, and to estimate how many cells will

be formed. When multiple cells form in the edge model, .e. the two-dimensional cartesian coordinate model, the internal cells have physical meaning, in that they are roll cells, and this type of cell is known to exist in porous media. In the case of the frustum, the assumption of radial symmetry used in Chapter 2 means that all the cells except the central one have a toroidal shape. Toroidal cells are not found in practice, but are a result of imposing a symmetry that it not felt in reality. It can be argued that if the radius of curvature of these toroidal cells is very large then they may be considered to approximate roll cells. This leaves the problem of the central cell, which could perhaps be considered to be an approximation to a hexagonal cell of the type which are known to be found in practice. However it is clear that, while it is of interest to examine the frustum which shows multiple cells, the results obtained from those cases are less meaningful than those obtained from the edge model.

When analysis indicates that multiple cells will be formed it is necessary to use a different expression to describe the locus of ignition points. It has been found that a suitable expression is:

$$FK = b\,(1 - 5/\sqrt{Ra^*}) \qquad (4.6)$$

For the edge model it is reasonable to approximate b=18.15, while for the frustum b=27.9. As discussed above, more reliance can be placed on the results from the edge model than on the frustum in this multiple flow cell situation, and hence for the purposes of the practitioner the locus of ignition points can be expressed as:

$$FK = 18.15\,(1 - 5/\sqrt{Ra^*}) \qquad (4.7)$$

The correct length scale in the situation when multiple cells are formed was found to be the length of the diagonal from the toe of the bed to the corner of the upper surface and the inner boundary of the edge cell. This length can be estimated *a priori* from the characteristics of the roll cell geometry described above. This would be done as follows. Firstly Eq. (4.5) is used to determine that multiple cells exist. It is possible to determine how many cells will form: this can be done because only an odd number of cells will form, and the hot-spot separation is 1-1.5 times the height of the layer. Once the number of cells has been decided, it is an easy matter to divide the stockpile into roll cells and an edge cell, because the widths of the roll cells are equal, and the outflow region of the edge

cell is also of the same width. In this way the required diagonal length can be estimated. Because all the ignition point computations except those for box and the wind rows were made for an angle of 30°, and because the diagonal length can be expressed in terms of the height, the constant in Eq. (4.7) has been corrected for the effect of the length scale, so that the parameters still appear exactly as defined in the nomenclature.

It can be seen that the asymptotic form of the ignition criterion for Ra large is the same as the criterion for thermal explosion or the conduction asymptotes for the one-dimensional models (Brooks et al.,1988a), indicating that the coal bed in this case is conduction-dominated because of the weak convection caused by the flow reversal. However compacting the bed would make it less safe.

In terms of physical parameters, the condition for safe stockpiling for large Ra can be expressed as:

$$D_p > D_{pi} = \frac{\beta \gamma \delta k_o \rho_a (1 - \epsilon) H^2 c_p \exp(-\gamma)}{18.15 k_e} \qquad (4.8)$$

4.3 The interior model

In Chapter 3 an approximate analysis was used to examine convection planforms in an infinite layer, and to derive a criterion for ignition points in this case. Considering an infinite layer allows the assumption of spatially-periodic solutions and allows far larger domains to be investigated than would be possible with a numerical method. In order to perform the analysis several simplifying assumptions had to be made over and above those made in Chapter 2. Only the case of a zero order reaction was considered, and this is known to be a very reasonable assumption. The positive exponential approximation was made, which is reasonable in view of the large activation energy of the chemisorption reaction. A more restrictive assumption was the replacement of the exponential temperature dependence in the energy equation with a quadratic expansion about $\theta=0$. It was shown that this approximation is likely to predict ignition points at parameter values larger than would occur in reality, i.e. the results are not conservative.

It was found that for this model the locus of ignition points was very

well described by the expression:

$$FK = 5.17 \tag{4.9}$$

The effect of roll cell size on the ignition point was found to be small, and the constant 5.17 in Eq. (4.9) represents the result for a roll cell size for which the horizontal separation of hot-spots was equal to the height of the layer. It appeared likely that this cell size would be formed preferentially in the layer. This is particularly interesting result, because a similar result was found in the numerical investigation of the edge which showed multiple cells, i.e. the hot-spot separation being 1-1.5 times the height of the bed. This was confirmed in the open-topped box simulations in section 2.6.2. This result allows one to be confident that the formation of multiple cells and their size can be predicted sufficiently accurately. One would not expect the two criteria to agree exactly, as the presence of boundaries in the numerical investigation will obviously affect the results (Joseph,1976). One can also see that Eqs.(4.7) and (4.9) are of the same functional form for large Ra, however the constants for the two cases are quite different, being 13.15 and 5.17. These differences are discussed in section 4.3. Eq. (4.9) can be expressed in terms of physical parameters as:

$$D_p > D_{pi} = \frac{\beta \gamma \delta k_o \rho_a (1 - \epsilon) H^2 c_p \exp(-\gamma)}{5.17 k_e} \tag{4.10}$$

4.3 Comparison of the small stockpile and interior models

As has already been discussed, it would not be expected that the ignition point criterion for the small stockpile with a single convection cell would be the same as the criterion for the stockpile with multiple convection cells. However one might expect that the expression for the numerical investigation of the latter case, Eq. (4.7) would agree with the one developed from the analysis of the infinite layer, Eq. (4.9). It has been shown that the two expressions are of essentially the same form, however the values of the constants that appear in the two expressions are quite different.

The most likely cause of this difference is the low order truncation used in the approximate analysis of the infinite layer. The truncation that was used to ensure reasonable computation times allowed only 2 terms to describe the vertical variation of the

velocity potential and temperature. This means that the position of the hot-spot could not be as close to the upper surface of the layer as might occur in practice. This may be expressed in another way by saying that the lower the order of the truncation, the more closely the solution will be forced to represent a conduction-only solution. As it is known that natural convection increases the critical value of the parameter at ignition over the conduction only solution, an excessively low order truncation would predict ignition at a smaller parameter value (FK_{crit}) than actually occurs. To be weighed against this is the knowledge that the quadratic approximation to the temperature exponential used in the approximate analysis will predict ig n at a larger FK than would occur in reality. It was found t e position of the hot-spot in the numerical investigations was w the upper surface of the bed, which is closer than was e infinite layer model (see figure 3.8). In the absence of rmation it is difficult to draw firm conclusions as to sion of Eqs. (4.7) and (4.9) is correct, although it would seem t e form of the expression has been well-defined for large Ra. Until further work is done it would seem to be best to use this expression realising that the correct value of the constant is between 5.17 and 18.15. Note that for the frustum with multiple cells the value of the constant would be ≈27.9 and that for small Ra there may be another term in the ignition criterion.

If one compares Eq. (4.3) with Eq. (4.9) it can be seen that for parameter values near their base case values ignition could always be expected to occur in the centre of a large bed, rather than at its edge. There are two situations where this might not be the case. For values of Ra^* close to unity the edge would be predicted to show ignition before the centre. However Eq. (4.3) is not valid for such small values of Ra^*, and at such values of Ra^* it is possible that a conduction only solution will exist in this parameter region, as has been seen in figure 3.2. In this case one would use a conduction asymptote expression to find the thermal explosion limit. The other situation in which the edge might show ignition before the centre of a large bed is for very small values of FK^*. This will arise for extremely unreactive coals, e.g. coals for which k_o is very small. Thus, for very large coal stockpiles of base case reactivity, ignition is predicted to occur in the centre of the bed. This also means that small beds which show only one convection cell will always be safer than very large beds, unless the reactivity of the coal is very low. This result shows that coal stockpiles on the extinguished branch will be made less safe by building walls around them and leaving the top open.

4.4 Storage of coal

It is not the purpose of this thesis to present detailed stockpiling procedures, for this the reader is referred to Glasser and Bradshaw,1989. Here only a few of the important points are mentioned. In order to use the ignition point criteria that have been developed, the practitioner must know the rate of reaction of the coal with oxygen, together with heat of the reaction and activation energy. The rate of reaction can be measured using a relatively simple apparatus (Smith,1989) while the heat of reaction and the activation energy are not found to vary much between coals and so the values given in Appendix A could be safely used. The practitioner has control over the particle size D_p, the voidage ϵ and the bed size H.

The particle size is defined as the total surface area per unit volume, S and for uniform spheres $S=6/D_p$, as was used throughout this thesis. For a sieved fraction of coal the following definition should be used:

$$S = \sum_{j=1}^{J} \frac{m_j}{D_{pj}} = \frac{1}{D_p} \qquad (4.12)$$

The reasons for using this expression are discussed in Brooks,1986 and Glasser and Bradshaw,1989.

Once a suitable stockpiling condition has been decided upon it must be ensured that these conditions are not altered during the laying of the stockpile. In particular, care must be taken to ensure that the bed is constructed without the formation of any unseen size distribution. Such a distribution can be disasterous if there is a particle size which is indicated as unsafe by the ignition criteria. There will almost certainly be a way for oxygen to reach the region with this particular dangerous particle size and ignition is an almost certain consequence. Such a situation could arise during compaction of a bed if particle breakage occurs, and could also arise due to the stacking method. As discussed in section 2.1.1, dropping the coal from a stacker results in a bed with extreme segregation of particles and should be avoided if it is economically possible to do so. The storage conditions will also have determined whether or not the bed lies on the ignited branch or the extinguished branch of solutions.

As has been discussed, the actions that are taken in the construction and maintenance of the stockpile are depend on whether or not the bed is oxygen limited or reaction rate limited.

Once the coal stockpile has been constructed it will also be necessary to monitor the coal regularly. In particular infra-red thermography can be used to indicate temperature anomalies, and oxygen probes and thermocouples can be used for more accurate on-the-spot assessments.

4.5 Conclusion

This chapter is concluded by a summary of the different ignition criteria, and when each should be used.

Small coal stockpiles of trapezoidal cross-section

This analysis is applicable to frusta, long trapezium-shaped beds and edges of large beds when only one convection cell is present. This can be determined by ensuring that the length of the flat upper surface is less than 1.5 times the height of the bed:

$$\frac{1 - A}{B} < 1.5 \qquad (4.13)$$

In this case the locus of ignition points is described by:

$$Ra^* = \frac{\sqrt{B^2 + 1}}{B} FK \qquad (4.3)$$

To ensure that the bed does not ignite the particle size D_p must be such that:

$$D_p > D_{pi} = \left[\frac{1 - \epsilon}{\epsilon} \right] \left[\frac{150\ \gamma^2\ \beta\ \mu\ 6\ k_o\ \exp(-\gamma)\ H \sqrt{B^2 + 1}}{\eta\ T_a\ \ g\ \rho_a\ \ B} \right]^{1/3} \qquad (4.4)$$

The interior of large coal stockiles

This analysis is appropriate for very large coal stockpiles when many Benard-like convection cells will be formed. Eq. (4.13) is used to determine whether or not multiple cells will form. Then knowing that an odd number of cells will be formed, that the horizontal separation of adjacent hot-spots will be 1-1.5 times the height of the layer, and that the roll cells are of equal width and the outflow region of the edge cell has the same width, it is possible to determine how many cells will form and what their size will be.

The locus of ignition points is described by:

$$FK = b\ (1 - 5/\sqrt{Ra^*}) \qquad (4.6)$$

To ensure that the bed does not ignite the particle size D_p must be such that for large Ra:

$$D_p > D_{pi} = \frac{\beta\ \gamma\ 6\ k_o\ \rho_a\ (1 - \epsilon)\ H^2\ c_p\ \exp(-\gamma)}{b\ k_e} \qquad (4.8)$$

For the infinite layer the value of b is 5.17, while for edges which show multiple cells the value is 18.15. The true value of b probably lies between these two values.

CHAPTER 5

CONCLUSION

In this thesis it has been shown that the critical parameters to determine the point of ignition in realistically-shaped coal stockpiles can be predicted adequately by simple algebraic relationships. These criteria were expressed in terms of easily measurable properties of the coal together with a measure of the size of the coal stockpile. Knowledge of the parameter values at the ignition point is a vital piece of information for the practitioner, because it delimits the regions of safe and conditionally safe stockpiling. For a stockpile of given size and coal reactivity, if the particle size is smaller than the ignition point particle size then the only steady-state condition of the bed is a burning situation. If the particle size is greater than the ignition point particle size, then it is likely that the stockpile can be safely stored indefinitely, provided that there are no large temperature perturbations to the bed (~hundreds °C) and provided that the particle size is not too close to the ignition point particle size. Although it is possible to store stockpiles of extremely fine coal, of particle size less than the ignition point particle size, for which the maximum temperature rise in the bed is acceptably low, the cost of crushing the coal to these sizes may be prohibitively high. It is also likely that such a bed would become less safe with time as the oxygen absorbing properties of the outer layer of the bed decrease, allowing oxygen ingress deep into the bed from where energy cannot easily be dissipated. A knowledge of the ignition point particle size is also vital in planning appropriate preventitive measures for stockpiles of a given particle size. For example, if the particle size is greater than the ignition point particle size then compaction of the coal bed will make the bed less safe, while for stockpiles with a particle size less than the ignition point particle size this action will make the bed safer.

In this work two approaches were taken to solving the equations describing the processes occurring in a coal stockpile. Small coal beds, i.e. those which show a predominantly unicellular flow pattern, were analysed using a numerical technique. This method was applied to various geometries: frusta, trapezoidal beds and the edges of infinitely long ones. The behaviour of the interiors of large coal stockpiles was examined using an approximate analytical method. By using one or both of the methods entire coal beds can be modelled, and

from this modelling effort criteria for the ignition point particle sizes for different situations were developed.

In the numerical analysis of small stockpile models, the finite element method was used to obtain results in geometries which closely resembled instrumented test coal heaps at a mine in South Africa. Using a two-dimensional formulation, trends predicted by simpler models were confirmed. In particular it was found that such coal beds show an ignition point, that the hot-spot is near the surface of the bed, that the surface of the bed is close to ambient temperature and that the consumption of oxygen for non-burning beds is very low. Many of these features are observed in real coal beds as well. A simple continuation procedure was imbedded in the finite element method and was used to calculate ignition points in frusta, trapezoids and edges.

Two types of behaviour were found to occur. For relatively small coal beds all the flow was found to enter the bed through the sloping side surface and to leave through the flat upper surface. In this case the locus of ignition points was well-described by the simple criterion for ignition that was derived by Brooks et al.,1988a for a one-dimensional chimney model of a coal stockpile. The correct length scale for use in this criterion was the length of the diagonal from the toe of the coal bed to the symmetry line at the upper surface. As the coal beds were made longer or flatter it was found that Bénard-like convection cells formed. In this situation the frustum model in which radial symmetry was assumed was no longer a good approximation to reality. The two-dimensional edge model was physically reasonable, and analysis of this model showed that the locus of ignition points was well-described by a different simple relationship to the one suitable for the beds with only one circulation pattern. The different functional forms of the two relationships indicates the fundamental mechanisms of transport in the beds are significantly different in the two cases. The asymptotic functional form of the relationship for the case when multiple cells formed was found to be the same as the form of the thermal explosion limit asymptote, or the conduction asymptotes of the one-dimensional models of Brooks et al.,1988a. This indicates the importance of conduction when the flow undergoes a 180° direction change.

From numerical experiments the conditions were determined for which multiple cells will form. These multiple cells have strongly characteristic features: an odd number of cells is formed, the horizontal separation of adjacent hot-spots is found to be 1-1.5 times

the height of the bed and the widths of the internal cells and the outflow region of the edge cell were equal. These characteristics make it possible to determine *a priori* when multiple cells will form.

These two simple criteria for the critical parameters at ignition are extremely useful to the practitioner. The criteria are simple algebraic expressions allowing rapid calculation of the parameters for ignition in terms of the coal properties.

The numerical work has several deficiencies which merit further research. The equations in the unsteady-state model are very stiff, and cannot be readily solved with commercial software. This means that the equations must be decoupled and solved as a mixture of steady and unsteady-state equations. This decoupling procedure involves trial and error and did not prove very successful when applied in this study. Further work is needed, as the unsteady-state results can be of considerable importance. This may be the case if a stockpile of coal is to be stored only for a short period. The steady-state behaviour of such a bed may well indicate high temperature burnout, but an unsteady-state analysis may indicate that this would happen only after the useful life of the stockpile.

In this work no solutions were found for beds very fine particles where the maximum temperature rise in the bed is acceptably small. Numerically this is a difficult problem, as several different length scales are now evident. In particular extremely steep gradients of concentration occur in a thin boundary layer on the bed surface. Numerical resolution of this layer while still retaining an adequate discretization of the remainder of the coal bed is very difficult and was not achieved in this work. A better approach would be to develop a two region model with different, simplified mechanisms in each region. This merits further investigation. It would also be of great interest to model the effects of particle size segregation. This could be quite easily implemented with the finite element program.

Because it is clearly extremely costly to solve numerically a coal bed in which many convection cells exist, unless only a few cells are to be modelled, an approximate analysis was made of the interior of a large coal stockpile. Assuming that the coal layer was laterally-unbounded allowed the assumption of spatially-periodic solutions. Infra-red thermography analysis of real coal beds appears to indicate that spatially-periodic convection cells do exist. The

Galerkin method is well-suited to the solution of this problem, as it allows very convenient representation of the periodicity. In order to use the Galerkin method several assumptions were made: most importantly the reaction was assumed to be of zero order and the boundaries of the bed were assumed to be at ambient temperature. Both of these assumptions had been shown to be reasonable in the numerical analysis. A continuation method was used to calculate ignition points in the infinite layer for a convection pattern of two-dimensional roll cells. It was found that the size of the roll cells had only a second order effect on the ignition point and that the locus of ignition points could be described by a relationship of the same functional form as was found in the numerical work for edges showing multiple cells for large Ra. However, the actual value of the critical parameter for ignition was different in the two cases, and although it is likely that the form of the criterion is correct, the value of the constant probably lies between the value obtained from the numerical work and that obtained from the approximate analysis. Because ignition was found to occur for large Ra in the infinite layer, no results were obtained for small Rayleigh numbers, and it was not possible to confirm the presence of the extra term in the ignition criterion for multiple flow cells obtained in the numerical work for small Ra. It was found that the preferred appeared to be one for which the hot-spot separation was height of the layer. This confirms the result that was the numerical work, and allows one to be confident that the form and sizes of Benard-like cells can be predicted.

This approximate analysis could be improved. In particular more powerful computer facilities would permit higher order approximating functions to be used. This would have the effect of moving the hot-spot closer to the top of the bed, and possibly changing the critical value of the parameter for ignition. A more powerful computer would also allow hexagons to be examined, although it is likely that hexagons would exhibit very similar behaviour to roll cells. The use of more suitable eigenvalue calculation routines would allow examination of the stability of the steady-state solutions, and perhaps also direct calcualtion of ignition points.

The ignition point criteria derived in this work are felt to be of great benefit to the coal mining industry. They allow easy calculation of the critical parameter values at ignition and are well-suited to use by the practitioner.

APPENDIX A

BASE CASE MODEL PARAMETERS

Ambient temperature	T_a	293 K
Ambient pressure	P_a	1.013×10^5 Pa
Density of air	ρ_a	1.18 kg/m^3
Density of solid	ρ_s	1.5×10^3 kg/m^3
Gas specific heat capacity	$(c_p)_g$	10^3 J/kg/K
Solid specific heat capacity	$(c_p)_s$	10^3 J/kg/K
Enthalpy of reaction	ΔH	$- 3 \times 10^8$ J/kmol
Dimensionless activation energy	γ	23.9
Voidage	ϵ	0.3
Bed thermal conductivity	k_e	0.2 W/m/K
Lewis number	Le	0.0333
Gas molecular mass	M	29 kg/kmol
Height of layer	H	15 m
Molecular diffusion coefficient	D	2×10^{-5} m^2/s
Gas viscosity	μ	1.8×10^{-5} kg/m/s
Coefficient of themal expansion	η	3.67×10^{-3} /K
Heat transfer coefficient	h	5 W/m^2/K

APPENDIX B

DESCRIPTION AND LISTING OF THE FINITE ELEMENT PROGRAM

In this appendix a listing is given of the finite element program described in Chapter 2, together with associated sample data files and some service programs. The version of the program that has been given is the most basic version that was used to obtain the results of Chapter 2. The version of the program which has the option to solve a mixture of stead and unsteady-state equations is necessarily more complex and has not been included here for space reasons. The service subroutines used to perform arc-length continuation have also been omitted for the same reason. Also included in this appendix are copies of two reports describing the finite element program. These two reports give further details on program structure, data files and other implementation details.

The following program (stored in files FEPDE FORTRAN and SUBS FORTRAN) was written in Fortran 77 by P. Anderson and S.M. Bradshaw. Two input data files are required, and examples are given after the program listing. In this form the program is written to solve the model defined by Eqs. (2.7)-(2.10) in a domain of trapezoidal cross section.

```
      BLOCK DATA DIMDAT
      IMPLICIT REAL*8 (A-H,O-Z)
      COMMON /XP/ XPARM(4)
       COMMON /DIMS/ INBDC, ILISTB, ICOORD, INLTOP, INF, IRHS, ISYSK,
     *               JNBDC, JLISTB, JNLTOP, JNF, JSYSK, INROPV, IAL, JAL
       COMMON /IO/ NINT, ITERM, NIN, NOUT, IPROFL, MESH, IERR, NTOUT,
     *             INPARM
      COMMON /FEMWRK/  RHS(410), AL(410,140),
     *        NROPV(410), RESDV(4,500), RESD(4), ERR(4),
     *        ERRAV(4), ERRCNT(4), ERRTOT(4), SCALE
      COMMON /BAND/ IBAND, IHBAND, ITOTDF
      COMMON /MTRIX/ SYSK(410,140), SYSM(410,140)
C     REAL*8 XKOA
       DATA INBDC /6/, ILISTB /140/, ICOORD /500/,INLTOP /500/,INF
     * /500/,
     * IRHS /410/, ISYSK /410/, JNBDC /80/, JNF/5/, JLISTB /5/,
     * JNLTOP /14/,  JSYSK /140/, INROPV /410/, IAL/410/, JAL /140/
      DATA NINT/3/, ITERM /4/, NIN /5/, NOUT /16/, IPROFL /7/,NTOUT /8/,
     *      IERR /9/, SCALE /10.0D25/, INPARM /1/
C
C       REAL*8   F(410),DELTAX(410),XTEMP(410),XOLD(410)
C     *         XMIN(410),XMAX(410)
C
C       COMMON /VARS1/ X(410), PAR(410), NEQN, NXEQN
C       COMMON /VAPS2/ VAR(410), IVAR(410)
C       COMMON /OUTVAR/ DELTA, NVP
C       COMMON /GPARAM/ H, TOL, NN, METH, MITER, NUMINT
C
C       DATA XMIN/9*-1./
C       DATA XMAX/6*5000.,1.,2*10./
C
      END
      IMPLICIT REAL*8(A-H,O-Z)
C       FOR ADAMS METHOD WK=20401, FOR STIFF METHOD WK=12001
      DIMENSION WK(12001), IWK(410), FNCVAL(410), FNCDER(410)
      DIMENSION VAR(410)
      EXTERNAL FUNC, MONT, TDERV, PDERV
      COMMON /XP/ XPARM(4)
      REAL*8  HESS(8), GRAD(3), WRKZ(12), XKOA
       COMMON /DIMS/ INBDC, ILISTB, ICOORD, INLTOP, INF, IRHS, ISYSK,
     *               JNBDC, JLISTB, JNLTOP, JNF, JSYSK, INROPV, IAL, JAL
       COMMON /IO/ NINT, ITERM, NIN, NOUT, IPROFL, MESH, IERR, NTOUT,
     *             INPARM
       COMMON /XTRACT/ NXTRCT, IVXTR(6), IEXLST(6,4,60), NODXTR(6)
      LOGICAL FIRST
      COMMON /PARAM/  RYLGH, HCOEF, DP, EPSI, EA, XKO, DOVA, TERM, XMU,
     *                PHI, ALPHA, PO, XLAM
      COMMON /GRPS/ XLEW, GAMMA, BETA, THIELE, RLLY, BIOT, DEE, CHI,
     *              TAU, ZETA, SIGMA
      COMMON /VAR/ NVAR
      COMMON /ELDAT/ NLTOP(500,14),COORD(500,3),NELE,IELTYP,NODEL,ITELS,
     *           NF(500,5), XX(30), YY(30),NODTOT, IDIMN, IDFEL,
     *NX,NY,
     *           IXPOS(500), IYPOS(500), NODSID
      COMMON /FEMWRK/  RHS(410), AL(410,140),
     *        NROPV(410), RESDV(4,500), RESD(4), ERR(4),
     *        ERRAV(4), ERRCNT(4), ERRTOT(4), SCALE
      COMMON /BAND/ IBAND, IHBAND, ITOTDF
      COMMON /MTRIX/ SYSK (410, 140), SYSM(410,140)
```

```
      COMMON /BNDRY/ NBNDRY(5,6,80), NBND(5), NBDC(6,80), LISTB(140,5)
      COMMON /SHPFN/ FUN(12), GDER(3,12)
      COMMON /FVALS/ FVAL(5,500), FLST(5,500)
      COMMON /JEOM/ XMAX, YMAX, CHRL, CRDSYS, IEQFRM, ISIDNM
      COMMON /CONT/ C0, CFCTMX, STEPS, STEPS1, STEPS2, ITRACE, ICONT,
     *              IFRST, ICHK  ITASK, IPAYN, DPUP, DPLOW
      COMMON /EXPT/ XEXP(10), YEXP(10), FEXP(10,10)
      COMMON /RELAX/ RELAX1, RELAX2, RELAX3
      COMMON /TMDAT/ TEND
      COMMON /DERFLG/ IFLAG1, IFLAG2, IFLAG3
      COMMON /RLNUM/ RALY, CFACT
      COMMON /ANGL/ ANGLE
      REAL*8 PARM(4)
      REAL*8 W1(3), W2(3), W3(3), W4(3), W5(4), W6(4,4)
C
C*                          **************************
C*                          *                        *
C*                          * INPUT DATA SECTION     *
C*                          *                        *
C*                          **************************
C
C                           INPUT OF NODAL GEOMETRY
C
C
      READ (NIN,*) NODTOT, IDIMN, NVAR
      READ (INPARM,*) XMAX, YMAX, CHRL, CRDSYS, IEQFRM
      READ (NIN,*) NX, NY
      IDFNOD=NVAR
      DO 1010 I=1,NODTOT
       READ (NIN,*) NODNUM, (COORD(NODNUM,J),J=1,IDIMN)
 1010 CONTINUE
C
C
C                              INPUT OF ELEMENT TOPOLOGY
C
C           IELTYP = 1   =>   3 noded triangular    elements
C                    2   =>   6   "       "             "
C                    3   =>  10   "       "             "
C                    4   =>   4   "   quadrilateral     "
C                    5   =>   8   "       "             "
C                    6   =>  12   "       "             "
C
C
      READ (NIN,*) IELTYP, ITELS, NODEL
      DO 1020 I=1,ITELS
        READ (NIN,*) IELNM, (NLTOP(IELNM,J+2),J=1,NODEL)
        NLTOP(IELNM,1) = IELTYP
        NLTOP(IELNM,2) = NODEL
 1020 CONTINUE
C
C                             INPUT OF NUMBER OF DEGREES OF FREEDOM
C                             PER NODE, INPUT OF BOUNDARY CON-
C                             DITIONS AND CONSTRUCTION OF NODAL
C                             FREEDOM ARRAY NF. ZEROING OF NORMALS
C
      DO 1030 IEQ=1,NVAR
      READ (NIN,*) NBND(IEQ)
      WRITE(ITERM,*)'BND ',ITBND, IEQ
      DO 1030 I=1,NBND(IEQ)
```

```
      READ (NIN,*) NBTYPE,NODSID, NUMNOD, (NBNDRY(IEQ,I,J+3),J=1,NUMNOD)
      NBNDRY(IEQ,I,1) = NBTYPE
      NBNDRY(IEQ,I,2) = NUMNOD
      NBNDRY(IEQ,I,3) = NODSID
 1030 CONTINUE
C           INPUT OF LIST OF NODES FOR WHICH EXTRACTED VALUES ARE REQD
      READ (NIN,*) NXTRCT
      DO 1031 I=1,NXTRCT
 1031 READ (NIN,*) IVXTR(I), NODXTR(I),
     *  (IEXLST(I,IVXTR(I),J),J=1,NODXTR(I))
      READ (INPARM,*) HCOEF, DP, EPSI, EA, XKO, XKEQ, DIFF, XMU
      READ (INPARM,*) TO, RHO, GRAV, HTCAP, DELTAH, ANGDEG
C     HCOEF= HEAT TRANSFER COEFFICIENT
C     DP=PARTICLE SIZE
C     EPSI=VOIDAGE
C     EA=ACTIVATION ENERGY
C     XKO=PRE-EXPONENTIAL FACTOR
C     XKEQ=TERMAL CONDUCTIVITY
C     DIFF=DIFFUSION COEFFICIENT
C     ALPHA= THERMAL DIFFUSIVITY
C     XMU=VISCOSITY
      ANGLE=3.14159265D0*ANGDEG/180.0D0
C     ALPHA=XKEQ/HTCAP/RHO
      XLAM=DP/20.0D-3
      PERM=DP*DP*EPSI**3/150.D0/(1.0D0-EPSI)**2
      RYLGH=GRAV*3.67D-3*TO*CHRL*RHO**2*PERM*HTCAP/XKEQ/XMU
      WRITE(ITERM,*)'DP RALLY',DP, RYLGH
      RLLY=RYLGH
      PHI=900.00D0
      PO=101325.00D0
C --- DEFINE DIMENSIONLESS GROUPS
        XLEW=EPSI*DIFF*RHO*HTCAP/XKEQ
        GAMMA=EA/8.314D0/TO
        BETA=DELTAH/0.029D0/TO/HTCAP/4.76D0
        BIOT=HCOEF*CHRL/XKEQ
        THIELE=6.0D0*XKO*RHO*HTCAP*(1.0D0-EPSI)*CHRL*CHRL
     *          /(XKEQ*DP)
        DEE=THIELE*DSQRT(RYLGH)*DEXP(-GAMMA)
        CHI=THIELE*THIELE/XLEW/RYLGH
        TAU=RYLGH/THIELE
        ZETA=RLLY*RLLY*GAMMA*BETA
        SIGMA=GAMMA/BETA
        R1=XMAX-YMAX/DTAN(ANGLE)
      WRITE(IERR,*)R1
        GEOMA=(XMAX-R1)/XMAX
        GEOMB=YMAX/XMAX
      WRITE(IERR,*)'LEWIS=', XLEW, 'GAMMA=', GAMMA
      WRITE(IERR,*)'BETA=', BETA
      WRITE(IERR,*)'BIOT=', BIOT, 'THIELE=', THIELE*DEXP(-GAMMA)
      WRITE(IERR,*)'RAYLEIGH=', RLLY
      WRITE(IERR,*)'DEE=', DEE, 'CHI=', CHI, 'TAU=', TAU
      WRITE(IERR,*)'ZETA=', ZETA, 'SIGMA=', SIGMA
      WRITE(IERR,*)'A=', GEOMA, 'B=', GEOMB
C     DOVA=DIFF/ALPHA*EPSI
C     XPARM(1)=RYLGH
C     XPARM(2)=HCOEF
      NPAR=3
      PARM(3)=RYLGH
C     PARM(4)=HCOEF
```

```
      READ (INPARM,*) ICHK
      READ (INPARM,*) CFCTMX, STEPS1, STEPS2, ITRACE, ICONT, ITASK
      READ (INPARM,*) DPUP, DPLOW
      READ (INPARM,*) RELAX1, RELAX2, RELAX3
      READ (INPARM,*) IREAD
C ---   Scale the domain to the required shape
      XMAX=XMAX/CHRL
      YMAX=YMAX/CHRL
      DO 2010 I=1,NODTOT
       COORD(I,1)=COORD(1,1)*XMAX
       COORD(I,2)=COORD(I,2)*YMAX
       COORD(I,1)=COORD(I,1)*(1.0-COORD(1,2)/DTAN(ANGLE)/XMAX)
2010  CONTINUE
C           Input/calculation of initial guesses for variables
C           and zeroing of normals
      IF (ITASK.EQ.5) THEN
       DO 1013 NOD=1,NODTOT
         READ(17,*)FVAL(1,NOD),FVAL(2,NOD),DUMMY3,DUMMY1,DUMMY2
1013   CONTINUE
       DO 1014 NOD=1,NODTOT
         FVAL(2,NOD)=(FVAL(2,NOD)+273.15D0-T0)/T0
1014   CONTINUE
C --- set SCALE = 1.0 for arc length continuation
C      SCALE=1.0D0
       GO TO 1012
      END IF
      IF(IREAD.EQ.1) THEN
        DO 5011 NOD=1,NODTOT
          READ(17,*)FVAL(1,NOD), FVAL(2,NOD), FVAL(3,NOD), DUM1, DUM2
          FVAL(2,NOD)=(FVAL(2,NOD)+273.15D0-T0)/T0
          FVAL(3,NOD)=FVAL(3,NOD)*4.76D0
          FLST(1,NOD)=FVAL(1,NOD)
          FLST(2,NOD)=FVAL(2,NOD)
          FLST(3,NOD)=FVAL(3,NOD)
5011    CONTINUE
      ELSE
        DO 1011 NOD=1,NODTOT
C         READ(17,*)FVAL(1,NOD),FVAL(2,NOD),FVAL(3,NOD),DUMMY1,DUMMY2
C         FVAL(2,NOD)=(FVAL(2,NOD)+273.15D0-T0)/T0
C         FVAL(3,NOD)=FVAL(3,NOD)*0.029/RHO*4.76
C         FVAL(1,NOD)=COORD(NOD,1)*(COORD(NOD,1)-1.0)*10.0
          FVAL(1,NOD)=1.0D0
          FLST(1,NOD)=FVAL(1,NOD)
          FVAL(2,NOD)=0.0D0
          FLST(2,NOD)=FVAL(2,NOD)
          FVAL(3,NOD)=0.9995679D0
C         FVAL(3,NOD)=0.0D0
          FLST(3,NOD)=FVAL(3,NOD)
1011    CONTINUE
      END IF
1012  CONTINUE
C           Set initial conditions on Dirichlet boundaries
      IF((ITASK.EQ.4).OR.(ITASK.EQ.6)) THEN
      DO 1036 IEQ=1,NVAR
        DO 1037 M=1,NBND(IEQ)
          IF (NBNDRY(IEQ,M,1).EQ.1) THEN
            NLIST=0
            DO 1038 N=1,NBNDRY(IEQ,M,2)
              NLIST=NLIST+1
```

```
                NDNUM=NBNDRY(IEQ,M,3+NLIST)
C               WRITE(ITERM,*)'NDNUM', NDNUM
                X=COORD(NDNUM,1)
                Y=COORD(NDNUM,2)
                FVAL(IEQ, NDNUM)=HU(X,Y,IEQ)
                FLST(IEQ, NDNUM)=FVAL(IEQ,NDNUM)
                WRITE(ITERM,*)FVAL(IEQ,NDNUM), IEQ, NDNUM
1038          CONTINUE
            ELSE
              CONTINUE
            END IF
1037      CONTINUE
1036    CONTINUE
        END IF
C           Combine initial cond's into system vector FNCVAL
        CALL COMBN (FVAL, NVAR, NODTOT, FNCVAL)
        WRITE(ITERM,*)'ICONT=',ICONT
C           'ITASK' = 0  -  CALCULATE SOLUTION ONCE
C           'ITASK' = 1  -  FIT PARAMETERS BY REPEATED EVALUATIONS
C           'ITASK' = 2  -  CALCULATE S.O.S SURFACE
C           'ITASK' = 4  -  SOLVE UNSTEADY STATE PROBLEM
C           'ITASK' = 5  -  STFADY STATE BY ARC LENGTH CONTINUATION
        IF (ITASK.EQ.4) THEN
           WRITE(ITERM,*)'READING TIME STEPPING DATA'
           READ (NIN,*) TSTART, TFINAL, NTSTEP
           TSTEP=(TFINAL-TSTART)/FLOAT(NTSTEP)
           CFACT=1.0D0
        END IF
        IFRST=1
C           READ IN EXPERIMENTAL MESH POINTS
C       READ (MESH,*) SCLX, SCLY
C       DPTH=DPTH*SCLY
C       READ (MESH,*) NEXPX, NEXPY
C       DO 1032 J=1,NEXPY
C         DO 1032 I=1,NEXPX
C       READ (MESH,*) XEXP(I), YEXP(J), FEXP(I,J)
C       XEXP(I)=XEXP(I)*SCLY
C       YEXP(J)=YEXP(J)*SCLY
C1032    FEXP(I,J)=FEXP(I,J)+273.15D0
C             SET UP CONVENTIONAL GRID REFERENCE POINTS
C       DO 99 I=1,NODTOT
C         IYPOS(I)=I/NX+1
C         IF((I/NX*NX).EQ.I) IYPOS(I)=IYPOS(I)-1
C         IXPOS(I)=I-NX*(IYPOS(I)-1)
C         XX(IXPOS(I))=COORD(I,1)
C99     YY(IYPOS(I))=COORD(I,2)
C
C
C
C                                SETUP NODAL FREEDOM ARRAY
C
        ITOTDF = 0
        DO 1050 I=1,NODTOT
        DO 1040 J=1,IDFNOD
           ITOTDF = ITOTDF + 1
           NF(I,J) = ITOTDF
 1040   CONTINUE
 1050 CONTINUE
        WRITE(ITERM,*)'ITOTDF=',ITOTDF
```

```
C
C                              CALCULATION OF SEMI-BANDWIDTH
C
      FIRST = .TRUE.
      IDIF = 0
      DO 1060 NELE=1,NELS
      CALL FREDIF(NELE, NLTOP, INLTOP, JNLTOP, NF, INF, JNF,IDFNOD,
     * FIRST, IDIF, ITEST)
 1060 CONTINUE
      IHBAND = IDIF + 1
      IBAND=2*IHBAND-1
      WRITE(4,*)'BANDWIDTH = ',IBAND
      IF (IBAND.GT.JSYSK) WRITE(ITERM,*)'MATRIX TOO SMALL'
C*********************************************************************************
      IF (ITASK.EQ.0) THEN
          WRITE(ITERM,*)'SINGLE CALCULATION PROCEEDING'
          C0=0.00D0
          STEPS=STEPS1
          WRITE(ITERM,*)'CALLING ERCHK'
          CALL ERCHK
C         CALL FUNC (NPAR,XPARM, FSOS)
          GO TO 241
      END IF
C*********************************************************************************
      IF (ITASK.EQ.1) THEN
          WRITE(ITERM,*)'FITTING PARAMETERS'
C          ZXMIN (FUNCT,NVAR,NSIG,MAXFN,IOPT,P1,HESS,GRAD,FVAL,WRK,IER)
C       CALL ZXMIN(FUNC, 2, 2, 140, 3, XPARM,HESS, GRAD, FSS, WRKZ, IER
C         TOLR=5.0*DSQRT(X02AAZ'RR))
C         CALL E04CCE (2, XPARM, FSS, TOLR, 3, W1, W2, W3, W4, W5, W6,
C    *      FUNC, MONT, 140, IFAIL)
       WRITE(ITERM,*)'IER, IFAIL = ',IER, IFAIL
          WRITE(NOUT,*)'SOS,PARAMS = ',FSS, XPARM(1), XPARM(2), XPARM(3)
          WRITE(NOUT,*) 'IER, IFAIL = ',IER  IFAIL
          WRITE(NOUT,*)'GRADIENTS '
          WRITE(NOUT,*)(GRAD(J),J=1,3)
          WRITE(NOUT,*)'HESS'
          WRITE(NOUT,*)(HESS(J),J=1,8)
       END IF
C*********************************************************************************
      IF (ITASK.EQ.2) THEN
        WRITE(ITERM,*)'CALCULATING LEAST-SQUARES DATA'
        RLY1=0.5*RYLGH
        RLY2=1.5*RYLGH
        RLSTP=(RLY2-RLY1)/6.0D0
        HCF1=0.5D0*HCOEF
        HCF2=1.50D0*HCOEF
        HCSTP=(HCF2-HCF1)/6.0D0
        HCF=1.0D0*HCOEF
        DO 242 RLY=RLY1,RLY2,RLSTP
          DO 242 HCF=HCF1,HCF2,HCSTP
          XPARM(1)=RLY
          XPARM(2)=HCF
          CALL FUNC(NPAR,XPARM,FSS)
242     WRITE(NOUT,*) FSS, RLY**2, HCF**2
      END IF
C*********************************************************************************
      IF (ITASK.EQ.4) THEN
        WRITE(ITERM,*)'UNSTEADY STATE SOLUTION'
```

```
C       Initialise IPAYN
        IPAYN=0
C       Initialise FNCDER
        DO 788 J=1,ITOTDF
            FNCDER(J)=0.0D0
788     CONTINUE
        CALL ASSM
C           INTEGRATE O.D.E.'S USING DGEAR: INITIALISE VARIABLES
        TEND=TSTART
        TDIF=TSTEP
        TOLR=1.0D-3
C           METH=1 -> Adams method    MITER=0 -> Functional itern.
C           METH=2 -> Stiff method
        METH=2
        MITER=0
        INDEX=1
      DO 789 ITSTEP=1,NTSTEP
        TEND=TEND+TDIF
        WRITE(ITERM,*) 'CALLING DGEAR'
        CALL DGEAR (ITOTDF, TDERV, PDERV, TIME, TSTEP, FNCVAL, TEND,
     *              TOLR, METH, MITER, INDEX, IWK, WK, IER)
        WRITE(4,*)'TEND, IER = ',TEND, IER
        CALL VECCOP (FNCVAL, ISYSK, RHS, ISYSK, ITOTDF, ITEST)
        CALL SEPRT (RHS, NVAR, NODTOT, FVAL)
C       CALL PRTANS
C       CALL PRTXTR
        IF (IER.GE.132) THEN
          WRITE (NOUT,*)'IER = ',IER
          STOP
        END IF
789   CONTINUE
      END IF
C*************************************************************************
      IF (ITASK.EQ.5) THEN
        WRITE(ITERM,*)'ARC LENGTH CONTINUATION'
C       REAL*8   F(9),DELTAX(9),XTEMP(9),XOLD(9),XMIN(9),XMAX(9)
C       REAL*8   JAC(9,9)
C
C       COMMON /VARS1/ X(9),PAR(9),NEQN,NXEQN
C       COMMON /VARS2/ VAR(9),IVAR(9)
C       COMMON /OUTVAR/ DELTA,NVP
C       COMMON /GPARAM/ H,TOL,NN,METH,MITER,NUMINT
C
C       DATA XMIN/9*-1./
C       DATA XMAX/6*5000.,1.,2*10./
C
C       ND  is ITOTDF + the number of parameters ie ITOTDF+1
        ND=ITOTDF+1
        VAR(ND)=XLAM
C       copy initial values into VAR(ND)
        DO 5 I=1,ITOTDF
            VAR(I)=FNCVAL(I)
5       CONTINUE
        READ(10,*) NSIG, ITMAX, NPOINT
        READ(10,*) IFLAG1, IFLAG2, IFLAG3
C       READ(10,*) H, TOL
        READ(10,*) HH, DIR
C       READ(10,*) NN, METH, MITER, NUMINT
C       READ(10,*) IVAR
```

```
C       READ(10,*) DELTA, NVP
C
        NEQN = ITOTDF
        NXEQN = NEQN+1
        NDE = NXEQN
C       DO 10 I = 1,NXEQN
C 10    X(I) = VAR(IVAR(I))
C       DO 20 I=NXEQN+1,ND
0         NXT=I-NXEQN
C20       PAR(NXT)=VAR(IVAR(I))
C
C       CALL PARA(ND, NEQN, VAR, NSIG, ITMAX, NPOINT
C     *            ,VMIN, VMAX, HH, DIR, FNCVAL, NDE, NODTOT)
C
      END IF
C*******************************************************************************
241   CALL PRTANS
      CALL PRTXTR
      STOP
      END
C ***************************************************************************** **********
C
C         SUBROUTINE TO CALCULATE S.O.S OF TEMPERATURE PROFILE ERRORS
      SUBROUTINE FUNC (NPAR, X, FSOS)
      IMPLICIT REAL*8 (A-H,O-Z)
      COMMON /FVALS/ FVAL(5,500), FLST(5,500)
      REAL*8 X(4), FMAT(60,60), FNTRP(60,60), WK(135)
      COMMON /ELDAT/ NLTOP(500,14),COORD(500,3),NELE,IELTYP,NODEL,ITELS,
     *           NF(500,5), XX(30), YY(30),NODTOT, IDIMN, IDFEL,
     *NX,NY,
     *           IXPOS(500), IYPOS(500), NODSID
      COMMCN /EXPT/ XEXP(10), YEXP(10), FEXP(10,10)
      COMMON /XTRACT/ NXTRCT, IVXTR(6), IEXLST(6,4,60), NODXTR(6)
      COMMON /CONT/ C0, CFCTMX, STEPS, STEPS1, STEPS2, ITRACE, ICONT,
     *              IFRST, ICHK, ITASK, IPAYN, DPUP, DPLOW
       COMMON /IO/ NINT, ITERM, NIN, NOUT, IPROFL, MESH, IERR, NTOUT,
     *             INPARM
C
C     C0=1.00
C     ICONT=0
      STEPS=STEPS2
C        If first time around, allow many continuation steps ('STEPS1')
      IF (IFRST.EQ.1) THEN
         STEPS=STEPS1
         C0=0.00D0
C        ICONT=0
         IFRST=0
      END IF
      NXE=9
      NYE=8
      IFMAT=30
      IFNTRP=30
      WRITE(4,*)'PARAMS ',X(1),X(2),X(3)
      CALL FELMNT
      DO 10 I=1,NODTOT
10    FMAT(IXPOS(I), IYPOS(I))=FVAL(2,I)
C     CALL IBCIEU (FMAT, IFMAT, XX, NX, YY,NY, XEXP, NXE, YEXP, NYE,
C    *      FNTRP, IFNTRP, WK, IER)
      FSOS=0.00D0
```

```
      DO 20 I=1,NXE
        DO 20 J=1,NYE
          FLG=1.0D0
          IF (FEXP(I,J).LT.300.00) FLG=0.00D0
          TNTRP=TREAL(FNTRP(I,J))
          IF ((ITASK.EQ.0).AND.(FLG.NE.0.00)) WRITE (IERR,*)
     *          TNTRP,FEXP(I,J)-273.15, XEXP(I), YEXP(J
20    FSOS=FSOS+FLG*(TNTRP+273.15-FEXP(I,J))**2
      WRITE(4,*)'SOS ',FSOS
      WRITE(4,*)
      WRITE(6,*) FSOS, X(1),X(2),X(3)
      RETURN
      END
C
      SUBROUTINE FELMNT
      IMPLICIT REAL*8(A-H,O-Z)
      REAL*8 JAC, JACIN, LDER
      DIMENSION ABSS(3,9), BELM(60,60), BELV(60), BN(60), BNTN(60,60),
     * BNTMP(12), BMTEMP(12,12),
     * COSIN(3), RMAT(60,60), ELK(60,60), GDERT(12,3),
     * GEOM(12,3),   JAC(3,3),JACIN(3,3), ABSCL(9),  LDER(3,12)
     *, P(3,3),
     * PD(3,12),NSTER(60), WGHT(9),BELV1(60),SRCE(60), QL(12)
     *, TMAT(12,12),
     * XTVEC(60), DERMAP(3,12)
      COMMON /XP/ XPARM(4)
       COMMON /DIMS/ INBDC, ILISTB, ICOORD, INLTOP, INF, IRHS, ISYSK,
     *              JNBDC, JLISTB, JNLTOP, JNF, JSYSK, INROPV, IAL, JAL
       COMMON /IO/ NINT, ITERM, NIN, NOUT, IPROFL, MESH, IERR, NTOUT,
     *            INPARM
C      COMMON /PARM/ PARAM(4)
       COMMON /VAR/ NVAR
       COMMON /ELDAT/ NLTOP(500,14),COORD(500,3),NELE,IELTYP,NODEL,ITELS,
     *           NF(500,5), XX(30), YY(30),NODTOT, IDIMN, IDFEL,
     *NX,NY,
     *           IXPOS(500), IYPOS(500), NODSID
       COMMON /XTRACT/ NXTRCT, IVXTR(6), IEXLST(6,4,60), NODXTR(6)
       COMMON /FEMWRK/  RHS(410), AL(410,140),
     *        NROPV(410), RESDV(4,500), RESD(4), ERR(4),
     *        ERRAV(4), ERRCNT(4), ERRTOT(4), SCALE
       COMMON /BAND/ IBAND, IHBAND, ITOTDF
       COMMON /MTRIX/ SYSK (410, 140), SYSM(410,140)
       COMMON /BNDRY/ NBNDRY(5,6,80), NBND(5), NBDC(6,80), LISTB(140,5)
       COMMON /SHPFN/ FUN(12), GDER(3,12)
       COMMON /FVALS/ FVAL(5,500), FLST(5,500)
       COMMON /RLNUM/ RALY, CFACT
       COMMON /JEOM/ XMAX, YMAX, CHRL, CRDSYS, IEQFRM, ISIDNM
       COMMON /PARAM/  RYLGH, HCOEF, DP, EPSI, EA, XK0, DOVA, PERM, XMU,
     *                 PHI, ALPHA, PO, XLAM
       COMMON /GRPS/ XLEW, GAMMA, BETA, THIELE, RLLY, BIOT, DEE, CHI,
     *              TAU, ZETA, SIGMA
       COMMON /CONT/ C0, CFCTMX, STEPS, STEPS1, STEPS2, ITRACE, ICONT,
     *              IFRST, ICHK, ITASK, IPAYN, DPUP, DPLOW
       COMMON /RELAX/ RELAX1, RELAX2, RELAX3
       COMMON /SPLIT/ IVAR, KK, K, NBTYPE, NODE, IFIRST
       REAL*8 CHPARM(4), MAPFUN(12), MAXVAL(5)
C
C                              PROBLEM SIZE DEPENDENT ARRAYS
C
```

```
C
      DATA IABSS /3/,IBELM/60/,IBELV /60/,IBN /60/,IBNTN /60/,ICOSIN/3/,
     * IRMAT /60/,IELK /60/, IFUN /12/, IGDER /3/,IGDERT /12/, IGEOM
     */12/,
     *  IJAC /3/, IJACIN /3/,IABSCL /9/, ILDER /3/, IP /3/, IPD /3/,
     * INSTER /60/,IWGHT /9/, JABSS /9/,JBELM/60/,JBNTN /60/,JCOORD /3/,
     *  ISRCE /60/, IXTVEC /60/,
     * JRMAT /60/, JELK /60/, JGDER /12/, JGDERT /3/, JGEOM /3/,JJAC
     */3/,
     * JJACIN /3/, JLDER /12/, JP /3/,JPD /12/
C
C                              PROBLEM SIZE DEPENDENT DATA STATEMENTS
C
C     DATA INBDC /6/, ILISTB /140/, ICOORD /500/, INLTOP /500/,INF /500/
C    *, IRHS /410/, ISYSK /410/, JNBDC /80/,JLISTB /5/, JNLTOP /14/,
C    * JSYSK /140/, INROPV /410/, IAL/410/, JAL /140/
C
C
      MPINCR=NODSID-1
      NODMAP=NODEL-NODSID+2
C
C
C
C     RYLGH=XPARM(1)
C     HCOEF=XPARM(2)
C                              SET 'RALY' TO MAX VALUE
C     RALY=RYLGH
C
C
C                              SET ITEST FOR FULL CHECKING
C
      IDFNOD=NVAR
      ITEST = 0
      IDGT=0
      IWKREA=50000
      NRHS=1
C
C*                             ****************************************
C*                             *                                      *
C*                             * SYSTEM STIFFNESS MATRIX ASSEMBLY *
C*                             *                                      *
C*                             ****************************************
C
C
      CALL MATNUL(SYSK, ISYSK, JSYSK, ITOTDF, IBAND, ITEST)
      CALL VECNUL(RHS, IRHS, ITOTDF, ITEST)
      IDFEL = NODEL*IDFNOD
      IF ((IELTYP.EQ.1).OR.(IELTYP.EQ.2).OR.(IELTYP.EQ.3)) THEN
         CALL QTRI7(WGHT, IWGHT, ABSS, IABSS, JABSS, NQP, ITEST)
      END IF
      IF ((IELTYP.EQ.4).OR.(IELTYP.EQ.5).OR.(IELTYP.EQ.6)) THEN
C        CALL QQUA4(WGHT, IWGHT, ABSS, IABSS, JABSS, NQP, ITEST)
         CALL QQUA9(WGHT, IWGHT, ABSS, IABSS, JABSS, NQP, ITEST)
      END IF
      DO 1100 NELE=1,ITELS
      CALL ELGEOM(NELE, NLTOP, INLTOP, JNLTOP, COORD, ICOORD,JCOORD,
     * GEOM, IGEOM, JGEOM, IDIMN, ITEST)
C
C                              INTEGRATION LOOP FOR ELEMENT MATRICES
```

```
C                              USING NQP QUADRATURE POINTS
C
      CALL MATNUL(ELK, IELK, JELK, IDFEL, IDFEL, ITEST)
      CALL VECNUL(SRCE, ISRCE, IDFEL, ITEST)
      DO 1090 IQUAD=1,NQP
      CALL MATNUL(RMAT, IRMAT, JRMAT, IDFEL, IDFEL, ITEST)
      CALL VECNUL(XTVEC, IXTVEC, IDFEL, ITEST)
C
C                              FORM SHAPE FUNCTION AND SPACE
C                              DERIVATIVES IN THE LOCAL CORRDINATES.
C                              TRANSFORM LOCAL DERIVATIVES TO GLOBAL
C                              COORDINATE SYSTEM
C
      XI = ABSS(1,IQUAD)/1.0000D0
      ETA = ABSS(2,IQUAD)/1.000000D0
      IF (IELTYP.EQ.1) THEN
        CALL TRIM3(FUN, IFUN, LDER, ILDER, JLDER, XI, ETA, ITEST)
        CALL TRIM3(MAPFUN, IFUN, DERMAP, ILDER, JLDER, XI, ETA, ITEST)
      END IF
      IF (IELTYP.EQ.4) THEN
        CALL QU4FN(FUN, IFUN, LDER, ILDER, JLDER, XI, ETA, ITEST)
        CALL QU4FN(MAPFUN, IFUN, DERMAP, ILDER, JLDER, XI, ETA, ITEST)
      END IF
      IF (IELTYP.EQ.5) THEN
        CALL QU8FN(FUN, IFUN, LDER, ILDER, JLDER, XI, ETA, ITEST)
        CALL QU4FN(MAPFUN, IFUN, DERMAP, ILDER, JLDER, XI, ETA, ITEST)
      END IF
C
C       Calculate Jacobian (mapping fn. deriv's * element geometry)
       CALL MLTXTR (DERMAP, ILDER, JLDER, GEOM, IGEOM, JGEOM, JAC, IJAC,
     *              JJAC, IDIMN, NODMAP, MPINCR)
C      CALL MATMUL(LDER, ILDER, JLDER, GEOM, IGEOM, JGEOM, JAC,IJAC,
C     * JJAC, IDIMN, NODEL, IDIMN, ITEST)
       CALL MATINV(JAC, IJAC, JJAC, JACIN, IJACIN, JJACIN, IDIMN, DET,
     * ITEST)
       CALL MATMUL(JACIN, IJACIN, JJACIN, LDER, ILDER, JLDER, GDER,IGDER,
     *              JGDER, IDIMN, IDIMN, NODEL, ITEST)
C
C                              CALCULATE (XI,ETA) IN GLOBAL (X,Y)
C                              COORDINATES AND FORM P MATRIX
C
       XMAP=0.0D0
       YMAP=0.0D0
       IMAP=0
       DO 8999 KL=1,NODMAP, MPINCR
       IMAP=IMAP+1
       XMAP=XMAP+GEOM(KL,1)*MAPFUN(IMAP)
8999   YMAP=YMAP+GEOM(KL,2)*MAPFUN(IMAP)
       X=XMAP
       Y=YMAP
C      CALL SCAPRD(GEOM(1,1), IGEOM, FUN, IFUN, NODEL, X, ITEST)
C      CALL SCAPRD(GEOM(1,2), IGEOM, FUN, IFUN, NODEL, Y, ITEST)
C
C                              FORM INTEGRAND ELEMENT STIFFNESS ELK
C
       QUOT = DABS(DET)*WGHT(IQUAD)
       DO 1082 IEQ=1,NVAR
        DO 1081 IVAR=1,NVAR
         DO 1080 I=1,NODEL
```

```
          DO 1070 J=1,NODEL
             CALL EQNS (F, X, Y, I, J, IEQ, IVAR, FUN, GDER, QUOT)
             TMAT(I,J)=F*QUOT
 1070     CONTINUE
          CALL SOURCT (F, X, Y, I, IEQ, FUN, GDER, NVAR)
          QL(I)=F*QUOT
 1080   CONTINUE
 1081  CALL ASMAT (TMAT, RMAT, IVAR, IEQ, NODEL)
 1082 CALL ASVEC (QL, XTVEC, IEQ,    DEL)
      CALL MATADD(ELK, IELK, JELK,    IRMAT, JRMAT, IDFEL,IDFEL,
     * ITEST)
      CALL VECADD(SRCE, ISRCE, XTVEC,    VEC, IDFEL, ITEST)
 1090 CONTINUE
C
C                              ASSEMBLY OF SYSTEM STIFFNESS MATRIX
C
      CALL DIRECT(NELE, NLTOP, INLTOP, JNLTOP, NF, INF, JNF,IDFNOD,
     * NSTER, INSTER, ITEST)
      CALL ASUSM(SYSK, ISYSK, JSYSK, ELK, IELK, JELK, NSTER,INSTER,
     * IHBAND, IDFEL, ITEST)
      CALL ASRHS(RHS, IRHS, SRCE, ISRCE, NSTER, INSTER, IDFEL,ITEST)
 1100 CONTINUE
C
C*                             ********************************************
C*                             *                                          *
C*                             * INSERTION OF BOUNDARY CONDITIONS *
C*                             *                                          *
C*                             ********************************************

      CALL QLIN3(WGHT, IWGHT, ABSCL, IABSCL, NQP, ITEST)
      DO 1230 IVAR=1,NVAR
       DO 1231 I=1,NBND(IVAR)
        DO 1231 J=1,40
          IFSTND=NBNDRY(IVAR, I, 4)
 1231     NBDC(I,J)=NBNDRY(IVAR, I, J)
      DO 1230 ITYPE=1,NBND(IVAR)
      NBTYPE = NBDC(ITYPE,1)
      NUMSID = NBDC(ITYPE,2)
      GO TO (1110, 1130, 1131), NBTYPE
C
C
C
C
C                                 'SPLIT' DIRICHLET BOUNDARY CONDITIONS
 1131  CALL SPLENO (ITEL , NLTOP, INLTOP, JNLTOP, ITYPE, NBDC,INBDC,
     * JNBDC, NUMSID, LISTE, ILISTB, JLISTB, ITEST)
      IF (NUMSID.EQ.0) WRITE(ITERM,*)'BOUNDARY ERROR',NVAR, ITYPE
      DO 1117 M=1,NUMSID
        IELNM = LISTB(M,1)
        ISIDNM = LISTB(M,2)
        NELE=IELNM
        LL=(ISIDNM-1)*NODSID-1)
C --- KK and KK1 are the first and second nodes on side ISIDNM
C --- and these are incremented in loop 1117 such that on
C --- each subsequent run through the loop the node called KK
C --- becomes the node called KK1 in the previous time through
C --- the loop
        DO 1117 N=1,NODSID-1
```

```
C --- IFIRST is the first node in the boundary list for SPLIT
          IF(N.EQ.1) THEN
C --- NODE =1 implies that the node is the first in the element
            NODE=1
          ELSE
            NODE=0
          END IF
          KK=NLTOP(NELE,3+LL+N-1)
          KK1=NLTOP(NELE,3+LL+N)
          K=NVAR*KK+(IVAR-NVAR)
          IF((KK.EQ.IFSTND).OR.(KK1.EQ.(IFSTND+N))) THEN
            IFIRST=1
          ELSE
            IFIRST=0
          END IF
          IF(ISIDNM.EQ.2) THEN
            DELTA=COORD(KK+1,1)-COORD(KK,1)
          END IF
          IF(ISIDNM.EQ.3) THEN
            DELTA=DSQRT((COORD(KK+1,1)-COORD(KK,1))**2+(COORD(KK+1,2)-
     *           COORD(KK,2))**2)
          END IF
          FVAL1=FVAL(1,KK)
          FVAL2=FVAL(1,KK1)
          DERIV=(FVAL2-FVAL1)/DELTA
          CALL DIRIC (DERIV, ISIDNM)
1117    CONTINUE
 1119 CONTINUE
      GO TO 1230
C
C                              PRESCRIBED VALUES  (DIRICHLET)
C
1110  DO 1120 J=1,NUMNOD
        KK = NBDC(ITYPE,J+3)
        K = NVAR*NBDC(ITYPE,J+3)+(IVAR-NVAR)
          CALL DIRIC (DERIV, ISIDNM)
 1120 CONTINUE
      GO TO 1230
C
C                            DERIVATIVES (NEUMANN AND CAUCHY)
C
1130  CALL SIDENO (ITELS, NLTOP. INLTOP, JNLTOP, ITYPE, NBDC,INBDC,
     * JNBDC, NUMSID, LISTB, ILISTB, JLISTB, ITEST)
      IF (NUMSID.EQ.0) WRITE(ITERM,*)'BOUNDARY ERROR', NVAR, ITYPE
      DO 1220 M=1,NUMSID
      IELNM = LISTB(M,1)
      NELE=IELNM
      ISIDNM = LISTB(M,2)
      CALL VECNUL(BELV, IBELV, IDFEL, ITEST)
      CALL VECNUL(BELV1, IBELV, IDFEL, ITEST)
      CALL MATNUL(BELM, IBELM, JBELM, IDFEL, IDFEL, ITEST)
C
C                              CONSTRUCT QUADRATURE RULE AND LOCAL
C                              GEOMETRY
C
      CALL ELGEOM(IELNM, NLTOP, INLTOP, JNLTOP, COORD, ICOORD,JCOORD,
     * GEOM, IGEOM, JGEOM, IDIMN, ITEST)
      IF ((IELTYP.EQ.1).OR.(IELTYP.EQ.2).OR.(IELTYP.EQ.3)) THEN
        CALL BQTRI(ABSS,IABSS,JABSS, ABSCL, IABSCL, NQP, ISIDNM,COEFF,
```

```
*              ITEST)
       END IF
       IF ((IELTYP.EQ.4).OR.(IELTYP.EQ.5).OR.(IELTYP.EQ.6)) THEN
         CALL BQQUA(ABSS,IABSS,JABSS, ABSCL, IABSCL, NQP, ISIDNM,COEFF,
*              ITEST)
       END IF
C
C                              PERFORM BOUNDARY INTEGRATION
C
       DO 1190 J=1,NQP
       CALL MATNUL(BNTN, IBNTN, JBNTN, IDFEL, IDFEL, ITEST)
       CALL VECNUL(BN, IBN, IDFEL, ITEST)
       XI = ABSS(1,J)/1.0D0
       ETA = ABSS(2,J)/1.0D0
       IF (IELTYP.EQ.1) THEN
         CALL TRIM3(FUN, IFUN, LDER  ILDER, JLDER, XI, ETA, ITEST)
         CALL TRIM3(MAPFUN, IFUN, DERMAP, ILDER, JLDER, XI, ETA, ITEST)
         CALL LINTRI(XI, ETA, GEOM, IGEOM, JGEOM, NODEL, ISIDNM,ULEN,
*              ITEST)
       END IF
       IF (IELTYP.EQ.4) THEN
         CALL QU4FN(FUN, IFUN, LDER, ILDER, JLDER, XI, ETA, ITEST)
         CALL QU4FN(MAPFUN, IFUN, DERMAP, ILDER, JLDER, XI, ETA, ITEST)
         CALL LINQUA(XI, ETA, GEOM, IGEOM, JGEOM, NODEL, ISIDNM,ULEN,
*              ITEST)
       END IF
       IF (IELTYP.EQ.5) THEN
         CALL QU8FN(FUN, IFUN, LDER, ILDER, JLDER, XI, ETA, ITEST)
         CALL QU4FN(MAPFUN, IFUN, DERMAP, ILDER, JLDER, XI, ETA, ITEST)
         CALL LINQUA(XI, ETA, GEOM, IGEOM, JGEOM, NODEL, ISIDNM,ULEN,
*              ITEST)
       END IF
       QUOT = ULEN*WGHT(J)*COEFF
C
C                              CALCULATE (XI,ETA) IN GLOBAL (X,Y)
C                              COORDINATES
C
       XMAP=0.0D0
       YMAP=0.0D0
       IMAP=0
       DO 8909 KL=1,NODMAP, MPINCR
       IMAP=IMAP+1
       XMAP=XMAP+GEOM(KL,1)*MAPFUN(IMAP)
8909   YMAP=YMAP+GEOM(KL,2)*MAPFUN(IMAP)
       X=XMAP
       Y=YMAP
C      CALL SCAPRD(GEOM(1,1), IGEOM, FUN, IFUN, NODEL, X, ITEST)
C      CALL SCAPRD(GEOM(1,2), IGEOM, FUN, IFUN, NODEL, Y, ITEST)
C
C                              CALCULATION OF THE NORMAL DIRECTION
C                              COSINES
C        Calculate Jacobian (mapping fn. deriv's * element geometry)
       CALL MLTXTR (DERMAP, ILDER, JLDER, GEOM, IGEOM, JGEOM, JAC, IJAC,
*              JJAC, IDIMN, NODMAP, MPINCR)
C      CALL MATMUL(LDER, ILDER, JLDER, GEOM, IGEOM, JGEOM, JAC,IJAC,
C     * JJAC, IDIMN, NODEL, IDIMN, ITEST)
       CALL MATINV(JAC, IJAC, JJAC, JACIN, IJACIN, JJACIN, IDIMN,DET,
*  ITEST)
       CALL MATMUL(JACIN, IJACIN, JJACIN, LDER, ILDER, JLDER, GDER,IGDER,
```

```
     *              JGDER, IDIMN, IDIMN, NODEL, ITEST)
      IF ((IELTYP.EQ.1).OR.(IELTYP.EQ.2).OR.(IELTYP.EQ.3)) THEN
C       CALL DCSTRI(JACIN,IJACIN, JJACIN, ISIDNM, COSIN, ICOSIN,ITEST)
      END IF
      IF ((IELTYP.EQ.4).OR.(IELTYP.EQ.5).OR.(IELTYP.EQ.6)) THEN
C       CALL DCSQUA(JACIN, IJACIN, JJACIN, ISIDNM, COSIN, ICOSIN,ITEST)
      END IF
C
      GO TO (1220, 1160), NBTYPE
C
C                              CAUCHY CONDITIONS
C
1160  VV=0.0D0
      DO 1181 IEQ=1,NVAR
        DO 1180 K=1,NODEL
          DO 1170 L=1,NODEL
            CALL BFUNM (F, X, Y, K, L, IEQ, IVAR, FUN, QUOT, ISIDNM,
     *                  GDER)
            BMTEMP(K,L) = F*QUOT
1170      CONTINUE
          CALL BFUNV (F, X, Y, K, IEQ, IVAR, FUN)
          BNTMP(K) = F*QUOT
1180    CONTINUE
1181  CALL ASMAT (BMTEMP, BNTN, IVAR, IEQ, NODEL)
      CALL ASVEC (BNTMP, BN, IEQ, NODEL)
      CALL MATADD(BELM, IBELM, JBELM, BNTN, IBNTN, JBNTN, IDFEL,IDFEL,
     * ITEST)
      CALL VECADD (BELV1, IBELV, BN, IBN, IDFEL, ITEST)
1190  CONTINUE
C
C
C                          ASSEMBLY OF BOUNDARY CONDITIONS
C
      CALL DIRECT(IELNM, NLTOP, INLTOP, JNLTOP, NF, INF, JNF,IDFNOD,
     * NSTER, INSTER, ITEST)
      GO TO (1220, 1210), NBTYPE
1210  CALL ASCSM(SYSK, ISYSK, JSYSK, BELM, IBELM, JBELM, NSTER,INSTER,
     * IHBAND, IDFEL, ITEST)
      CALL ASRHS(RHS, IRHS, BELV1, IBELV, NSTER, INSTER, IDFEL,ITEST)
1220  CONTINUE
1230  CONTINUE
      RETURN
      END
```

```
      SUBROUTINE ASMAT(A, B, IVAR, IEQ, NODEL)
      IMPLICIT REAL*8 (A-H,O-Z)
      REAL*8 A(12,12), B(60,60)
      COMMON /VAR/ NVAR
      IOFST=IEQ-NVAR
      JOFST=IVAR-NVAR
      DO 10 I=1,NODEL
         II=NVAR*I+IOFST
         DO 10 J=1,NODEL
            JJ=NVAR*J+JOFST
10          B(II,JJ)=A(I,J)
      RETURN
      END
C
      SUBROUTINE ASVEC(V, W, IEQ, NODEL)
      IMPLICIT REAL*8 (A-H,O-Z)
      REAL*8 V(12), W(60)
      COMMON /VAR/ NVAR
      IOFST=IEQ-NVAR
      DO 10 I=1,NODEL
10          W(NVAR*I+IOFST)=V(I)
      RETURN
      END
C
      SUBROUTINE USSEQN (F, X, Y, I, J, IEQ, IVAR, FUN, GDER, QUOT)
      IMPLICIT REAL*8 (A-H,O-Z)
      COMMON /PARAM/ RYLGH, HCOEF, DP, EPSI, EA, XKO, DOVA, PERM, XMU,
     *               PHI, ALPHA, PO, XLAM
      COMMON /GRPS/ XLEW, GAMMA, BETA, THIELE, RLLY, BIOT, DEE, CHI,
     *              TAU, ZETA, SIGMA
      COMMON /RLNUM/ RALY, CFACT
      COMMON /CONT/ CO, CFCTMX, STEPS, STEPS1, STEPS2, ITRACE, ICONT,
     *              IFRST, ICHK, ITASK, IPAYN, DPUP, DPLOW
      REAL*8 FUN(12), GDER(3,12)
      F=0.00D0
C           Contributions from equation 1
        IF (IEQ.EQ.1) THEN
           IF (IVAR.EQ.1) THEN
              F=-GDER(1,I)*GDER(1,J)-GDER(2,I)*GDER(2,J)
     *          -FUN(I)*GDER(1,J)/X
           END IF
           IF (IVAR.EQ.2) THEN
              F=0.00D0
           END IF
           IF (IVAR.EQ.3) THEN
              F=0.00D0
           END IF
        END IF
C           Contributions from equation 2
        IF (IEQ.EQ.2) THEN
           IF (IVAR.EQ.1) THEN
              F=0.00D0
           END IF
           IF (IVAR.EQ.2) THEN
              F=FUN(I)*FUN(J)/PHI
           END IF
           IF (IVAR.EQ.3) THEN
              F=0.00D0
           END IF
```

```
          END IF
C           CONTRIBUTIONS FROM EQUATION 3
          IF (IEQ.EQ.3) THEN
             IF (IVAR.EQ.1) THEN
                F=0.00D0
             END IF
             IF (IVAR.EQ.2) THEN
                F=0.00D0
             END IF
             IF (IVAR.EQ.3) THEN
                F=FUN(I)*FUN(J)/EPSI
             END IF
          END IF
        RETURN
        END
C
C
C
C
C   This file contains the equations for the unsteady problem
        SUBROUTINE EQNS (F, X, Y, I, J, IEQ, IVAR, FUN, GDER, QUOT)
        IMPLICIT REAL*8 (A-H,O-Z)
        COMMON /RLNUM/ RALY, CFACT
        COMMON /CONT/ C0, CFCTMX, STEPS, STEPS1, STEPS2, ITRACE, ICONT,
       *              IFRST, ICHK, ITASK, IPAYN, DPUP, DPLOW
        COMMON /ELDAT/ NLTOP(500,14),COORD(500,3),NELE,IELTYP,NODEL,ITELS,
       *            NF(500,5), XX(30), YY(30),NODTOT, IDIMN, IDFEL,
       *NX,NY,
       *            IXPOS(500), IYPOS(500), NODSID
        COMMON /PARAM/ RYLGH, HCOEF, DP, EPSI, EA, XK0, DOVA, PERM, XMU,
       *               PHI, ALPHA, P0 ,XLAM
        COMMON /GRPS/ XLEW, GAMMA, BETA, THIELE, RLLY, BIOT, DEE, CHI,
       *              TAU, ZETA, SIGMA
        COMMON /JEOM/ XMAX, YMAX, CHRL, CRDSYS, IEQFRM, ISIDNM
        COMMON /IO/ NINT, ITERM, NIN, NOUT, IPROFL, MESH, IERR, NTOUT,
       *            INPARM
C       CRDSYS=0 SELECTS CARTESIAN COORDINATES, =1 SELECTS CYLINDRICAL
C       IEQFRM=0 SELECTS CONCENTRATION FORM, =1 SELECTS PHI**2 FORM
        REAL*8 FUN(12), GDER(3,12)
        RALLY=RALY
C       SELECT APPROPRIATE EQUATION SET FOR COORDINATE SYSTEM CRDSYS=0
C       FOR CARTESIAN
        IF(CRDSYS.EQ.0.0)THEN
C             Contributions from equation 1
        IF (IEQ.EQ.1) THEN
          IF (IVAR.EQ.1) THEN
             F=-GDER(1,I)*GDER(1,J)
       *     -GDER(2,I)*GDER(2,J)
             RETURN
          END IF
          IF (IVAR.EQ.2) THEN
             F=RLLY*(DPUP-(DPUP-DPLOW)*(DSIN(3.1415D0/2.0D0*
       *       (CFACT-1.0D0)/(CFCTMX-1.0D0))))**2/DP**2
       *       *FUN(I)*GDER(1,J)
             RETURN
          END IF
          IF(IVAR.EQ.3) THEN
            F=0.0D0
            RETURN
```

```
          END IF
        END IF
C
C            Contributions from equation 2
        IF (IEQ.EQ.2) THEN
          IF (IVAR.EQ.1) THEN
             F=0.00D0
             RETURN
          END IF
          IF (IVAR.EQ.2) THEN
             F=(+DFXY(2,1)*FUN(I)*GDER(1,J)-DFXY(1,1)*FUN(I)*
     *          GDER(2,J))+GDER(1,I)*GDER(1,J)+GDER(2,I)*GDER(2,J)
             RETURN
          END IF
          IF(IVAR.EQ.3) THEN
            F=0.0D0
            RETURN
          END IF
        END IF
C              CONTRIBUTIONS FROM EQUATION 3
        IF(IEQ.EQ.3) THEN
          IF(IVAR.EQ.1) THEN
            F=0.0D0
            RETURN
          END IF
          IF(IVAR.EQ.2) THEN
            F=0.0D0
            RETURN
           END IF
           IF(IVAR.EQ.3) THEN
             IF(IEQFRM.EQ.2)THEN
             F=+DFXY(2,1)*FUN(I)*GDER(1,J)
     *         -DFXY(1,1)*FUN(I)*GDER(2,J)
     #         +XLEW*(GDER(1,I)*GDER(1,J)+GDER(2,I)*GDER(2,J))
               RETURN
             END IF
             IF(IEQFRM.EQ.1)THEN
             F=+DFXY(2,1)*FUN(I)*GDER(1,J)*FUN(J)
     #         -DFXY(1,1)*FUN(I)*GDER(2,J)*FUN(J)
     #       +XLEW*(GDER(1,I)*GDER(1,J)*FUN(J)-DFXY(1,3)*GDER(1,J)*FUN(I)
     *       +GDER(2,I)*GDER(2,J)*FUN(J)-DFXY(2,3)*GDER(2,J)*FUN(I))
             RETURN
             END IF
           END IF
        END IF
        END IF
C*************************************.*************************************
C            EQUATIONS IN CYLINDRICAL COORDINATES
C*****************************************************************************
        IF(CRDSYS.EQ.1.)THEN
C              Contributions from equation 1
        IF (IEQ.EQ.1) THEN
          IF (IVAR.EQ.1) THEN
             F=-GDER(1,I)*GDER(1,J)-FUN(I)*GDER(1,J)/X
     *       -GDER(2,I)*GDER(2,J)
             RETURN
          END IF
          IF (IVAR.EQ.2) THEN
             F=RLLY*(DPUP-(DPUP-DPLOW)*(DSIN(3.1415D0/2.0D0*
```

```
*       (CFACT-1.0D0)/(CFCTMX-1.0D0))))**2/DP**2
*       *FUN(I)*GDER(1,J)*X
        RETURN
      END IF
      IF(IVAR.EQ.3) THEN
        F=0.'D0
        RETURN
      END IF
    END IF
C
C           Contributions from equation 2
    IF (IEQ.EQ.2) THEN
      IF (IVAR.EQ.1) THEN
        F=0.00D0
        RETURN
      END IF
      IF (IVAR.EQ.2) THEN
        F=(+DFXY(2,1)*FUN(I)*GDER(1,J)/X-DFXY(1,1)*FUN(I)*
*         GDER(2,J)/X)+GDER(1,I)*GDER(1,J)+GDER(2,I)*GDER(2,J)
*         -FUN(I)*GDER(1,J)/X
        RETURN
      END IF
      IF(IVAR.EQ.3) THEN
        F=0.0D0
        RETURN
      END IF
    END IF
C             CONTRIBUTIONS FROM EQUATION 3
    IF(IEQ.EQ.3) THEN
      IF(IVAR.EQ.1) THEN
        F=0.0D0
        RETURN
      END IF
      IF(IVAR.EQ.2) THEN
        F=0.0D0
        RETURN
      END IF
      IF(IVAR.EQ.3) THEN
        IF(IEQFRM.EQ.0) THEN
        F=+DFXY(2,1)*FUN(I)*GDER(1,J)/X
#         -DFXY(1,1)*FUN(I)*GDER(2,J)/X
#     +XLEW*(GDER(1,I)*GDER(1,J)-GDER(1,J)*FUN(I)/X
*         +GDER(2,I)*GDER(2,J))
          RETURN
        END IF
        IF(IEQFRM.EQ.1) THEN
        F=+DFXY(2,1)*FUN(I)*GDER(1,J)*FUN(J)/X
#         -DFXY(1,1)*FUN(I)*GDER(2,J)*FUN(J)/X
#     +XLEW*(GDER(1,I)*GDER(1,J)*FUN(J)-GDER(1,J)*FUN(J)*FUN(I)/X
*         -DFXY(1,3)*GDER(1,J)*FUN(I)
*         +GDER(2,I)*GDER(2,J)*FUN(J)
*         -DFXY(2,3)*GDER(2,J)*FUN(I))
          RETURN
        END IF
      END IF
    END IF
    WRITE(4,*)'ERROR - IEQ OR IVAR > NEQ',IEQ,IVAR
    RETURN
```

```
      END
C
C
C
      SUBROUTINE BFUNM (F, X, Y, K, L, IEQ, IVAR, FUN, QUOT, ISIDE,
     *                  GDER)
      IMPLICIT REAL*8 (A-H,O-Z)
      COMMON /IO/ NINT, ITERM, NIN, NOUT, IPROFL, MESH, IERR, NTOUT,
     *           INPARM
      COMMON /ELDAT/ NLTOP(500,14),COORD(500,3),NELE,IELTYP,NODEL,ITELS,
     *           NF(500,5), XX(30), YY(30),NODTOT, IDIMN, IDFEL,
     *NX,NY,
     *           IXPOS(500), IYPOS(500), NODSID
      COMMON /JEOM/ XMAX, YMAX, CHRL, CRDSYS, IEQFRM, ISIDNM
      COMMON /PARAM/ RYLGH, HCOEF, DP, EPSI, EA, VKO, DOVA, PERM, XMU,
     *               PHI, ALPHA, PO, XLAM
      COMMON /GRPS/ XLEW, GAMMA, BETA, THIELE, RLLY, BIOT, DEE, CHI,
     *              TAU, ZETA, SIGMA
      COMMON /ANGL/ ANGLE
      REAL*8 FUN(12), GDER(3,12)
      F=0.00D0
        IF(IEQ.EQ.1) THEN
         IF (IVAR.EQ.1) THEN
            F=0.00D0* FUN(K)*FUN(L)
            RETURN
         END IF
         IF (IVAR.EQ.2) THEN
            F=0.00D0*FUN(K)*FUN(L)
            RETURN
         END IF
         IF (IVAR.EQ.3) THEN
            F=0.00D0*FUN(K)*FUN(L)
            RETURN
         END IF
        END IF
C
        IF(IEQ.EQ.2) THEN
         IF (IVAR.EQ.1) THEN
            F=0.00D0* FUN(K)*FUN(L)
            RETURN
         END IF
         IF (IVAR.EQ.2) THEN
            IF(ISIDE.EQ.2) THEN
              IF(CRDSYS.EQ.1.0) THEN
                VELN=-DFXY(1,1)/X
               ELSE
                VELN=-DFXY(1,1)
               END IF
             END IF
            IF(ISIDE.EQ.3) THEN
              IF(CRDSYS.EQ.1.0) THEN
                VELN=DFXY(2,1)*DSIN(ANGLE)/X
               ELSE
                VELN=DFXY(2,1)*DSIN(ANGLE)
               END IF
             END IF
            IF(ISIDE.EQ.2) THEN
             IF(VELN.GT.0.0D0) THEN
              F=BIOT*FUN(K)*FUN(L)
```

```
            RETURN
           ELSE
            F=(BIOT+VELN)*FUN(K)*FUN(L)
            RETURN
           END IF
          END IF
          IF(ISIDE.EQ.3) THEN
           IF(VELN.GT.0.0D0) THEN
            F=BIOT*FUN(K)*FUN(L)
            RETURN
           ELSE
            F=(BIOT+VELN)*FUN(K)*FUN(L)
            RETURN
           END IF
          END IF
        END IF
        IF (IVAR.EQ.3) THEN
          F=0.00D0*FUN(K)*FUN(L)
          RETURN
        END IF
      END IF
C
      IF(IEQ.EQ.3) THEN
       IF (IVAR.EQ.1) THEN
          F=0.00D0* FUN(K)*FUN(L)
          RETURN
       END IF
       IF (IVAR.EQ.2) THEN
          F=0.00D0*FUN(K)*FUN(L)
          RETURN
       END IF
       IF (IVAR.EQ.3) THEN
          F=0.00D0*FUN(K)*FUN(L)
          RETURN
       END IF
      END IF
     RETURN
     END
C
     SUBROUTINE BFUNV (F, X, Y, K, IEQ, IVAR, FUN)
     IMPLICIT REAL*8 (A-H,O-Z)
     COMMON /JEOM/ XMAX, YMAX, CHRL, CRDSYS, IEQFRM, ISIDNM
     COMMON /PARAM/ RYLGH, HCOEF, DP, EPSI, EA, XKO, DOVA, PERM, XMU,
    *               PHI, ALPHA, PO, XLAM
     COMMON /GRPS/ XLEW, GAMMA, BETA, THIELE, RLLY, BIOT, DEE, CHI,
    *              TAU, ZETA, SIGMA
     COMMON /ANGL/ ANGLE
     REAL*8 FUN(12)
     F=0.00D0
     IF (IEQ.EQ.1) THEN
        F= 0.00D0*FUN(K)
        RETURN
     END IF
     IF (IEQ.EQ.2) THEN
        F=0.00D0
        RETURN
     END IF
     IF (IEQ.EQ.3) THEN
        F= 0.00D0*FUN(K)
```

```
          RETURN
        END IF
        RETURN
        END
C
        SUBROUTINE DIRIC (DERIV, ISIDE)
        IMPLICIT REAL*8 (A-H,O-Z)
        COMMON /SPLIT/ IVAR, KK, K, NBTYPE, NODE, IFIRST
        COMMON /JEOM/ XMAX, YMAX, CHRL, CRDSYS, IEQFRM, ISIDNM
        COMMON /IO/ NINT, ITERM, NIN, NOUT, IPROFL, MESH, IERR, NTOUT,
       *            INPARM
        COMMON /VAR/ NVAR
        COMMON /ELDAT/ NLTOP(500,14),COORD(500,3),NELE,IELTYP,NODEL,ITELS,
       *            NF(500,5), XX(30), YY(30),NODTOT, IDIMN, IDFEL,
       *NX,NY,
       *            IXPOS(500), IYPOS(500), NODSID
        COMMON /FEMWRK/  RHS(410), AL(410,140),
       *        NROPV(410), RESDV(4,500), RESD(4), ERR(4),
       *        ERRAV(4), ERRCNT(4), ERRTOT(4), SCALE
        COMMON /BAND/ IBAND, IHBAND, ITOTDF
        COMMON /MTRIX/ SYSK(410,140), SYSM(410,140)
        COMMON /CONT/ C0, CFCTMX, STEPS, STEPS1, STEPS2, ITRACE, ICONT,
       *             IFRST, ICHK, ITASK, IPAYN, DPUP, DPLOW
C           TEST FOR BOUNDARY CONDITION 'SPLIT'
C       LSTSID=1
C       IF(ISIDE.NE.LSTSID) THEN
C         LSTSID=ISIDE
C         IFIRST=1
C       END IF
        IF(NBTYPE.EQ.1) GO TO 11
        IF ((IELTYP.EQ.1).OR.(IELTYP.EQ.3)) THEN
          IF ((ISIDE.EQ.2).AND.(DERIV.LT.0.0D0)) GO TO 10
          IF ((ISIDE.EQ.3).AND.(DERIV.LT.0.0D0)) GO TO 10
          GO TO 11
        ELSE
C --- LSTNOD=2 implies that the last node was a derivative
          IF(IFIRST.EQ.1) THEN
            IF((NODE.EQ.1).AND.(DERIV.LT.0.0D0)) THEN
              LSTNOD=2
              RETURN
            END IF
            IF((NODE.EQ.1).AND.(DERIV.GE.0.0D0)) THEN
              LSTNOD=1
              GO TO 11
            END IF
            IF((NODE.NE.1).AND.(LSTNOD.EQ.2)) THEN
              RETURN
            END IF
            IF((NODE.NE.1).AND.(LSTNOD.EQ.1).AND.(DERIV.GE.0.0D0)) THEN
              GO TO 11
            END IF
            IF((NODE.NE.1).AND.(LSTNOD.EQ.1).AND.(DERIV.LT.0.0D0)) THEN
              LSTNOD=2
              GO TO 11
            END IF
          ELSE
            IF((NODE.EQ.1).AND.(LSTNOD.EQ.2)) THEN
              RETURN
            END IF
```

```
            IF((NODE.EQ.1).AND.(LSTNOD.NE.2).AND.(DERIV.GE.0.0D0)) THEN
              LSTNOD=1
              GO TO 11
            END IF
            IF((NODE.EQ.1).AND.(LSTNOD.NE.2).AND.(DERIV.LT.0.0D0)) THEN
              LSTNOD=2
              RETURN
            END IF
            IF((NODE.NE.1).AND.(DERIV.GE.0.0D0)) THEN
              LSTNOD=1
              GO TO 11
            END IF
            IF((NODE.NE.1).AND.(DERIV.LT.0.0D0)) THEN
              LSTNOD=2
              GO TO 11
            END IF
          END IF
        END IF
11        X = COORD(KK,1)
          Y = COORD(KK,2)
          IF(ITASK.NE.4) THEN
C       Payne-Irons on K matrix
            SYSK(K,IHBAND) = SYSK(K,IHBAND)*SCALE
            RHS(K) = SYSK(K,IHBAND)*H(X,Y,IVAR)
          END IF
          IF((ITASK.EQ.4).AND.(IPAYN.EQ.1)) THEN
C       Payne-Irons on mass matrix
            SYSM(K,IHBAND) = SYSM(K,IHBAND)*SCALE
          END IF
 10     RETURN
        END
C


        DOUBLE PRECISION FUNCTION H(X,Y,IVAR)
        IMPLICIT REAL*8 (A-H,O-Z)
        COMMON /JEOM/ XMAX, YMAX, CHRL, CRDSYS, IEQFRM, ISIDNM
        COMMON /PARAM/ RYLGH, HCOEF, DP, EPSI, EA, XKO, DOVA, PERM, XMU,
       *               PHI, ALPHA, PO, XLAM
        COMMON /GRPS/ XLEW, GAMMA, BETA, THIELE, RLLY, BIOT, DEE, CHI,
       *              TAU, ZETA, SIGMA
        COMMON /RLNUM/ RALY, CFACT
        COMMON /CONT/ CO, CFCTMX, STEPS, STEPS1, STEPS2, ITRACE, ICONT,
       *              IFRST, ICHK, ITASK, IPAYN, DPUP, DPLOW
        H=0.0D0
        IF (IVAR.EQ.1) H=1.00D0
        IF (IVAR.EQ.2) THEN
          H=0.0D0
        END IF
        IF(IVAR.EQ.3) THEN
C         H=XMOLWT*CO/RHOG/MOLFRAC
            IF(IEQFRM.EQ.0) THEN
              H=0.029D0*8.523D0/1.177023D0*4.76
              RETURN
            END IF
            IF(IEQFRM.EQ.1) THEN
              H=DSQRT(0.029D0*8.523D0/1.177023D0*4.76)
              RETURN
            END IF
        END IF
```

```
      RETURN
      END
C
      DOUBLE PRECISION FUNCTION HU(X,Y,IVAR)
      IMPLICIT REAL*8 (A-H,O-Z)
      COMMON /JEOM/ XMAX, YMAX, CHRL, CRDSYS, IEQFRM, ISIDNM
      COMMON /PARAM/ RYLGH, HCOEF, DP, EPSI, EA, XKO, DOVA, PERM, XMU,
     *               PHI, ALPHA, PO, XLAM
      COMMON /GRPS/ XLEW, GAMMA, BETA, THIELE, RLLY, BIOT, DEE, CHI,
     *              TAU, ZETA, SIGMA
      COMMON /RLNUM/ RALY, CFACT
      COMMON /CONT/ CO, CFCTMX, STEPS, STEPS1, STEPS2, ITRACE, ICONT,
     *              IFRST, ICHK, ITASK, IPAYN, DPUP, DPLOW
      HU=0.0D0
      IF (IVAR.EQ.2) HU=1.00D0
      IF (IVAR.EQ.1) THEN
        HU=1.0D-6
      END IF
      IF(IVAR.EQ.3) THEN
C       HU=XMOLWT*CO/RHOG/MOLFRAC
          IF(IEQFRM.EQ.0) THEN
            HU=0.029D0*8.523D0/1.177023D0*4.76
            RETURN
          END IF
          IF(IEQFRM.EQ.1) THEN
            HU=DSQRT(0.029D0*8.523D0/1.177023D0*4.76)
            RETURN
          END IF
      END IF
      RETURN
      END
C
C
C  This file contains the source terms for the unsteady problem
C
      SUBROUTINE SOURCT (F, X, Y, I, IEQ, FUN, GDER, NVAR)
      IMPLICIT REAL*8 (A-H,O-Z)
      COMMON /PARAM/ RYLGH, HCOEF, DP, EPSI, EA, XKO, DOVA, PERM, XMU,
     *               PHI, ALPHA, PO, XLAM
      COMMON /GRPS/ XLEW, GAMMA, BETA, THIELE, RLLY, BIOT, DEE, CHI,
     *              TAU, ZETA, SIGMA
      COMMON /JEOM/ XMAX, YMAX, CHRL, CRDSYS, IEQFRM, ISIDNM
      COMMON /RLNUM/ RALY, CFACT
      COMMON /CONT/ CO, CFCTMX, STEPS, STEPS1, STEPS2, ITRACE, ICONT,
     *              IFRST, ICHK, ITASK, IPAYN, DPUP, DPLOW
      COMMON /IO/ NINT, ITERM, NIN, NOUT, IPROFL, MESH, IERR, NTOUT,
     *            INPARM
      REAL*8 FUN(12), GDER(3,12)
      F=0.00D0
      FX=0.00D0
      FY=0.00D0
      TMPRT=TREAL(FXY(2))+273.15D0
C     E  BROOKS=58198
      EOVR=EA/8.314D0
C     CHOOSE FORM OF RATE EXPRESSION FOR EQUATION FORM
      IF(IEQFRM.EQ.0) THEN
            CONC=FXY(3)
            IF(NVAR.EQ.2) THEN
               CONC=0.9995679D0
```

```
            END IF
         END IF
         IF(IEQFRM.EQ.1) THEN
               CONC=FXY(3)*FXY(3)
         END IF
C        TERM=-EOVR/TMPRT
C        TERM=-EOVR/293.0D0
         TERM=-GAMMA/(1.0D0+FXY(2))
         RA=DEXP(TERM)
C        DIVIDE RATE BY 2 FOR PHI**2 EQUATION FORMULATION
         IF(IEQFRM.EQ.1)RA=RA/2.
         IF (IEQ.EQ.1) THEN
            F=0.0
            RETURN
         END IF
         IF (IEQ.EQ.2) THEN
            F=THIELE*BETA*CONC*FUN(I)*RA/
     *      (DPUP-(DPUP-DPLOW)*(DSIN(3.1415D0/2.0D0*(CFACT-1.0D0)/
     *      (CFCTMX-1.0D0))))*DP
            RETURN
         END IF
         IF(IEQ.EQ.3) THEN
            F=-THIELE*FUN(I)*CONC*RA/
     *      (DPUP-(DPUP-DPLOW)*(DSIN(3.1415D0/2.0D0*(CFACT-1.0D0)/
     *      (CFCTMX-1.0D0))))*DP
            RETURN
         END IF
         RETURN
         END
C
C
C
         SUBROUTINE SEPRT (RHS, NVAR, NTNOD, FVAL)
         IMPLICIT REAL*8 (A-H,O-Z)
         REAL*8 RHS(410), FVAL(5,500)
         DO 10 IEQ=1,NVAR
           IOFST=IEQ-NVAR
           DO 10 NOD=1,NTNOD
10       FVAL(IEQ,NOD)=RHS(NVAR*NOD+IOFST)
         RETURN
         END
C
C
         SUBROUTINE MLTXTR (ARAY1, I1, J1, ARAY2, I2, J2, ARAY3, I3, J3,
     *        NDIM, MXMLT, INCR)
         IMPLICIT REAL*8 (A-H,O-Z)
         REAL*8 ARAY1(I1,J1), ARAY2(I2,J2), ARAY3(I3,J3)
         DO 10 I=1,NDIM
           DO 10 J=1,NDIM
             ARAY3(I,J)=0.00D0
             KCNTR=0
               DO 10 K=1,MXMLT, INCR
C                    Single increment for map function
                 KCNTR=KCNTR+1
10       ARAY3(I,J)=ARAY3(I,J)+ARAY1(I,KCNTR)*ARAY2(K
         RETURN
         END
C
         SUBROUTINE COMBN (FNVAL, NVAR, NTNOD, MAX)
```

```
      IMPLICIT REAL*8 (A-H,O-Z)
      COMMON /IO/ NINT, ITERM, NIN, NOUT, IPROFL, MESH, IERR, NTOUT,
     *            INPARM
      REAL*8 VMIX(410), FNVAL(5,500)
      DO 10 IEQ=1,NVAR
        IOFST=IEQ-NVAR
        DO 10 NOD=1,NTNOD
10    VMIX(NVAR*NOD+IOFST)=FNVAL(IEQ,NOD)
      RETURN
      END
C
      DOUBLE PRECISION FUNCTION FXY(IVAR)
      IMPLICIT REAL*8 (A-H,O-Z)
      COMMON /FVALS/ FVAL(5,500), FLST(5,500)
      COMMON /VAR/ NVAR
      COMMON /SHPFN/ FUN(12), GDER(3,12)
      COMMON /ELDAT/ NLTOP(500,14),COORD(500,3),NELE,IELTYP,NODEL,ITELS,
     *           NF(500,5), XX(30), YY(30),NODTOT, IDIMN, IDFEL,
     *NX,NY,
     *           IXPOS(500), IYPOS(500), NODSID
      FXY=0.00D0
      DO 10 I=1,NODEL
        NOD=NLTOP(NELE, I+2)
        IOFST=IVAR-NVAR
10    FXY=FXY+FUN(I)*FVAL(IVAR,NOD)
      RETURN
      END
C
      DOUBLE PRECISION FUNCTION DFXY (IDRN, IVAR)
      IMPLICIT REAL*8 (A-H,O-Z)
      COMMON /FVALS/ FVAL(5,500), FLST(5,500)
      COMMON /VAR/ NVAR
      COMMON /SHPFN/ FUN(12), GDER(3,12)
      COMMON /ELDAT/ NLTOP(500,14),COORD(500,3),NELE,IELTYP,NODEL,ITELS,
     *           NF(500,5), XX(30), YY(30),NODTOT, IDIMN, IDFEL,
     *NX,NY,
     *           IXPOS(500), IYPOS(500), NODSID
      DFXY=0.00D0
      DO 10 I=1,NODEL
        NOD=NLTOP(NELE, I+2)
10    DFXY=DFXY+GDER(IDRN,I)*FVAL(IVAR,NOD)
      RETURN
      END
C
      DOUBLE PRECISION FUNCTION TREAL(TDIML)
      IMPLICIT REAL*8 (A-H,O-Z)
      TREAL=(1.0D0+TDIML)*293.0D0-273.15D0
      RETURN
      END
C
      SUBROUTINE PRTANS
      IMPLICIT REAL*8 (A-H,O-Z)
      COMMON /FVALS/ FVAL(5,500), FLST(5,500)
      COMMON /ELDAT/ NLTOP(500,14),COORD(500,3),NELE,IELTYP,NODEL,ITELS,
     *           NF(500,5), XX(30), YY(30),NODTOT, IDIMN, IDFEL,
     *NX,NY,
     *           IXPOS(500), IYPOS(500), NODSID
      COMMON /VAR/ NVAR
      COMMON /IO/ NINT, ITERM, NIN, NOUT, IPROFL, MESH, IERR, NTOUT,
```

```
*            INPARM
      COMMON /JEOM/ XMAX, YMAX, CHRL, CRDSYS, IEQFRM, ISIDNM
      DO 10 NOD=1,NODTOT
      IF(IEQFRM.EQ.0) THEN
         WRITE (NOUT,5) FVAL (1,NOD), TREAL(FVAL(2,NOD)),
*              FVAL(3,NOD)/4.76,
*DACOS(1.0D0-COORD(NOD,1))*2.0D0/3.142D0*CHRL
*              , COORD(NOD,2)*CHRL
5        FORMAT(5F16.8)
      END IF
      IF(IEQFRM.EQ.1) THEN
         WRITE (NOUT,*) FVAL (1,NOD), TREAL(FVAL(2,NOD)),
*              FVAL(3,NOD)**2/4.76,COORD(NOD,1)
*              , COORD(NOD,2)
      END IF
10    CONTINUE
      RETURN
      END

      SUBROUTINE PRTXTR
      IMPLICIT REAL*8 (A-H,O-Z)
      COMMON /XTRACT/ NXTRCT, IVXTR(6), IEXLST(6,4,60), NODXTR(6)
      COMMON /FVALS/ FVAL(5,500), FLST(5,500)
      COMMON /ELDAT/ NLTOP(500,14),COORD(500,3),NELE,IELTYP,NODEL,ITELS,
*            NF(500,5), XX(30), YY(30),NODTOT, IDIMN, IDFEL,
*NX,NY,
*            IXPOS(500), IYPOS(500), NODSID
      COMMON /JEOM/ XMAX, YMAX, CHRL, CRDSYS, IEQFRM, ISIDNM
      COMMON /IO/ NINT, ITERM, NIN, NOUT, IPROFL, MESH, IERR, NTOUT,
*            INPARM
      DO 20 I=1,NXTRCT
       ITOT=0
       IFGLST=1
       DO 30 J=1,NODXTR(I)
         NMNOD=IEXLST(I,IVXTR(I),J)
         IF(IVXTR(I).EQ.1) THEN
C --- Calculate the number of flow reversals
           FLOW1=FVAL(IVXTR(I),NMNOD)
           FLOW2=FVAL(IVXTR(I),NMNOD+1)
C --- sign of the flow
           SIGN=FLOW2-FLOW1
           IF(SIGN.GE.0.0D0) THEN
             IFLG=1
           ELSE
             IFLG=0
           END IF
C --- If the flow direction is different from previous increment ITOT
           IF(IFGLST.NE.IFLG) ITOT=ITOT+1
           IFGLST=IFLG
C          WRITE(IPROFL,*) FVAL(IVXTR(I), NMNOD),
C     *     COORD(NMNOD,1), COORD(NMNOD,2)
         ELSE
         IF(IVXTR(I).EQ.2) THEN
           WRITE(IPROFL,*) TREAL(FVAL(IVXTR(I), NMNOD)),
     *     COORD(NMNOD,1), COORD(NMNOD,2)
         ELSE
         IF(IVXTR(I).EQ.3) THEN
           WRITE(IPROFL,*) FVAL(IVXTR(I), NMNOD)/4.76,
     *     COORD(NMNOD,1), COORD(NMNOD,2)
```

```
          END IF
          END IF
          END IF
30       CONTINUE
         WRITE(NOUT,*)'NUMBER OF FLOW CELLS',ITOT
20      CONTINUE
        RETURN
        END
C
        SUBROUTINE SOLVE
        IMPLICIT REAL*8 (A-H,O-Z)
C
C*                          ************************
C*                          *                      *
C*                          * EQUATION SOLUTION    *
C*                          *                      *
C*                          ************************
C
         COMMON /DIMS/ INBDC, ILISTB, ICOORD, INLTOP, INF, IRHS, ISYSK,
      *                JNBDC, JLISTB, JNLTOP, JNF, JSYSK, INROPV, IAL, JAL
         COMMON /VAR/ NVAR
         COMMON /ELDAT/ NLTOP(500,14),COORD(500,3),NELE,IELTYP,NODEL,ITELS,
      *            NF(500,5), XX(30), YY(30),NODTOT, IDIMN, IDFEL,
      *NX,NY,
      *            IXPOS(500), IYPOS(500), NODSID
         COMMON /FEMWRK/  RHS(410), AL(410,140),
      *        NROPV(410), RESDV(4,500), RESD(4), ERR(4),
      *        ERRAV(4), ERRCNT(4), ERRTOT(4), SCALE
         COMMON /BAND/ IBAND, IHBAND, ITOTDF
         COMMON /MTRIX/ SYSK(410,140), SYSM(410,140)
         COMMON /FVALS/ FVAL(5,500), FLST(5,500)
         ITEST=0
         CALL GAUSOL (SYSK, ISYSK, JSYSK, AL, IAL, JAL, ITOTDF, IHBAND,
      *   NROPV, INROPV, RHS, IRHS, ITEST)
         CALL SEPRT(RHS, NVAR, NODTOT, FVAL,
         RETURN
         END
C
C
         SUBROUTINE ERCHK
         IMPLICIT REAL*8 (A-H,O-Z)
         DIMENSION ABSS(3,9), BELM(60,60), BELV(60), BN(60), BNTN(60,60),
      * BNTMP(12), BMTEMP(12,12),
      * COSIN(3), RMAT(60,60), ELK(60,60), GDERT(12,3),
      * GEOM(12,3),   JAC(3,3),JACIN(3,3), ABSCL(9),  LDER(3,12)
      *, P(3,3),
      * PD(3,12),NSTER(60), WGHT(9),BELV1(60),SRCE(60), QL(12)
      *, TMAT(12,12),
      * XTVEC(60), DERMAP(3,12)
         COMMON /XP/ XPARM(4)
          COMMON /DIMS/ INBDC, ILISTB, ICOORD, INLTOP, INF, IRHS, ISYSK,
      *               JNBDC, JLISTB, JNLTOP, JNF, JSYSK, INROPV, IAL, JAL
         COMMON /IO/ NINT, ITERM, NIN, NOUT, IPROFL, MESH, IERR, NTOUT,
      *            INPARM
C        COMMON /PARM/ PARAM(4)
         COMMON /VAR/ NVAR
         COMMON /ELDAT/ NLTOP(500,14),COORD(500,3),NELE,IELTYP,NODEL,ITELS,
      *            NF(500,5), XX(30), YY(30),NODTOT, IDIMN, IDFEL,
      *NX,NY,
```

```
*            IXPOS(500), IYPOS(500), NODSID
      COMMON /XTRACT/ NYTRCT, IVXTR(6), IEXLST(6,4,60), NODXTR(6)
      COMMON /FEMWRK/  RHS(410), AL(410,140),
     *        NROPV(410), RESDV(4,500), RESD(4), ERR(4),
     *        ERRAV(4), ERRCNT(4), ERRTOT(4), SCALE
      COMMON /BAND/ IBAND, IHBAND, ITOTDF
      COMMON /MTRIX/ SYSK(410,140), SYSM(410,140)
      COMMON /BNDRY/ NBNDRY(5,6,80), NBND(5), NBDC(6,80), LISTB(140,5)
      COMMON /SHPFN/ FUN(12), GDER(3,12)
      COMMON /FVALS/ FVAL(5,500), FLST(5,500)
      COMMON /RLNUM/ RALY, CFACT
      COMMON /CONT/ C0, CFCTMX, STEPS, STEPS1, STEPS2, ITRACE, ICONT,
     *              IFRST, ICHK, ITASK, IPAYN, DPUP, DPLOW
      COMMON /JEOM/ XMAX, YMAX, CHRL, CRDSYS, IEQFRM, ISIDNM
      COMMON /PARAM/ RYLGH, HCOEF, DP, EPSI, EA, XKO, DOVA, PERM, XMU,
     *               PHI, ALPHA, PO, XLAM
      COMMON /GRPS/ XLEW, GAMMA, BETA, THIELE, RLLY, BIOT, DEE, CHI,
     *              TAU, ZETA, SIGMA
      COMMON /RELAX/ RELAX1, RELAX2, RELAX3
      REAL*8 CHPARM(4), MAPFUN(12), MAXVAL(5)
      STEPS=STEPS2
C        If first time around, allow many continuation steps ('STEPS1')
      IF (IFRST.EQ.1) THEN
         STEPS=STEPS1
         C0=0.00D0
         IFRST=0
      END IF
      IDFNOD=NVAR
      ITEST=0
      IDGT=0
      IWKREA=50000
      NRHS=1
C     CALL MATNUL(FLST, 4, NODTOT, NVAR, NODTOT, ITEST)
C     iteration (if necessary) begins here

      CFSTP=(CFCTMX-C0)/STEPS
      IPCNTR=0
      IF (ICONT.EQ.0) THEN
         NITER=0
         CFACT=1.00D0
         CFCTMX=CFACT-0.01D0
      END IF
10001 DO 10000 CFACT=1.0D0, CFCTMX+0.01D0, 1.0D0
      IF(ICONT.EQ.1) WRITE(ITERM,*)' CFACT  = ',CFACT
      NITER=0
9000  CALL FELMNT
      IF (NITER.GT.300) THEN
         WRITE(ITERM,*) 'ITERATION LIMIT EXCEEDED, CFACT = ',CFACT,
     .      ERR(1), ERR(2), ERR(3)
         WRITE(NOUT,*) 'ITERATION LIMIT EXCEEDED, CFACT = ', CFACT,
     .      ERR(1), ERR(2), ERR(3), ERRAV(1), ERRAV(2), ERRAV(3)
         CALL PRTANS
         CALL PRTXTR
         STOP
      END IF
      NITER=NITER+1
      IPCNTR=IPCNTR+1
      CALL SOLVE
C
```

```
C           CALCULATE RESIDUALS
C
      TMAX=0.0D0
      DO 127 IVAR=1,NVAR
        RESD(IVAR)=0.00D0
        ERR(IVAR)=0.00D0
        ERRAV(IVAR)=0.0D0
        ERRCNT(IVAR)=0.0D0
        ERRTOT(IVAR)=0.0D0
        MAXVAL(IVAR)=0.00D0
      DO 127 NOD=1,NODTOT
        FV=FVAL(IVAR,NOD)
        IF (DABS(FV).GT.MAXVAL(IVAR)) MAXVAL(IVAR)=DABS(FV)
127   CONTINUE
      DO 126 IVAR=1,NVAR
        DO 125 NOD=1,NODTOT
          IF(FVAL(2,NOD).LT.0.0D0) FVAL(2,NOD)=0.0D0
C         IF(FVAL(2,NOD).GT.2.5D0) FVAL(2,NOD)=2.50D0
          IF(FVAL(3,NOD).LT.0.0D0) FVAL(3,NOD)=0.0D0
          IF(FVAL(3,NOD).GT.0.9995679D0) FVAL(3,NOD)=0.9995679D0
          FV=FVAL(IVAR,NOD)
          IF(IVAR.EQ.2) THEN
            RSDV=(FVAL(IVAR,NOD)-FLST(IVAR,NOD))/MAXVAL(IVAR)
          ELSE
            RSDV=(FVAL(IVAR,NOD)-FLST(IVAR,NOD))/FVAL(IVAR,NOD)
          END IF
          ERRTOT(IVAR)=ERRTOT(IVAR)+RSDV
          RESDV(IVAR,NOD)=RSDV
          IF (DABS(RSDV).GT.DABS(ERR(IVAR))) ERR(IVAR)=RSDV
            IF(IVAR.EQ.1) THEN
              FVAL(IVAR,NOD)=(FVAL(IVAR,NOD)
     *        +RELAX1*FLST(IVAR,NOD))/(RELAX1+1.0D0)
            ELSE
            IF(IVAR.EQ.2) THEN
              FVAL(IVAR,NOD)=(FVAL(IVAR,NOD)
     *        +RELAX2*FLST(IVAR,NOD))/(RELAX2+1.0D0)
            ELSE
            IF(IVAR.EQ.3) THEN
              FVAL(IVAR,NOD)=(FVAL(IVAR,NOD)
     *        +RELAX3*FLST(IVAR,NOD))/(RELAX3+1.0D0)
            END IF
            END IF
            END IF
          FLST(IVAR,NOD)=FV
          IF(IVAR.EQ.2)THEN
            TTEST=FVAL(IVAR,NOD)
            IF(TTEST.GT.TMAX)THEN
             TMAX=TTEST
             NDTMAX=NOD
            END IF
          END IF
125     RESD(IVAR)=RESD(IVAR)+RESDV(IVAR,NOD)**2
        ERRAV(IVAR)=ERRTOT(IVAR)/FLOAT(NODTOT)
        ERRCNT(IVAR)=0.0D0
        DO 128 NOD=1,NODTOT
            IF(RESDV(IVAR,NOD).GT.ERRAV(IVAR)) THEN
              ERRCNT(IVAR)=ERRCNT(IVAR)+1.0D0
            END IF
128     CONTINUE
```

```
126   CONTINUE
      RESD(1)=DSQRT(RESD(1))/NODTOT
      RESD(2)=DSQRT(RESD(2))/NODTOT
C     WRITE(ITERM,*) 'ERRORS ',ERR(1), ERR(2)
      IF (ITRACE.EQ.1) THEN
        WRITE(ITERM,*) 'MAX NORM ERR ',ERR(1), ERR(2), ERR(3)
        WRITE(ITERM,*) 'AVG ERR ', ERRAV(1), ERRAV(2), ERRAV(3)
        WRITE(ITERM,*) '# OF NODES WITH ERROR EXCEEDING ERRAV'
        WRITE(ITERM,*) ERRCNT(1), ERRCNT(2), ERRCNT(3)
        WRITE(ITERM,*) TREAL(TMAX), COORD(NDTMAX,1)*CHRL
     *               , COORD(NDTMAX,2)*CHRL
        WRITE(ITERM,*)'DP',
     *     DPUP-(DPUP-DPLOW)*(DSIN(3.1415D0/2.0D0*(CFACT-1.0D0)/
     *    (CFCTMX-1.0D0)))
      END IF
      IF(ICONT.EQ.1) GO TO 637
      WRITE(NTOUT,*) TREAL(TMAX)+273.15, COORD(NDTMAX,1)*CHRL
     *               , COORD(NDTMAX,2)*CHRL
637   IF (ICHK.NE.1) THEN
C       IF((RESD(1).GT.0.040).OR.(RESD(2).GT.0.01))  GO TO 9000
        IF ((DABS(ERRAV(1)).GT.1.0D-3).OR.(DABS(ERRAV(2)).GT.1.0D-3)
     *     .OR.(DABS(ERRAV(3)).GT.1.0D-3)) GO TO 9000
      END IF
C     IF(ICONT.EQ.1) THEN
C       IF((TREAL(TMAX)+273.15).GE.360.0D0) THEN
C         CFCTMX=(CFCTMX-CFACT)*10.0D0
C         CFSTP=1.0D0
C         C0=1.0D0
C         GO TO 10001
C       END IF
C     END IF
      IF (ICHK.EQ.1) THEN
         ICNV=0
         WRITE(ITERM,*)' ARE ERRORS OK ?'
         READ (NINT,*)ICNV
         IF (ICNV.NE.1) GOTO 9000
      END IF
C     IF ((IPCNTR/ITRACE)*ITRACE.EQ.IPCNTR) THEN
      WRITE(ITERM,*)'CONTINUATION FACTOR = ',CFACT
C     END IF
      REWIND(UNIT=2)
      WRITE(2,5) CFACT
      DO 10 NOD=1,NODTOT
         WRITE (2,5) FVAL (1,NOD), TREAL(FVAL(2,NOD)),
     *              FVAL(3,NOD)/4.76,COORD(NOD,1)*CHRL
     *              , COORD(NOD,2)*CHRL
5        FORMAT(5F16.8)
10    CONTINUE
C     IF((TREAL(TMXLST)-TREAL(TMAX)).GT.30.0D0) GO TO 10000
      WRITE(NOUT,*)'CFACT=', CFACT
      WRITE(NOUT,*)'RAYLEIGH', RLLY*
     *  (DPUP-(DPUP-DPLOW)*(DSIN(3.1415D0/2.0D0*(CFACT-1.0D0)/
     *  (CFCTMX-1.0D0))))**2/DP**2
      WRITE(NOUT,*)'THIELE', THIELE/
     *  (DPUP-(DPUP-DPLOW)*(DSIN(3.1415D0/2.0D0*(CFACT-1.0D0)/
     *  (CFCTMX-1.0D0))))*DP
     *                          *DEXP(-GAMMA)
      WRITE(NOUT,*)'DP',
     *   DPUP-(DPUP-DPLOW)*(DSIN(3.1415D0/2.0D0*(CFACT-1.0D0)/
```

```
     *  (CFCTMX-1.0D0)))
      WRITE(NOUT,*) TREAL(TMAX)+273.15, COORD(NDTMAX,1)*CHRL
     *              , COORD(NDTMAX,2)*CHRL
      CALL PRTXTR
      TMXLST=TMAX
10000 CONTINUE
C --- Reset CFACT
      IF(ICONT.EQ.0) CFACT=1.0D0
 8010 FORMAT (16I5)
 8020 FORMAT (I5, 6F10.0)
 9010 FORMAT (//25H ***** NODAL GEOMETRY *****//1H )
 9020 FORMAT (1H , 16I5)
 9030 FORMAT (1H , 15, 6F10.5)
 9040 FORMAT (//27H ***** ELEMENT TOPOLOGY *****//1H )
 9050 FORMAT (//30H ***** BOUNDARY CONDITIONS *****//1H )
 9060 FORMAT (//27H ***** NODAL POTENTIALS *****//1H )
      RETURN
      END
C
C
      SUBROUTINE ASSM
      IMPLICIT REAL*8 (A-H,O-Z)
      REAL*8 JAC, JACIN, LDER
      REAL*8 CHPARM(4), MAPFUN(12), MAXVAL(5)
      DIMENSION ABSS(3,9), BELM(60,60), BELV(60), BN(60), BNTN(60,60),
     * BNTMP(12), BMTEMP(12,12),
     * COSIN(3), RMMAT(60,60), ELM(60,60), GDERT(12,3),
     * GLOM(12,3),   JAC(3,3),JACIN(3,3), ABSCL(9),  LDER(3,12)
     *, P(3,3),
     * PD(3,12),NSTER(60), WGHT(9),BELV1(60),SRCE(60), QL(12)
     *, TMMAT(12,12),
     * XTVEC(60), DERMAP(3,12)
       COMMON /DIMS/ INBDC, ILISTB, ICOORD, INLTOP, INF, IRHS, ISYSK,
     *               JNBDC, JLISTB, JNLTOP, JNF, JSYSK, INROPV, IAL, JAL
      COMMON /IO/ NINT, ITERM, NIN, NOUT, IPROFL, MESH  IERR, NTOUT,
     *            INPARM
C     COMMON /PARM/ PARAM(4)
      COMMON /VAR/ NVAR
      COMMON /ELDAT/ NLTOP(500,14),COORD(500,3),NELE,IELTYP,NODEL,ITELS,
     *           NF(500,5), XX(30), YY(30),NODTOT, IDIMN, IDFEL,
     *NX,NY,
     *           IXPOS(500), IYPOS(500), NODSID
      COMMON /XTRACT/ NXTRCT, IVXTR(6), IEXLST(6,4,60), NODXTR(6)
      COMMON /FEMWRK/  RHS(410), AL(410,140),
     *        NROPV(410), RESDV(4,500), RESD(4), ERR(4),
     *        ERRAV(4), ERRCNT(4), ERRTOT(4), SCALE
      COMMON /BAND/ IBAND, IHBAND, ITOTDF
      COMMON /MTRIX/ SYSK(410,140), SYSM(410,140)
      COMMON /BNDRY/ NBNDRY(5,6,80), NBND(5), NBDC(6,80), LISTB(140,5)
      COMMON /SHPFN/ FUN(12), GDER(3,12)
      COMMON /FVALS/ FVAL(5,500), FLST(5,500)
      COMMON /RLNUM/ RALY, CFACT
      COMMON /CONT/ C0, CFCTMX, STEPS, STEPS1, STEPS2, ITRACE, ICONT,
     *              IFRST, ICHK, ITASK, IPAYN, DPUP, DPLOW
      COMMON /SPLIT/ IVAR, KK, K, NBTYPE, NODE, IFIRST
C
C                          PROBLEM SIZE DEPENDENT ARRAYS
C
C
```

```
      DATA IABSS /3/,IBELM/60/,IBELV /60/,IBN /60/,IBNTN /60/,ICOSIN/3 ,
     * IRMMAT /60/,IELM /60/, IFUN /12/, IGDER /3/,IGDERT /12/, IGEOM
     */12/,
     *  IJAC /3/, IJACIN /3/,IABSCL /9/, ILDER /3/, IP /3/, IPD /3/,
     * INSTER /60/,IWGHT /9/, JABSS /9/,JBELM/60/,JBNTN /60/,JCOORD /3/,
     *  ISRCE /60/, IXTVEC /60/,
     * JRMMAT /60/, JELM /60/, JGDER /12/, JGDERT /3/, JGEOM /3/,JJAC
     */3/,
     * JJACIN /3/, JLDER /12/, JP /3/,JPD /12/
C
C
      WRITE(ITERM,*) 'INSIDE ASSM'
      MPINCR=NODSID-1
      NODMAP=NODEL-NODSID+2
      IDFNOD=NVAR
      ITEST = 0
      IDGT=0
      IWKREA=50000
      NRHS=1
C
C*                          ****************************************
C*                          *                                      *
C*                          *       MASS       MATRIX ASSEMBLY    *
C*                          *                                      *
C*                          ****************************************
C
C
      CALL MATNUL(SYSM, ISYSK, JSYSK, ITOTDF, IBAND, ITEST)
      IDFEL = NODEL*IDFNOD
      IF ((IELTYP.EQ.1).OR.(IELTYP.EQ.2).OR.(IELTYP.EQ.3)) THEN
         CALL QTRI7(WGHT, IWGHT, ABSS, IABSS, JABSS, NQP, ITEST)
      END IF
      IF ((IELTYP.EQ.4).OR.(IELTYP.EQ.5).OR.(IELTYP.EQ.6)) THEN
C        CALL QQUA9(WGHT, IWGHT, ABSS, IABSS, JABSS, NQP, ITEST)
         CALL QQUA4(WGHT, IWGHT, ABSS, IABSS, JABSS, NQP, ITEST)
      END IF
      DO 1100 NELE=1,ITELS
      CALL ELGEOM(NELE, NLTOP, INLTOP, JNLTOP, COORD, ICOORD,JCOORD,
     * GEOM, IGEOM, JGEOM, IDIMN, ITEST)
C
C                            INTEGRATION LOOP FOR ELEMENT MATRICES
C                            USING NQP QUADRATURE POINTS
C
      CALL MATNUL(ELM, IELM, JELM, IDFEL, IDFEL, ITEST)
      DO 1090 IQUAD=1,NQP
      CALL MATNUL(RMMAT, IRMMAT, JRMMAT, IDFEL, IDFEL, ITEST)
C
C                            FORM SHAPE FUNCTION AND SPACE
C                            DERIVATIVES IN THE LOCAL CORRDINATES.
C                            TRANSFORM LOCAL DERIVATIVES TO GLOBAL
C                            COORDINATE SYSTEM
C
      XI = ABSS(1,IQUAD)/1.00000D0
      ETA = ABSS(2,IQUAD)/1.00000D0
      IF (IELTYP.EQ.1) THEN
        CALL TRIM3(FUN, IFUN, LDER, ILDER, JLDER, XI, ETA, ITEST)
        CALL TRIM3(MAPFUN, IFUN, DERMAP, ILDER, JLDER, XI, ETA, ITEST)
      END IF
```

```
      IF (IELTYP.EQ.4) THEN
        CALL QU4FN(FUN, IFUN, LDER, ILDER, JLDER, XI, ETA, ITEST)
        CALL QU4FN(MAPFUN, IFUN, DERMAP, ILDER, JLDER, XI, ETA, ITEST)
      END IF
      IF (IELTYP.EQ.5) THEN
        CALL QU8FN(   FUN, IFUN,   LDER, ILDER, JLDER, XI, ETA, ITEST)
        CALL QU4FN(MAPFUN, IFUN, DERMAP, ILDER, JLDER, XI, ETA, ITEST)
      END IF
C
      IF (IELTYP.EQ.6) THEN
        CALL QU12FN(FUN, IFUN, LDER, ILDER, JLDER, XI, ETA, ITEST)
        CALL QU4FN(MAPFUN, IFUN, DERMAP, ILDER, JLDER, XI, ETA, ITEST)
      END IF
C           Calculate Jacobian (mapping fn. deriv's * element geom.)
      CALL MLTXTR (DERMAP, ILDER, JLDER, GEOM, IGEOM, JGEOM, JAC,IJAC,
     *             JJAC, IDIMN, NODMAP, MPINCR)
      CALL MATINV(JAC, IJAC, JJAC, JACIN, IJACIN, JJACIN, IDIMN, DET,
     * ITEST)
C     CALL MLTXTR(JACIN, IJACIN, JJACIN, LDER, ILDER, JLDER, GDER,IGDER,
C    *            JGDER, IDIMN, NODMAP, MPINCR)
      CALL MATMUL(JACIN, IJACIN, JJACIN, LDER, ILDER, JLDER, GDER,IGDER,
     *            JGDER, IDIMN, IDIMN, NODEL, ITEST)
C                          CALCULATE (XI,ETA) IN GLOBAL (X,Y)
C                          COORDINATES AND FORM P MATRIX
C
      XMAP=0.0D0
      YMAP=0.0D0
      IMAP=0
      DO 8999 KL=1,NODMAP, MPINCR
      IMAP=IMAP+1
      XMAP=XMAP+GEOM(KL,1)*MAPFUN(IMAP)
8999  YMAP=YMAP+GEOM(KL,2)*MAPFUN(IMAP)
      X=XMAP
      Y=YMAP
C     CALL SCAPRD(GEOM(1,1), IGEOM, FUN, IFUN, NODEL, X, ITEST)
C     CALL SCAPRD(GEOM(1,2), IGEOM, FUN, IFUN, NODEL, Y, ITEST)
C
C                              FORM INTEGRAND ELEMENT STIFFNESS ELM
C
      QUOT = DABS(DET)*WGHT(IQUAD)
      DO 1082 IEQ=1,NVAR
       DO 1081 IVAR=1,NVAR
        DO 1080 I=1,NODEL
         DO 1070 J=1,NODEL
            CALL USSEQN (F, X, Y, I, J, IEQ, IVAR, FUN, GDER, QUOT)
            TMMAT(I,J)=QUOT*F
 1070    CONTINUE
 1080   CONTINUE
 1081  CALL ASMAT (TMMAT, RMMAT, IVAR, IEQ, NODEL)
 1082 CONTINUE
      CALL MATADD(ELM, IELM, JELM, RMMAT, IRMMAT, JRMMAT, IDFEL,IDFEL,
     * ITEST)
 1090 CONTINUE
C
C                              ASSEMBLY OF MASS MATRIX
C
      CALL DIRECT(NELE, NLTOP, INLTOP, JNLTOP, NF, INF, JNF,IDFNOD,
     * NSTER, INSTER, ITEST)
C     CALL ASSYM(SYSM, ISYSK, JSYSK, ELM, IELM, JELM, NSTER,INSTER,
```

```
C     * IHBAND, IDFEL, ITEST)
      CALL ASUSM(SYSM, ISYSK, JSYSK, ELM, IELM, JELM, NSTER,INSTER,
     * IHBAND, IDFEL, ITEST)
 1100 CONTINUE
C
C*                          ****************************************
C*                          *                                      *
C*                          * INSERTION OF BOUNDARY CONDITIONS     *
C*                          *                                      *
C*                          ****************************************

      CALL QLIN3(WGHT, IWGHT, ABSCL, IABSCL, NQP, ITEST)
      DO 1230 IVAR=1,NVAR
       DO 1231 I=1,NBND(IVAR)
        DO 1231 J=1,40
          IFSTND=NBNDRY(IVAR, I, 4)
1231      NBDC(I,J)=NBNDRY(IVAR, I, J)
      DO 1230 ITYPE=1,NBND(IVAR)
      NBTYPE = NBDC(ITYPE,1)
      NUMNOD = NBDC(ITYPE,2)
      GO TO (1110, 1230, 1131), NBTYPE
C
C
C
C
C
C                             'SPLIT' DIRICHLET BOUNDARY CONDITIONS
1131  CALL SIDENO (ITELS, NLTOP, INLTOP, JNLTOP, ITYPE, NBDC,INBDC,
     * JNBDC, NUMSID, LISTB, ILISTB, JLISTB, ITEST)
      IF (NUMSID.EQ.0) WRITE(ITERM,*)'BOUNDARY ERROR',NVAR, ITYPE
      DO 1119 M=1,NUMSID
        IELNM = LISTB(M,1)
        ISIDNM = LISTB(M,2)
        NELE=IELNM
        LL=(ISIDNM-1)*(NODSID-1)
C --- KK and KK1 are the first and second nodes on side ISIDNM
C --- and these are incremented in loop 1117 such that on
C --- each subsequent run through the loop the node called KK
C --- becomes the node called KK1 in the previous time through
C --- the loop
        DO 1117 N=1,NODSID-1
C --- IFIRST is the first node in the boundary list for SPLIT
          IF(N.EQ.1) THEN
C --- NODE =1 implies that the node is the first in the element
            NODE=1
          ELSE
            NODE=0
          END IF
          KK=NLTOP(NELE,3+LL+N-1)
          KK1=NLTOP(NELE,3+LL+N)
          K=NVAR*KK+(IVAR-NVAR)
          IF((KK.EQ.IFSTND).OR.(KK1.EQ.(IFSTND+1))) THEN
            IFIRST=1
          ELSE
            IFIRST=0
          END IF
          IF(ISIDNM.EQ.2) THEN
            DELTA=COORD(KK+1,1)-COORD(KK,1)
          END IF
```

```
            IF(ISIDNM.EQ.3) THEN
              DELTA=DSQRT((COORD(KK+1,1)-COORD(KK,1))**2+(COORD(KK+1,2)-
     *             COORD(KK,2))**2)
            END IF
            FVAL1=FVAL(1,KK)
            FVAL2=FVAL(1,KK1)
            DERIV=(FVAL2-FVAL1)/DELTA
            CALL DIRIC (DERIV, ISIDNM)
 1117     CONTINUE
  1119 CONTINUE
       GO TO 1230
C
C                              PRESCRIBED VALUES  (DIRICHLET)
C
 1110  DO 1120 J=1,NUMNOD
         KK = NBDC(ITYPE,J+3)
         K = NVAR*NBDC(ITYPE,J+3)+(IVAR-NVAR)
           CALL DIRIC (DERIV, ISIDNM)
  1120 CONTINUE
       GO TO 1230
C
 1230  CONTINUE
C       Reset IPAYN
       IPAYN=0
C      CALL CHORDN (SYSM, ISYSK, JSYSK, ITOTDF, IHBAND, ITEST)
       CALL GAURDN (SYSM, ISYSK, JSYSK, AL, IAL, JAL, ITOTDF, IHBAND,
     *              NROPV, INROPV, ITEST)
       WRITE(ITERM,*) 'EXITING ASSM'
C      IF (ITEST.NE.999) WRITE(4,*)'ITEST GAURDN = ',ITEST
C      IF (ITEST.NE.999) STOP
       RETURN
       END
C
C           TDERV evaluates derivatives for unsteady solution
       SUBROUTINE TDERV (NDE, TIME, FNCVAL, FNCDER)
       IMPLICIT REAL*8 (A-H,O-Z)
        COMMON /DIMS/ INBDC, ILISTB, ICOORD, INLTOP, INF, IRHS, ISYSK,
     *                JNBDC, JLISTB, JNLTOP, JNF, JSYSK, INROPV, IAL, JAL
       COMMON /XP/ XPARM(4)
       COMMON /FEMWRK/  RHS(410), AL(410,140),
     *         NROPV(410), RESDV(4,500), RESD(4), ERR(4),
     *         ERRAV(4), ERRCNT(4), ERRTOT(4), SCALE
       COMMON /BAND/ IBAND, IHBAND, ITOTDF
       COMMON /MTRIX/ SYSK (410,140), SYSM(410,140)
       COMMON /FVALS/ FVAL(5,500), FLST(5,500)
       COMMON /IO/ NINT, ITERM, NIN, NOUT, IPROFL, MESH, IERR, NTOUT,
     *             INPARM
       REAL*8 FNCVAL(410), FNCDER(410), WORK1(410), WORK2(410)
       WRITE(ITERM,*) 'INSIDE TDERV'
       CALL SEPRT(FNCVAL, NVAR, NODTOT, FVAL)
       CALL FELMNT
       CALL MVUSB(SYSK, ISYSK, JSYSK, FNCVAL, NDE, WORK1, NDE,
     *            ITOTDF, IHBAND, ITEST)
       CALL VECSUB (WORK1, ISYSK, RHS, ISYSK, NDE, ITEST)
C      CALL CHOSUB (SYSM, ISYSK, JSYSK, WORK1, ISYSK, NDE, IHBAND,
C     * ITEST)
       CALL GAUSUB (SYSM, ISYSK, JSYSK, AL, IAL, JAL, NDE, IHBAND, NROPV
     *             ,INROPV, WORK1, ISYSK, ITEST)
       CALL VECCOP (WORK1, ISYSK, FNCDER, ISYSK, NDE, ITEST)
```

```
      WRITE(ITERM,*) 'EXITING TDERV'
      RETURN
      END
C
C
      SUBROUTINE MONT(FMIN, FMAX, SIM, N, IS, NCALL)
      IMPLICIT REAL*8 (A-H,O-Z)
      REAL*8 SIM(4,4)
C     WRITE(4,*)((SIM(I,J),J=1,2),I=1,3)
C     WRITE(4,*)
      RETURN
      END
C
C
      SUBROUTINE PDERV(N, X, Y, YJAC)
      IMPLICIT REAL*8 (A-H,O-Z)
      REAL*8 Y(N), YJAC(N)
      RETURN
      END
```

The following file (NDQ63 DATA) contains the finite element mesh data for use with the finite element program. In this case the mesh is a 6 by 6 array of 8 noded quadrilateral elements with boundary conditions as for figure 2.1.

133	2	3
6	6	
1	0.0000000	0.0000000
2	0.0833333	0.0000000
3	0.1[illegible]666	0.0000000
4	0.2500000	0.0000000
5	0.3333333	0.0000000
6	0.4166666	0.0000000
7	0.5000000	0.0000000
8	0.5833333	0.0000000
9	0.6666666	0.0000000
10	0.7500000	0.0000000
11	0.8333333	0.0000000
12	0.9166666	0.0000000
13	1.0000000	0.0000000
14	0.0000000	0.0833333
15	0.1666666	0.0833333
16	0.3333333	0.0833333
17	0.5000000	0.0833333
18	0.6666666	0.0833333
19	0.8333333	0.0833333
20	1.0000000	0.0833333
21	0.0000000	0.1666666
[illegible]	0833333	0.1666666
	1666666	0.1666666
	2500000	0.1666666
[illegible]	0.3333333	0.1666666
26	4166666	0.1666666
27	5000000	0.1666666
28	0.5833333	0.1666666
29	0.6666666	0.1666666
30	0.7500000	0.1666666
31	0.8333333	0.1666666
32	0.9166666	0.1666666
33	1.0000000	0.1666666
34	0.0000000	0.2500000
35	0.1666666	0.2500000
36	0.3333333	0.2500000
37	0.5000000	0.2500000
38	0.6666666	0.2500000
39	0.8333333	0.2500000
40	1.0000000	0.2500000
41	0.0000000	0.3333333
42	0.0833333	0.3333333
43	0.1666666	0.3333333
44	0.2500000	0.3333333
45	0.3333333	0.3333333
46	0.4166666	0.3333333
47	0.5000000	0.3333333
48	0.5833333	0.3333333
49	0.6666666	0.3333333
50	0.7500000	0.3333333
51	0.8333333	0.3333333
52	0.9166666	0.3333333
53	1.0000000	0.3333333
54	0.0000000	0.4166666
55	0.1666666	0.4166666
56	0.3333333	0.4166666
57	0.5000000	0.4166666

58	0.6666666	0.4166666
59	0.8333333	0.4166666
60	1.0000000	0.4166666
61	0.0000000	0.5000000
62	0.0833333	0.5000000
63	0.1666666	0.5000000
64	0.2500000	0.5000000
65	0.3333333	0.5000000
66	0.4166666	0.5000000
67	0.5000000	0.5000000
68	0.5833333	0.5000000
69	0.6666666	0.5000000
70	0.7500000	0.5000000
71	0.8333333	0.5000000
72	0.9166666	0.5000000
73	1.0000000	0.5000000
74	0.0000000	0.5833333
75	0.1666666	0.5833333
76	0.3333333	0.5833333
77	0.5000000	0.5833333
78	0.6666666	0.5833333
79	0.8333333	0.5833333
80	1.0000000	0.5833333
81	0.0000000	0.6666666
82	0.0833333	0.6666666
83	0.1666666	0.6666666
84	0.2500000	0.6666666
85	0.3333333	0.6666666
86	0.4166666	0.6666666
87	0.5000000	0.6666666
88	0.5833333	0.6666666
89	0.6666666	0.6666666
90	0.7500000	0.6666666
91	0.8333333	0.6666666
92	0.9166666	0.6666666
93	1.0000000	0.6666666
94	0.0000000	0.7500000
95	0.1666666	0.7500000
96	0.3333333	0.7500000
97	0.5000000	0.7500000
98	0.6666666	0.7500000
99	0.8333333	0.7500000
100	1.0000000	0.7500000
101	0.0000000	0.8333333
102	0.0833333	0.8333333
103	0.1666666	0.8333333
104	0.2500000	0.8333333
105	0.3333333	0.8333333
106	0.4166666	0.8333333
107	0.5000000	0.8333333
108	0.5833333	0.8333333
109	0.6666666	0.8333333
110	0.7500000	0.8333333
111	0.8333333	0.8333333
112	0.9166666	0.8333333
113	1.0000000	0.8333333
114	0.0000000	0.9166666
115	0.1666666	0.9166666
116	0.3333333	0.9166666

```
      117          0.5000000          0.9166666
      118          0.6666666          0.9166666
      119          0.8333333          0.9166666
      120          1.0000000          0.9166666
      121          0.0000000          1.0000000
      122          0.0833333          1.0000000
      123          0.1666666          1.0000000
      124          0.2500000          1.0000000
      125          0.3333333          1.0000000
      126          0.4166666          1.0000000
      127          0.5000000          1.0000000
      128          0.5833333          1.0000000
      129          0.6666666          1.0000000
      130          0.7500000          1.0000000
      131          0.8333333          1.0000000
      132          0.9166666          1.0000000
      133          1.0000000          1.0000000
  5    36    8
  1     1   14   21   22   23   15    3    2
  2     3   15   23   24   25   16    5    4
  3     5   16   25   26   27   17    7    6
  4     7   17   27   28   29   18    9    8
  5     9   18   29   30   31   19   11   10
  6    11   19   31   32   33   20   13   12
  7    21   34   41   42   43   35   23   22
  8    23   35   43   44   45   36   25   24
  9    25   36   45   46   47   37   27   26
 10    27   37   47   48   49   38   29   28
 11    29   38   49   50   51   39   31   30
 12    31   39   51   52   53   40   33   32
 13    41   54   61   62   63   55   43   42
 14    43   55   63   64   65   56   45   44
 15    45   56   65   66   67   57   47   46
 16    47   57   67   68   69   58   49   48
 17    49   58   69   70   71   59   51   50
 18    51   59   71   72   73   60   53   52
 19    61   74   81   82   83   75   63   62
 20    63   75   83   84   85   76   65   64
 21    65   76   85   86   87   77   67   66
 22    67   77   87   88   89   78   69   68
 23    69   78   89   90   91   79   71   70
 24    71   79   91   92   93   80   73   72
 25    81   94  101  102  103   95   83   82
 26    83   95  103  104  105   96   85   84
 27    85   96  105  106  107   97   87   86
 28    87   97  107  108  109   98   89   88
 29    89   98  109  110  111   99   91   90
 30    91   99  111  112  113  100   93   92
 31   101  114  121  122  123  115  103  102
 32   103  115  123  124  125  116  105  104
 33   105  116  125  126  127  117  107  106
 34   107  117  127  128  129  118  109  108
 35   109  118  129  130  131  119  111  110
 36   111  119  131  132  133  120  113  112
2
1 3 11  14  21  34  41  54  61  74  81  94 101
      114
1 3 11  12  11  10   9   8   7   6   5   4   3
        2
```

```
2
2  3  37     1   14   21   34   41   54   61   74   81   94
           101  114  121  122  123  124  125  126  127  128
           129  130  131  132  133  120  113  100   93   80
            73   60   53   40   33   20   13
1  3  11    12   11   10    9    8    7    6    5    +    3
             2
1
3  3  26   121  122  123  124  125  126  127  128  129  130
           131  132  133  120  113  100   93   80   73   60
            53   40   33   20   13   12
1
1    12    121  122  123  124  125  126  127  128  129  130
           131  132
```

The following file (INPARM2 DATA) contains the physical parameters of the model and the flags to control the program operation. In this case the problem to be solved is an ignition point calculation in Cartesian coordinates.

```
30.00E0   15.0E0    30.0        0.0         0
5.0       55.00E-3   0.1       58198.      10.0    0.20       2.0E-5   1.8E-5
293.0     1.177023  9.81        1.0E3     300.0E3   30.0E0
0
55.0       35.0       1.0        1          1          0
55.00E-3             15.0E-3
1.0       1.0         1.0
0
```

The following program SNODE FORTRAN written in Fortran 77 by P. Anderson generates a mesh of 4-noded quadrilateral elements with optional mesh crushing.

```
C --- Program to generate a mesh of 4-noded elements
      REAL A(2),B(2)
      INTEGER IBND(4,300)
      DATA MESH /8/
      A(1)=0.00E0
      B(1)=1.00E0
      A(2)=0.00E0
      B(2)=1.00E0
      XW=B(1)-A(1)
      YW=B(2)-A(2)
C --- Choose where to crush mesh
C           1-U 2-BOTH 3-L 4-R 5-? 6-L&M&R
      IMESHX=2
      IMESHY=2
      NODX=11
      NODY=11
      NELX=NODX-1
      NELY=NODY-1
      NELS=NELX*NELY
      NNODS=NODX*NODY
      WRITE(6,*) NNODS, 2, 2
      WRITE(6,*) NODX, NODY
      DO 10 IY=1,NODY
        Y=FMESH(IY, NODY, A(2), B(2), IMESHY)
        DO 10 IX=1,NODX
          NNOD=NNOD+1
          X=FMESH(IX, NODX, A(1), B(1), IMESHX)
10        WRITE(6,*)NNOD, X, Y
      WRITE(6,*) 1, NELS, 4
      DO 5 IELNM=1,NELS
        NROW=IELNM/NELX
        RTIO=IELNM/NELX
        IF ((NROW*NELX).NE.IELNM) THEN
          NROW=INT(RTIO)+1
        END IF
        IRST=(NROW-1)*NODX+1
        IELPOS=IELNM-(NROW-1)*NELX
        IBLFT=IRST+IELPOS-1
        ITLFT=IBLFT+NODX
        ITPRT=ITLFT+1
        IBTRT=IBLFT+1
        WRITE(6,*)IELNM, IBLFT, ITLFT, ITPRT, IBTRT
5     CONTINUE
      WRITE(6,*)
      NP=0
      DX=XW/NELX
      DY=YW/NELY

      DO 40 I=1,NODY
40    IBND(1,I)=I*NODX-NODX+1

      DO 30 I=1,NODX
        J=NODX-I
30    IBND(2,I)=NNODS-J

      DO 50 I=1,NODY
        J=NODY-I+1
50    IBND(3,I)=J*NODX
```

```
      DO 20 I=1,NODX
        J=NODX-I+1
20    IBND(4,I)=J

      DO 60 I=1,4
60    WRITE(6,70)(IBND(I,J),J=1,20)
70    FORMAT (6X,10(I3,1X))
      STOP
      END
C
      REAL FUNCTION FMESH (I, N, A, B, IMESH)
C     1-U 2-BOTH 3-L 4-R 5-? 6-L&M&R
      PI=3.14159
      FMESH=0.00E0
      XI=FLOAT(I-1)
      XN=FLOAT(N-1)
      FRC1=XI/XN*PI*2.0
      FRC=XI/XN
         IF (IMESH.EQ.1) F=A+(B-A)*FRC
         IF (IMESH.EQ.2) F=(0.5*(A-B)*COS(PI*FRC)+(A+B)/2.0)
         IF (IMESH.EQ.3) F=(B-A)*(1.0-COS(FRC*PI/2.0))
         IF (IMESH.EQ.4) F=(B-A)*(SIN(FRC/2.0*PI))
         IF (IMESH.EQ.5) F=(4.0/9.0*FRC**3-6.0/19.0*FRC**2+FRC/10.0)
         IF (IMESH.EQ.6) F=(FRC1/2.0-SIN(2.0*FRC1)/4.0)/PI
      FMESH=F
      RETURN
      END
```

The following program SNODEQ FORTRAN written in Fortran 77 by P. Anderson generates a mesh of 8-noded quadrilateral elements.

```
C --- Program to generate a mesh of 8-noded elements
      INTEGER ILTOP(500,10), NBND(300)
      REAL COORD(500,2)
      NELX=8
      NELY=8
      N1X=2*NELX+1
      N2X=NELX+1
      N3X=N1X+N2X
      N1Y=2*NELY+1
      N2Y=NELY+1
      N3Y=N1Y+N2Y
      NNODY=2*NELY+1
      ITNOD=NELY*(N1X+N2X)+N1X
      WRITE(6,*) ITNOD, 2, 2
      WRITE(6,*) 2, 2
      ITELS=NELX*NELY
      DO 1) NELE=1,ITELS
        R=NELE/NELX
        IROW=INT(R)
        IEPOS=NELX
        IF ((NELE/NELX*NELX).NE.NELE) THEN
           IEPOS=NELE-INT(R)*NELX
           IROW=INT(R)+1
        END IF
        NSTRT=(3*NELX+2)*(IROW-1)+1
        IBL=NSTRT+2*(IEPOS-1)
        ILTOP(NELE,1)=IBL
        IF (IEPOS.EQ.1)  NSTRTM=ILTOP(NELE,1)+2*NELX+1
        IF (IEPOS.EQ.1)  NSTRTT=ILTOP(NELE,1)+N1X+N2X
        IML=NSTRTM+IEPOS-1
        ILTOP(NELE,2)=IML
        ITL=NSTRTT+2*(IEPOS-1)
        ILTOP(NELE,3)=ITL
        IMT=ILTOP(NELE,3)+1
        ILTOP(NELE,4)=IMT
        ITR=ILTOP(NELE,4)+1
        ILTOP(NELE,5)=ITR
        IMR=ILTOP(NELE,2)+1
        ILTOP(NELE,6)=IMR
        IBR=ILTOP(NELE,1)+2
        ILTOP(NELE,7)=IBR
        IMB=ILTOP(NELE,1)+1
        ILTOP(NELE,8)=IMB
10    CONTINUE
15    FORMAT(3X,I3,3X,8(I3,2X))
      DO 90 NOD=1,ITNOD
      IROW=NOD/N3X+1
        IF (NOD/N3X*N3X.NE.NOD) THEN
          IROW=NOD/N3X+1
        END IF
        IF (NOD/N3X*N3X.EQ.NOD) IROW=IROW-1
        ISTRT=(IROW-1)*N3X+1
        IYPOS=2*(IROW-1)
C                 IN FIRST LEVEL
        TEST=(1.0*NOD-1.0*ISTRT+1.0)/(1.0*N1X)
        IF (TEST.LT.1.00E0) THEN
           LEV=1
           INPOS=NOD-ISTRT
           X=       INPOS/FLOAT(N1X-1)
```